

THE UNIVERSITY OF CALGARY

PHASE EQUILIBRIA IN GAS HYDRATE FORMING SYSTEMS IN THE
PRESENCE OF ELECTROLYTES OR METHANOL, AND ESTIMATION
OF INTERACTION PARAMETERS IN EQUATIONS OF STATE

by

PETROS ENGLEZOS

A THESIS

SUBMITTED TO THE FACULTY OF GRADUATE STUDIES
IN PARTIAL FULFILLMENT OF THE REQUIREMENT FOR THE
DEGREE OF
DOCTOR OF PHILOSOPHY

DEPARTMENT OF CHEMICAL AND PETROLEUM ENGINEERING

CALGARY, ALBERTA

JUNE, 1990

© PETROS ENGLEZOS



National Library
of Canada

Bibliothèque nationale
du Canada

Canadian Theses Service Service des thèses canadiennes

Ottawa, Canada
K1A 0N4

The author has granted an irrevocable non-exclusive licence allowing the National Library of Canada to reproduce, loan, distribute or sell copies of his/her thesis by any means and in any form or format, making this thesis available to interested persons.

The author retains ownership of the copyright in his/her thesis. Neither the thesis nor substantial extracts from it may be printed or otherwise reproduced without his/her permission.

L'auteur a accordé une licence irrévocable et non exclusive permettant à la Bibliothèque nationale du Canada de reproduire, prêter, distribuer ou vendre des copies de sa thèse de quelque manière et sous quelque forme que ce soit pour mettre des exemplaires de cette thèse à la disposition des personnes intéressées.

L'auteur conserve la propriété du droit d'auteur qui protège sa thèse. Ni la thèse ni des extraits substantiels de celle-ci ne doivent être imprimés ou autrement reproduits sans son autorisation.

ISBN 0-315-61905-8

Canada

THE UNIVERSITY OF CALGARY
FACULTY OF GRADUATE STUDIES

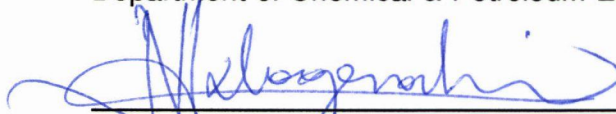
The undersigned certify that they have read, and recommend to the
Faculty of Graduate Studies for Acceptance, a thesis entitled,

"PHASE EQUILIBRIA IN GAS HYDRATE FORMING SYSTEMS IN THE
PRESENCE OF ELECTROLYTES OR METHANOL, AND ESTIMATION OF
INTERACTION PARAMETERS IN EQUATIONS OF STATE"

submitted by Petros Englezos in partial fulfillment of the requirements for the degree of
Doctor of Philosophy in Engineering.



Dr. P.R. Bishnoi, (Supervisor)
Department of Chemical & Petroleum Engineering



Dr. N.E. Kalogerakis
Department of Chemical & Petroleum Engineering



Dr. R.A. Heidemann
Department of Chemical & Petroleum Engineering



Dr. G. Karim
Department of Mechanical Engineering



Dr. P. Handa, (External)
National Research Council of Canada

Date June 19, 1990

ABSTRACT

Gas hydrates are solid crystalline materials formed by the inclusion of certain molecules into the voids created by a three dimensional network of water molecules. The water molecules are linked together with hydrogen bonds. There is a great interest in the academia and in the industry to know the physical properties and the conditions under which these compounds are formed. The present thesis deals with the determination of the equilibrium conditions in multicomponent systems capable of forming gas hydrates. Particularly, it is concerned with the experimental and theoretical determination of the inhibiting effect of electrolytes on the vapor-aqueous liquid-hydrate equilibrium conditions and on the calculation of the inhibiting effect of methanol.

A new experimental apparatus was designed and built. Its main component is a variable volume high pressure cell which is immersed in a temperature controlled bath. The cell is equipped with two marine-type windows made of plexiglas. The windows allow visual observation of the cell contents. The apparatus is shown to provide measurements which are reproducible and consistent with the measurements in other laboratories. Experimental equilibrium data for ethane hydrate formation in the presence of single and mixed electrolyte solutions of NaCl, KCl, CaCl₂ and KBr were obtained using this apparatus. Fifty experiments were performed at temperatures between 265.36 and 282.98 K. First, data on hydrate formation in pure water and in single electrolyte solutions were obtained. Second, data on hydrate formation in four solutions of binary

salt mixtures and a solution of the ternary salt mixture from NaCl, KCl and CaCl₂ were collected. Finally, a four-component aqueous solution was prepared and hydrate formation experiments were conducted.

A predictive method for calculating the incipient equilibrium formation conditions for hydrocarbon gas hydrates in the presence of single or mixed electrolytes was developed. The method utilizes the statistical thermodynamics model of van der Waals and Platteeuw to describe the solid hydrate phase, the electrolyte activity coefficient model of Pitzer or that of Meissner to describe the aqueous electrolyte solution and the Trebble-Bishnoi equation of state for the vapor phase. The method is able to predict very accurately all the available experimental data in the literature as well as all the data obtained in this work.

A method was also developed for the calculation of the inhibiting effect of methanol on the equilibrium hydrate formation conditions. The method is distinguished from another method available in the literature because it uses only an equation of state to model all the fluid phases instead of three different models. The predictions were found to agree well with the experimental data available in the literature. The method is also used to calculate the amount of methanol required to inhibit hydrate formation in a natural gas stream and to calculate the amounts of methanol distributed in the vapor and liquid phases.

In the above methods the accuracy of the predictions relies on the ability of the thermodynamic models to describe the phases. The use of adjustable parameters, called binary interaction parameters, in

equations of state improves dramatically their ability to represent the phase behavior of binary systems. In this work, a computationally efficient method for the estimation of these parameters is presented. It uses binary vapor-liquid equilibrium data and consists of a least squares estimation procedure to find the best combination of interaction parameters and a maximum likelihood estimation procedure to determine the statistically best parameter values. When three phase equilibrium data are available, they can easily be included in the parameter estimation database. The additional computational requirements are negligible. In addition, a constrained least squares interaction parameter estimation method was proposed. It enables the calculation of such parameters which when used in the thermodynamic model (equation of state) prevent the prediction of erroneous liquid phase separation. All the above estimation methods were illustrated with examples using the Trebble-Bishnoi equation of state.

Finally, the phenomenon of the supersaturation of the aqueous liquid phase with methane prior to methane hydrate nucleation was examined. An attempt was made to relate the limits of supersaturation with the liquid phase stability limits. In addition, tangent plane analysis for the identification of the phase behavior was performed for this system.

ACKNOWLEDGEMENTS

I wish to express my sincere gratitude to Dr. P. Raj Bishnoi, not only for his guidance, encouragement and advice during the thesis work but also for providing the academic freedom to pursue my scientific interests and for sharing frequently his wisdom. His suggestions and comments all these years covered matters beyond the borders of thermodynamics and chemical engineering and therefore are sincerely appreciated.

It was a great pleasure to work with Dr. Nicolas Kalogerakis. I thank him for his continuous interest and the time and advice he provided with tremendous enthusiasm during the thesis work.

I became fascinated with chemical thermodynamics and decided to do my Ph.D. work in this discipline after taking Dr. Heidemann's graduate course. For this reason and for the very useful discussions we had, I sincerely thank him.

Also, I thank Dr. Mark Trebble for the useful discussions we had.

The meticulous work by Adolf Kohl and the technical help by Ian Mikalson, Mike Grigg, Dan Fantini and Vince Kraus from the chemical engineering workshop and that by John McRae are greatly appreciated.

Thanks are also due to Norma Wilson, Jeanie Streets, Judy McDonald and Sherry Flynn for their help which they always provided with a smile.

Thanks to Mr. Pankaj Dholabhai for a very good cooperation and also to all the graduate students I have worked with during my studies.

Several organizations contributed to the successful completion of this thesis.

The financial support provided by the scholarship trusts of *Alberta Research Council* and *Izaak Walton Killam Memorial* is sincerely appreciated.

Also, I acknowledge the financial support from the *Natural Science and Engineering Research Council of Canada* (NSERC), the NSERC - Strategic and the *Energy Mines and Resources, Canada*.

I sincerely thank my uncle Chris Antonopoulos and his family for their love, help and support.

I am especially indebted to my wife Vangie for her love, understanding and companionship during my Ph.D. years. She endured with patience my obsession with research and the frustrations that come with it.

Finally, I express my deepest gratitude to my mother Maria and my brother Demetrios for their love, support and dedication.

Dedicated to my family:

my mother Maria, my brother Demetrios and my wife Evangelia.

TABLE OF CONTENTS

	Page
ABSTRACT	iii
ACKNOWLEDGEMENTS	vi
TABLE OF CONTENTS	ix
LIST OF TABLES	xiii
LIST OF FIGURES	xv
LIST OF SYMBOLS	xx
1. INTRODUCTION	1
1.1 Gas Hydrates	1
1.2 Thermodynamics of Gas Hydrates in the Presence of Inhibitors	5
1.2.1 Experimental Studies	6
1.2.2 Computational Studies	9
1.3 Scope of the Study	13
2. BACKGROUND AND ANALYSIS OF HYDRATE PHASE EQUILIBRIA COMPUTATIONS AND RESEARCH OBJECTIVES	16
2.1 Phase Equilibrium in Gas Hydrate Forming Systems	16
2.2 Thermodynamic Models	17
2.2.1 Hydrate Phase	17
2.2.2 Vapor Phase	22
2.2.3 Aqueous Liquid Phase	24
2.3 Predictive Methods for Incipient Hydrate Formation Conditions	26
2.3.1 Gas Hydrate Formation in Pure Liquid Water	26

2.3.2	Gas Hydrate Formation in the Presence of Inhibitors	28
2.4	Flash Calculations in Systems Containing Gas Hydrates	30
2.5	Interaction Parameter Estimation for Equations of State	32
2.5.1	Problem Statement for Binary VLE Data Regression	37
2.5.2	Estimation Methods	39
2.6	Research Objectives	42
3.	PREDICTION OF THE INCIPIENT HYDRATE FORMATION CONDITIONS IN AQUEOUS ELECTROLYTE SOLUTIONS	45
3.1	Methodology	45
3.2	Activity of Water	47
3.2.1	Single Electrolyte Solutions	48
3.2.2	Mixed Electrolyte Solutions	50
3.3	Results and Discussion	51
4.	PREDICTION OF THE INCIPIENT HYDRATE FORMATION CONDITIONS IN THE PRESENCE OF METHANOL	58
4.1	Methodology	58
4.1.1	Computational Procedure	61
4.2	Results and Discussion	63
4.3	Methanol Dehydration Unit	84
5.	EXPERIMENTAL APPARATUS AND PROCEDURE	88
5.1	Background on Gas Hydrate Experimental Methods	88
5.1.1	Visual Methods	89

5.1.2	Non-visual Methods	96
5.1.3	Experimental Data Using the Kinetics Apparatus	96
5.2	Design of a New Experimental Apparatus	100
5.2.1	Apparatus	100
5.2.2	The Equilibrium Cell	103
5.3	Experimental Procedure	108
5.4	The Validity of the Experimental Apparatus and the Procedure	110
6.	EXPERIMENTAL RESULTS	112
6.1	Experimental Data with the New Experimental Apparatus	112
7.	GIBBS FREE ENERGY ANALYSIS OF THE CH ₄ -H ₂ O SYSTEM	121
7.1	Solubility of Methane in Water, Supersaturation and Nucleation	121
7.1.1	Limits of Stability for the Methane-Water System	125
7.2	Gibbs Free Energy Analysis for the Phase Behavior	128
7.2.1	Gibbs Free Energy Change of Mixing	128
7.2.2	Results and Discussion	130
8.	INTERACTION PARAMETER ESTIMATION IN EQUATIONS OF STATE USING BINARY VLE DATA	138
8.1	Unconstrained Estimation	138
8.1.1	Proposed Implicit Least Squares Estimation Procedure	138
8.1.2	Proposed Implicit Maximum Likelihood Estimation	

	Procedure	139
8.1.3	Computation of the Parameter Estimates	142
8.1.4	Numerical Results and Discussion	143
8.2	Constrained Least Squares Estimation	152
8.2.1	Prediction of Erroneous Liquid Phase Separation	152
8.2.2	Formulation of the Constrained Estimation Problem	157
8.2.3	Proposed Solution Method	159
8.2.4	Computational Algorithm	161
8.2.5	Numerical Results and Discussion	163
8.2.6	A Systematic Approach to the Interaction Parameter Estimation Problem in Equations of State	175
9.	SIMULTANEOUS REGRESSION OF BINARY VLE AND VLLE DATA	183
9.1	Introduction and Problem Statement	183
9.2	Proposed Implicit ML and LS Estimation Procedures	184
9.3	Simultaneous Regression of Binary VLE and VLLE Data	187
9.4	Numerical Results and Discussion	188
9.4.1	Effect of Inconsistent Data	195
10.	CONCLUSIONS AND RECOMMENDATIONS	202
10.1	Conclusions	202
10.2	Recommendations	205
	REFERENCES	207

LIST OF TABLES

<i>Table</i>	<i>Title</i>	<i>Page</i>
1.1	Physical Properties of Hydrate Lattices	2
2.1	Reported Values for the Thermodynamic Reference Properties of Gas Hydrates	23
4.1	Binary Interaction Parameters for the Trebble-Bishnoi EOS	60
4.2	Molar Composition of the Natural Gas Mixtures	77
4.3	Equilibrium Phase Compositions for the CO ₂ -H ₂ O-CH ₃ OH System	78
4.4	Equilibrium Phase Compositions for a Multicomponent Gas- Water-Methanol System	79
4.5	Equilibrium Phase Compositions for a Multicomponent Gas- Water-Methanol System	80
4.6	Equilibrium Phase Compositions for the CH ₄ -H ₂ O-CH ₃ OH System	81
4.7	Equilibrium Phase Compositions for the Ethane - Water - Methanol System	82
4.8	Equilibrium Phase Compositions for the Propane - Water Methanol System	83
4.9	Water and Methanol Flows per One Million Moles of Dry Natural Gas II	87
5.1	Experimentally Determined Methane Hydrate Formation Pressures in the Presence of Aqueous Solutions of Sodium Chloride and Potassium Chloride	98

6.1	Experimental Data on Ethane Hydrate Formation Pressures in Pure Water	114
6.2	Experimental Data on Ethane Hydrate Formation Pressures in Aqueous Solutions of Single Salts	115
6.3	Experimental Data on Ethane Hydrate Formation Pressures in Aqueous Solutions of Mixed Salts	116
6.4	Experimental Data on Ethane Hydrate Formation Pressures in Aqueous Solutions of Mixed Salts	117
7.1	Experimental Mole Fractions of Methane at Nucleation, Two Phase Equilibrium Mole Fractions and Limits of Stability	124
7.2	Experimental and Calculated Solubilities of Methane in Water	126
8.1	Parameter Estimates for the Methane-Methanol System.	144
8.2	Parameter Estimates for the CO_2 - CH_3OH System.	147
8.3	Parameter Estimates for the Propane-Methanol System.	150
8.4	Binary Interaction Parameter Estimates for the CO_2 - <i>n</i> -Hexane System.	165
8.5	Binary Interaction Parameter Estimates for the <i>n</i> -Hexane-Ethanol System.	170
9.1	Interaction Parameters for the H_2S - H_2O System Using the VLE and VLLE Data by Selleck et al. (1952)	189
9.2	Interaction Parameters for the H_2S - H_2O System Using the VLLE Data by Carroll and Mather and the Correct VLE Data by Selleck et al.	197
9.3	Root Mean Square Deviations in Three Phase Equilibrium Calculations	201

LIST OF FIGURES

<i>Figure</i>	<i>Title</i>	<i>Page</i>
1.1	Cavities and Unit Cells for Gas Hydrate Structures	3
1.2	Experimental and Calculated Incipient Hydrate Formation Conditions for C_2H_6 and the Inhibiting Effect of CH_3OH	7
2.1	Equilibrium Phase Fractions for a Condensate-Water System at 278 K (Bishnoi et al. 1989a)	33
2.2	Vapor Liquid Equilibrium Calculations for the Methane - Methanol System	35
3.1	Experimental and Predicted Pressures for Methane Hydrate Formation in Aqueous Sodium Chloride Solution	52
3.2	Experimental and Predicted Pressures for Propane Hydrate Formation in Aqueous Sodium Chloride Solution	54
3.3	Experimental and Predicted Pressures for Cyclopropane Hydrate Formation in Aqueous KCl and $CaCl_2$ Solutions	56
4.1	Computational Flow Diagram	62
4.2	Inhibiting Effect of Methanol on Methane Hydrate Formation	65
4.3	Inhibiting Effect of Methanol on Propane Hydrate Formation	66
4.4	Inhibiting Effect of Methanol on CO_2 Hydrate Formation	67
4.5	Inhibiting Effect of Methanol on Hydrate Formation from a Mixture of 89.51 mole % Methane and 10.49 mole % Ethane	68
4.6	Inhibiting Effect of Methanol on Hydrate Formation from a Mixture of 95.01 mole % Methane and 4.99 mole % Propane	70

4.7	Inhibiting Effect of Methanol on Hydrate Formation from a Mixture of 91.12 mole % Methane and 8.88 mole % Propane	71
4.8	Inhibiting Effect of Methanol on Hydrate Formation from a Mixture of 90.09 mole % Methane and 9.91 mole % CO ₂	72
4.9	Inhibiting Effect of Methanol on Hydrate Formation from a Mixture of 69.75 mole % Methane and 30.25 mole % CO ₂	73
4.10	Inhibiting Effect of Methanol on Hydrate Formation from Natural Gas Mixture I	75
4.11	Inhibiting Effect of Methanol on Hydrate Formation from Natural Gas Mixture II	76
4.12	Methanol Dehydration Unit	86
5.1	The Experimental Apparatus for Hydrate Kinetic Studies	94
5.2	The Constant Volume High Pressure Cylindrical Cell	95
5.3	Experimental and Predicted Pressures for Methane Hydrate Formation in Aqueous Solutions of NaCl and a Mixture of NaCl and KCl	99
5.4	Block Diagram of the Experimental Apparatus	101
5.5	Schematic of the Experimental Apparatus	102
5.6	A Cross Section of the Equilibrium Cell	104
5.7	A Cross Section of the Equilibrium Cell	105
5.8	The Stirring Mechanism Assembly	107
5.9	Comparison of the Experimental Data Obtained in this Work and the Data of Other Workers	111
6.1	Experimental Data and Predicted Ethane Hydrate Formation Pressures in Aqueous Salt Solutions	118

6.2	Experimental Data and Predicted Ethane Hydrate Formation Pressures in Aqueous Salt Solutions	119
6.3	Experimental Data and Predicted Ethane Hydrate Formation Pressures in Aqueous Salt Solutions	120
7.1	Experimental Gas Consumption Curve for Methane Hydrate Formation in a Semi-batch Reactor Containing 300 cm ³ of Distilled and De-ionized Water	122
7.2	Gibbs Free Energy Change of Mixing for Methane-Water at 0.82 MPa and 274 K	132
7.3	Gibbs Free Energy Change of Mixing for Methane-Water in Liquid Phase, in the Vicinity of Zero Methane Mole Fraction	133
7.4	Gibbs Free Energy Change of Mixing for Methane-Water in Vapor Phase, in the Vicinity of Unity Methane Mole Fraction	134
7.5	Gibbs Free Energy Change of Mixing for Methane-Water in Hydrate Phase	135
7.6	Gibbs Free Energy Change of Mixing for Methane-Water at 2.88 MPa and 274 K	136
7.7	Gibbs Free Energy Change of Mixing for Methane-Water at 3.82 MPa and 274 K	137
8.1	Vapor-Liquid Equilibrium for the Methane-Methanol System	146
8.2	Vapor-Liquid Equilibrium for the CO ₂ - CH ₃ OH System	148
8.3	Vapor-Liquid Equilibrium for the Propane-Methanol System	151
8.4	Prediction of Erroneous Liquid Phase Separation Using the Interaction Parameters from Unconstrained LS Estimation	154
8.5	The Stability Function with Interaction Parameters	

from Unconstrained Least Squares Estimation for the CO ₂ - n-Hexane System	156
8.6 Selection of Lower Bound for ϕ	162
8.7 VLE Predictions for CO ₂ -n-Hexane with Interaction Parameters from Constrained Least Squares Estimation	166
8.8 The Stability Function with Interaction Parameters from Constrained Least Squares Estimation for the CO ₂ - n-Hexane System	167
8.9 The Minimum Value of the Stability Function at each Temperature with Interaction Parameters from ULS and CLS Estimation	168
8.10 VLE Predictions for the n-Hexane-Ethanol System with Interaction Parameters from Unconstrained LS Estimation	171
8.11 VLE Predictions for the n-Hexane-Ethanol System with Interaction Parameters from Constrained LS Estimation	172
8.12 The Minimum Value of the Stability Function at each Temperature with Interaction Parameters from ULS and CLS Estimation	173
8.13 Gibbs Free Energy Change of Mixing for the n-Hexane - Ethanol System	174
8.14 A Systematic Approach for the Interaction Parameter Estimation Problem in Equations of State	176
8.15 VLE Predictions for the n-Pentane-Acetone System.	179
8.16 The Minimum Value of the Stability Function at each Temperature with Interaction Parameters from ULS and	

	CLS Estimation	180
8.17	VLE Predictions for the Propane-Methanol System with Interaction Parameters from Constrained LS Estimation	181
9.1	VLE for the Hydrogen Sulfide-Water System. (—) Zero Interaction Parameters. (...) Parameters Obtained by Simultaneous LS Regression of Selleck's VLE and VLLE Data	191
9.2	VLE for the H ₂ S-H ₂ O System. (—) Parameters Obtained by ML Regression of Selleck's VLE Data. (...) Parameters Obtained by Simultaneous ML Regression of Selleck's VLE and VLLE Data	192
9.3	Three Phase Pressure-Temperature Locus for H ₂ S-H ₂ O. (—) Parameters from Simultaneous ML Estimation. (...) Parameters from ML Estimation Using VLE Data. (- - -) Zero Interaction Parameters	194
9.4	VLE for the Hydrogen Sulfide-Water System. (—) Parameters Obtained by the ML Regression of Selleck's VLE and VLLE Data. (...) Parameters Obtained by the ML Regression of Selleck's Correct VLE Data and Mather's VLLE Data	198
9.5	Three Phase Temperature-Pressure Locus for H ₂ S-H ₂ O. (—) Parameters Obtained by the ML Regression of Selleck's VLE and VLLE Data. (- - -) Parameters Obtained by the ML Regression of Selleck's Correct VLE Data and Mather's VLLE Data	200

LIST OF SYMBOLS

a_w	activity of water
a, b, c, d	equation of state parameters
A, B	fitted constants in Eq. 5
C	Langmuir constant, 1/MPa
C^*	constant in Eq. 6
C_p	heat capacity, J/mol K
e	residual vector (VLE data regression)
f	fugacity, MPa
G	Gibbs free energy
h	enthalpy, J/mol
H	enthalpy, J/mol
I	ionic strength
$\mathbf{k} = (k_a, k_b, k_c, k_d)^T$	EOS interaction parameter vector
L_h	hydrocarbon liquid
m	molality
M	number of VLLE data points
n	number of moles
N	number of VLE data points
N_s	number of components in a system
N_h	number of hydrate forming components
P	pressure, MPa
Q	weighting matrix for VLE residuals
Q^*	constant in Eq. 6

r	radial distance from center of cavity, m
\mathbf{r}	residual vector (VLLE data regression)
R	universal gas constant, J/mol K
R_i	type i cavity radius, m
T	temperature, K
\mathbf{u}	vector of "precisely" known parameters
\mathbf{V}	covariance matrix
V	volume, m^3
v	molar volume, m^3/mol
\mathbf{W}	weighting matrix for VLLE residuals
$W(r)$	cell potential function, J
x	liquid mole fraction
y	vapor mole fraction
\mathbf{z}	vector of state variables
z_+, z_-	ion charges

Greek Letters

β	constant in Eq. 8
γ	activity coefficient
$\delta_o, \delta_1, \delta_2$	Pitzer's model adjustable parameters
ε	vector of measurement errors
ζ	hydrate mole fraction
η_1, η_2	independent variables
θ	degree of occupancy in hydrate cavities

θ	degree of occupancy in hydrate cavities
κ	Boltzman's constant, J/K
λ	weighting factor (chapter 9)
λ	Langrange multiplier (chapter 8)
μ	chemical potential, J/mol
ν	stoichiometric number of moles
ν_i	number of cavities of type i
ξ	positive constant (chapter 8)
ξ_1, ξ_2	dependent variables (chapter 2)
π	ratio of circle's periphery to the diameter
ρ_1, ρ_2	constants defined in Eqns 40, 41
σ	standard deviation
Σ	variance-covariance matrix
ϕ	stability function

Subscripts

el	electrolyte
eq	V-H-L equilibrium conditions (chapter 7)
exp	experimental
i	index
j	index
k	index
LS	least squares

ML	maximum likelihood
mx	mixing
T _x	temperature, liquid mole fraction
TP	temperature, pressure
w	water

Superscripts

*	Vapor-liquid metastable equilibrium conditions
calc	calculated
I	liquid-I
II	liquid-II
j	index
H	hydrate
L	liquid
L ^o	pure liquid water
mix	mixing
MT	empty lattice
o	reference conditions of 273.15 K and zero absolute pressure
o	pure component state (in chapter 7)
V	vapor
VL	vapor-liquid
VLL	vapor-liquid-liquid
^	experimental

Πάντα ρεῖ, πάντα χωρεῖ, οὐδὲν μένει, δις εἰς τὸν αὐτὸν ποταμὸν οὐκ ἂν εμβαίῃς.
Everything flows and nothing stays, you can't step twice into the same river.

Heraclitus, 6th century B.C.

Προαιρεῖσθαι τε δεῖ ἀδύνατα εἰκότα μᾶλλον ἢ δυνατὰ ἀπίθανα.
Probable impossibilities are to be preferred to improbable possibilities.

Aristotle, 384-322 B.C.

Tempora mutantur, et nos mutamur in illis.
Times change, and we change with them.

Emperor Lothar, 795-855.

Il n'existe pas de sciences appliquees, mais seulement des applications de la science.

Louis Pasteur, 1822-1895.

Let the good not be the enemy of the best.

Professor Peter Danckwerts.

Every aspect of nature may be approached by poetry or experiment as well as by reason, and indeed such is the usual order in history.

C. Truesdell, Rational Thermodynamics.

1. INTRODUCTION

1.1 Gas Hydrates

Gas hydrates are aqueous clathrates. The term is applied to the crystals which are formed by the combination of water with many gases and volatile liquids. The water molecules through hydrogen bonding are capable of forming a three dimensional lattice-like structure containing cavities. These cavities can be occupied by molecules of gases and volatile liquids whose molecular diameter is smaller than the diameter of the cavity. By the inclusion of these molecules, the structure by itself thermodynamically unstable is stabilized. Each cavity structure (polyhedron) may contain one guest molecule. The interaction between the host water molecules and the guest gas molecule is not chemical and appears to be primarily of the van der Waals type, even for polar guest molecules.

The gas hydrates, from a thermodynamic viewpoint, may be considered as solid solutions of guest molecules in the host water lattice. Therefore, they are nonstoichiometric compounds. The gas hydrates are formed in two cubic structures (I and II). The properties of hydrate lattices are summarized in Table 1.1. In Figure 1.1 the unit cells and individual cavities of gas hydrate structures are shown. Detailed information about the physical properties of hydrates as well as their technological significance and environmental implications can be found in four books (Davidson, 1973; Makogon, 1981; Berez and Balla-Achs,

Table 1.1 Physical Properties of Hydrate Lattices.

	<i>Structure I</i>	<i>Structure II</i>
Number of Cavities per Unit Cell		
<i>Small</i>	2	16
<i>Large</i>	6	8
Cavity Radius, Å		
<i>Small</i>	3.97	3.91
<i>Large</i>	4.30	4.73
Number of Molecules of Water per Unit Cell	46	136
Typical Hydrate Forming Gases	CH_4 , C_2H_6 C_2H_4 , CO_2	C_3H_8 , $i-C_4H_{10}$

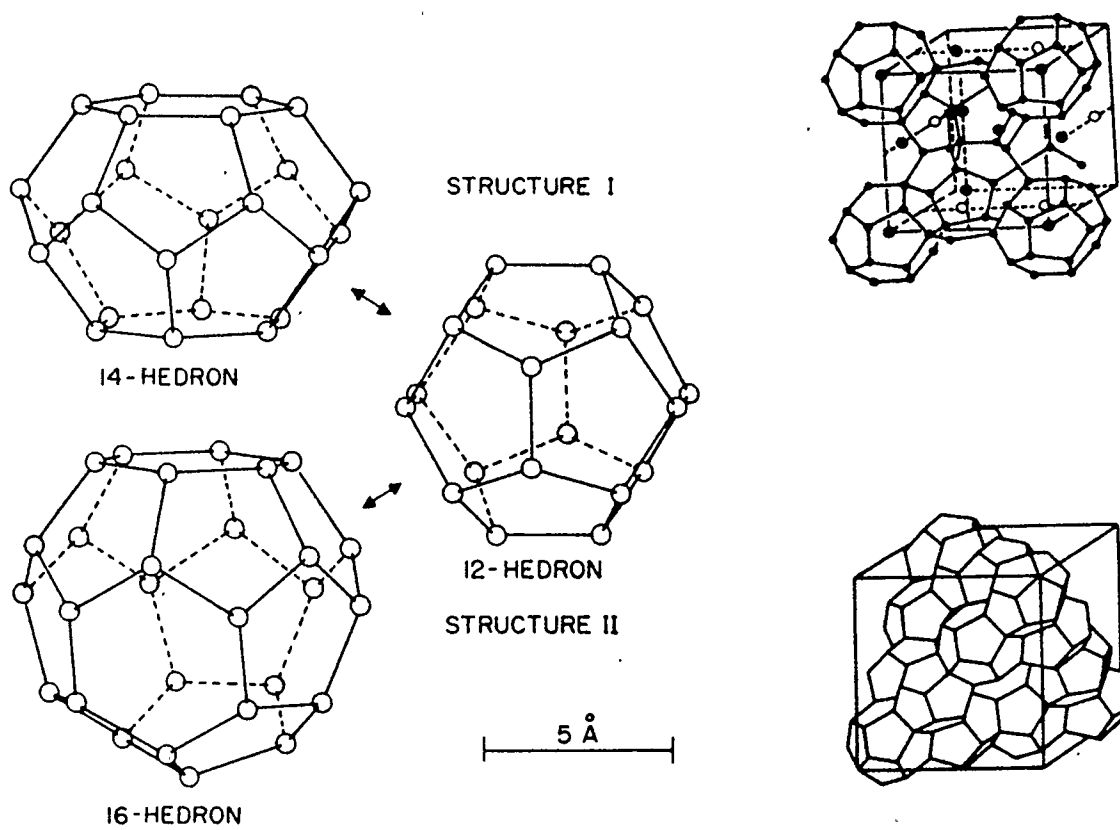


Figure 1.1 Cavities and Unit Cells for Gas Hydrate Structures

1983; Sloan, (1989), in a recent review (Holder et al. 1988), and in a French scientific journal (Makogon, 1987).

The natural gas components like methane, ethane, propane etc. are known to form gas hydrates. They have significant technological importance. Because of their solid nature, gas hydrates may block hydrocarbon transportation lines and plug process piping, valves, orifice plates, chokes, wellheads and flowlines. Recently, Barker and Gomez (1989) reported two case histories of deep water hydrate occurrence and the problems encountered in drilling operations. Hammerschmidt (1934) showed that the blocking of natural gas transportation lines was due to hydrate formation. That was the point where hydrates ceased to be of academic interest only and the oil and gas industry became actively involved in gas hydrates research. The interest was directed towards knowing the equilibrium hydrate forming conditions for natural gases and establishing methods to prevent hydrate occurrence. A common industrial practice is to use inhibiting agents to prevent the hydrate formation. Electrolytes and alcohols such as methanol suppress the formation of hydrates.

Gas hydrate formation also presents an opportunity for designing useful processes. For example, it offers the possibility of developing water desalination, gas storage and gas separation facilities (Knox et al. 1961; Barduhn et al. 1962; Roo et al. 1983; Berecz and Balla-Achs, 1983; Sloan, 1989). Hydrates of natural gas are also an energy resource. Huge quantities of natural gas in the hydrate state exist in the permafrost regions of the world and on ocean floors. These hydrate

reserves could be used for the recovery of the gas under a proper economic environment (Makogon, 1981; 1987; Sloan, 1989).

Chemical and petroleum engineers are primarily interested to know the equilibrium conditions for hydrate formation for a given hydrocarbon-water mixture in the absence or presence of inhibitors like electrolytes or alcohols. Also they are interested to examine the factors affecting the nucleation of hydrate crystals and the rate of formation and decomposition. The phenomena associated with the kinetics of gas hydrate formation and decomposition have only recently been investigated (Vysniauskas and Bishnoi, 1983; 1985; Kim et al., 1987, Englezos et al., 1987a; 1987b; Smirnov, 1987; Englezos et al., 1990a; Bishnoi et al., 1989b).

Extensive experimental and theoretical equilibrium studies for many gas hydrate forming substances and their mixtures in the absence of inhibiting substances have been carried out. On the other hand, systematic experimental studies for hydrate formation in the presence of inhibitors have only recently appeared. These data are useful for the validation of computational methods for the prediction of hydrate equilibria and in the design of industrial processes. In the present work, the equilibrium in the presence of inhibitors is studied.

1.2 Thermodynamics of Gas Hydrates in the Presence of Inhibitors

One of the most important aspects of the thermodynamics of gas hydrates is the determination of the incipient hydrate formation

conditions both experimentally and theoretically. In Figure 1.2 the experimental and calculated incipient hydrate formation conditions for ethane are shown (Englezos et al. 1990b). The parameters for the curves are methanol concentration in the liquid phase expressed in weight percent. The inhibiting action of methanol is evident. At a given pressure the temperature at which hydrates are formed becomes lower with the addition of methanol or at a given temperature hydrates begin to form at a higher pressure. The magnitude of the temperature depression or pressure rise depends on the amount of the inhibitor.

During the five decades following Hammerschmidt's observation regarding the blocking of natural gas transmission lines, an enormous effort has been devoted to hydrate thermodynamics research in industry and academia. The main objective was to provide data like those shown in the figure and also generalized predictive methods and correlations for computing the curves similar to the ones shown in Figure 1.2. It is noted that the majority of these studies has focused on hydrate formation from pure water. The four books which were cited earlier provide a systematic and detailed source of these studies. In addition, the review by Byk and Fomina (1968) is also very informative.

1.2.1 Experimental Studies

A large number of experimental data similar to those shown in Figure 1.2 have been collected. Recently, Holder et al. (1988) and Sloan (1989) have published literature surveys about the experimentally

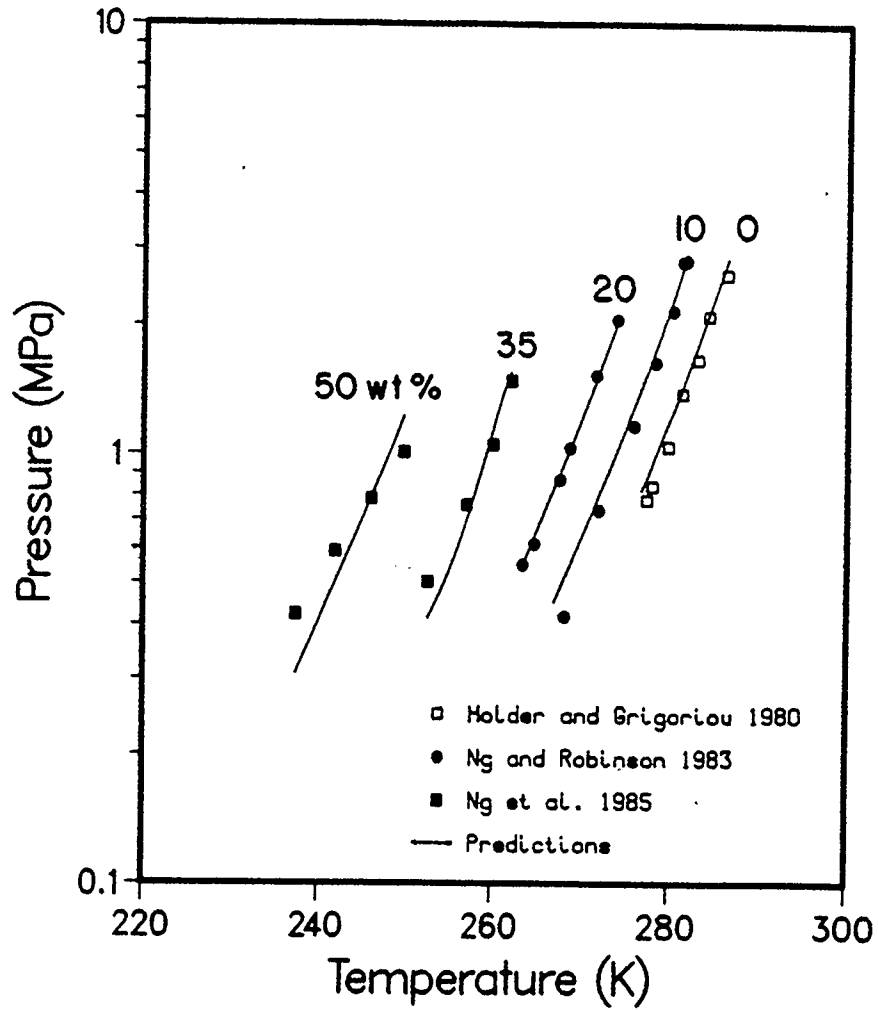


Figure 1.2 Experimental and Calculated Incipient Hydrate Formation Conditions for C_2H_6 and the Inhibiting Effect of CH_3OH

investigated hydrate forming systems. The majority of the experimental studies were focused on the formation from pure water. In the present work only the experimental studies concerning the inhibiting effects of electrolytes and methanol will be mentioned. However, reference to several experimental studies for hydrate formation in pure water will be given in the section describing the various experimental procedures in chapter 5.

The inhibiting effect of various organic and inorganic chemicals on hydrate formation was studied first by Hammerschmidt (1939). Deaton and Frost (1946) presented incipient hydrate formation curves for natural gases in the presence of methanol, NaCl, CaCl₂, NH₃ and ethanol. These graphs were useful for pipeline and other design purposes by the then fast growing U.S oil and gas industry. Bond and Russell (1949) studied hydrogen sulfide hydrate formation in the presence of methanol, NaCl and CaCl₂. Kobayashi studied methane hydrate formation in the presence of ethanol and NaCl aqueous solutions (Sloan, 1989). Significant experimental work has also been carried out in the Soviet Union (Makogon, 1981) and Hungary (Berecz and Balla-Achs, 1983).

Systematic experimental studies on the effect of methanol and ethylene glycol have only recently been presented (Menten et al. 1981; Ng and Robinson, 1983; 1984; Ng et al. 1985; 1987). Experimental studies on the inhibiting effect of electrolytes have been carried out by Knox et al. (1961), Menten et al. (1981), Roo et al. (1983), Kubota et al. (1984), and Paranjpe et al. (1987). In these studies the effect of only single salts, mainly NaCl or KCl, was studied.

The corrosive action of the aqueous electrolyte solutions prevented their wide use as inhibiting agents. However, possible development of water desalination and underground gas storage facilities were the reasons for obtaining the above mentioned hydrate formation data. Since the natural environment of hydrate occurrence is usually seawater or groundwater, which contains a number of salts, and also the drilling muds contain mixtures of various salts, there is a need to obtain experimental hydrate formation data in the presence of mixed electrolytes. Such data have been obtained recently in our laboratory (Dholabhai, 1989; Englezos et al. 1990a).

1.2.2 Computational Studies

Significant effort has also been devoted to the development of methodologies for the calculation of the equilibrium hydrate formation conditions. The first computation method was based on the distribution coefficient or K-value concept and it was introduced by Wilcox, Carson and Katz (1941). Another method at that time was proposed by Professor Katz (Sloan, 1989). One can estimate the hydrate formation pressure given the temperature and gas gravity.

The breakthrough in calculating hydrate forming conditions occurred with the presentation of a statistical mechanical model for the chemical potential of water in the hydrate phase (van der Waals and Platteeuw, 1959). The model uses the Lennard-Jones potential to describe the interaction of a gas molecule with the water molecule of the lattice.

McKoy and Sinanoglu (1963) used the Kihara potential. Parrish and Prausnitz (1972) were the first to present an algorithm for the calculation of the incipient hydrate formation conditions for gas mixtures. Subsequently, the algorithm was improved by Holder et al. (1980). Ng and Robinson (1976; 1977) extended the calculation procedure to the hydrate formation in condensed systems. They also proposed an empirical correction to the van der Waals-Platteeuw model in order to improve the predictions for gas mixtures.

The above mentioned algorithm is suitable for calculating the incipient hydrate formation conditions in pure water. It does not account for the effect of inhibitors like methanol and salts. Hammerschmidt (1939) proposed an empirical equation for the calculation of the depression effect of alcohols. It is widely used in the industry although its reliability is variable (Ng and Robinson, 1985).

Anderson and Prausnitz (1986) presented a thermodynamics based method for calculating the inhibiting effect of methanol. Methanol is not incorporated in the hydrate lattice (Davidson, 1981). Hence, they were able to use the van der Waals-Platteeuw model to describe the hydrate phase. They used the Redlich-Kwong equation of state (Redlich and Kwong, 1948) for the vapor phase, the UNIQUAC activity coefficient model for the liquid phase and Henry's constants for the calculation of the fugacities of components in their supercritical state (N_2 and CH_4) in the liquid phase. Furthermore, empirical correlations were used for calculating the molar volumes, partial molar volumes at infinite dilution and the fugacities of hypothetical liquid water below the

ice-point temperature.

In order to avoid using so many thermodynamic models, the use of an equation of state to describe all the fluid phases seems to be the proper approach. Englezos et al. (1990b) utilized the Trebble-Bishnoi equation of state (Trebble and Bishnoi, 1987; 1988). The calculated results generally compare very well with the experimental data.

For the calculation of the hydrate forming conditions from aqueous single salt solutions a method was proposed by Menten et al. (1981). It is based on calculating the activity of water by using freezing point depression data. However, this method of calculating the activity of water is not accurate enough and cannot be extended to mixed salt solutions. Englezos and Bishnoi (1988a) presented a computer implementable methodology for the prediction of hydrate formation conditions in systems containing light hydrocarbon gases and aqueous solutions of single or mixed electrolytes. The method does not require any adjustable parameters and predicts all the available experimental data very well (Englezos and Bishnoi, 1988a; Dholabhai et al. 1990).

In addition to incipient hydrate formation calculations, situations may arise where we need to know the amount and type of hydrates formed from a multicomponent mixture. Bishnoi et al. (1989a) presented a methodology for the isobaric-isothermal flash calculations for systems containing solid hydrates in addition to fluid phases. The hydrate is treated as a solid solution. Mole fractions of the components present in the lattice can be defined appropriately. They will be given in a later chapter. It is noted that the multiphase-multicomponent flash problem

was solved by a novel methodology proposed by Gupta (Gupta, 1989).

Another important aspect of the hydrate thermodynamics is the calculation of the water concentration of a hydrocarbon vapor or liquid in equilibrium with hydrates. Experimental data and calculation methods were presented by Sloan et al. (1976) for methane hydrate, by Song and Kobayashi (1982) for methane-propane hydrate, by Sloan et al. (1987) for ethane, propane liquid hydrate equilibrium, and by Song and Kobayashi (1987) for carbon dioxide hydrate.

Relevant to the problem of developing predictive methods for hydrate equilibria is the problem of interaction parameter estimation for thermodynamic models. These models utilize adjustable parameters in order to improve their correlational and predictive capabilities. The parameters are usually obtained from the regression of phase equilibrium data. The models are nonlinear in these parameters and as a result, iterative techniques are used for the solution of the estimation problem. In this work, the modelling of the fluid phases is done with the Trebble-Bishnoi equation of state. This model can utilize up to four binary interaction parameters. Using this equation of state for evaluation purposes, Englezos et al. (1989a; 1990c) presented a computationally very efficient method for the estimation of interaction parameters particularly suitable for models with more than one such parameters.

Finally, a better insight on hydrate formation has been gained by calculating the stability limits of the liquid phase for the methane-water system (Englezos and Bishnoi, 1988b).

1.3 Scope of the Study

The central theme of the thesis is phase equilibrium in gas hydrate forming systems in the presence of electrolytes and methanol. Particularly, experimental and computational studies are presented for hydrate-vapor-aqueous liquid equilibrium. The approach taken is based on classical thermodynamics. The following objectives were identified:

- (a) Design and construction of a new apparatus for the study of hydrate equilibria, and collection of experimental data on hydrate formation in aqueous mixed electrolyte solutions. Such data are not available in the literature.
- (b) Development of efficient computational methodologies for the prediction of the incipient hydrate formation conditions in the presence of electrolytes or methanol.
- (c) Development of statistically based and computationally efficient interaction parameter estimation procedures for equations of state.
- (d) Application of the thermodynamic stability theory to gas hydrate nucleation.

In chapter 1 the reader is introduced to the subject of gas hydrates. Background information on the thermodynamics of gas hydrate forming systems is given.

In chapter 2 the specific research objectives of the thesis are delineated. However, before that the phase equilibrium problem is defined, the thermodynamic models and previous solution methods are presented. In addition, the problem of interaction parameter estimation for equations of state is stated together with the background information on the subject.

In chapters 3 and 4 the proposed predictive methodologies for the incipient hydrate formation in the presence of electrolytes and methanol respectively, are presented. An important design problem, a methanol dehydration unit, is also presented together with other results.

The experimental design of the new apparatus, the procedure to perform the experiments, the experimental data as well as a survey of the experimental methods are presented in chapters 5 and 6.

In chapter 7 the stability analysis and the tangent plane analysis of the phase behavior for the methane-water system are presented.

In chapter 8 procedures for efficient interaction parameter estimation for equations of state are proposed and evaluated using the Trebble-Bishnoi equation of state. Vapor liquid equilibrium (VLE) data are used for the estimation. In addition, a methodology is presented for the calculation of binary interaction parameters for equations of state subject to liquid phase stability requirements. Based on these estimation methods, a practical approach for the efficient estimation of

binary interaction parameters for equations of state is presented. The approach is particularly suitable for equations of state with more than one binary interaction parameters.

In chapter 9 the estimation procedures for VLE data are extended in order to be used for binary vapor liquid liquid equilibrium (VLLE) data.

Finally, conclusions and recommendations for further work are presented in chapter 10.

2. BACKGROUND AND ANALYSIS OF HYDRATE PHASE EQUILIBRIA COMPUTATIONS AND RESEARCH OBJECTIVES

In this chapter an analysis of the problem of determining the phase equilibria in a multicomponent system capable of forming gas hydrates is presented. The problem is defined and the appropriate background is provided. In particular, the thermodynamic models which are available for the description of the phases and the existing solution methods are presented. In addition, the background on the problem of interaction parameter estimation for equations of state is provided. The needs for new or improved thermodynamic models and solution methods are identified and the specific research objectives of the thesis are set.

2.1 Phase Equilibria in Gas Hydrate Forming Systems

In a multicomponent hydrate forming system the phases of aqueous liquid, ice, hydrocarbon liquid, vapor, hydrate of structure I and hydrate of structure II may be present. If the ice phase is present, it is assumed to be pure. When one is interested in the incipient hydrate formation conditions (i.e. the minimum pressure at a fixed temperature where the first hydrate crystals appear) then, depending on the hydrate forming components, either hydrate of structure I or II exists. The second hydrate structure requires a higher pressure to be formed. In the thesis, the hydrate phase, which may be I or II, is denoted by H.

At pressures above the quadruple point where vapor is absent and

the aqueous liquid, hydrocarbon liquid and hydrate phases coexist, the pressure changes sharply with only a slight increase in temperature. This happens because the phases are relatively incompressible and highly immiscible. Ng and Robinson (1976, 1977) measured phase equilibrium of this type and suggested a Clapeyron type equation to obtain the P-T locus. In this study the condensed hydrocarbon phase will not be included in the analysis. Natural gas type systems will be considered. Hence, the phases that constitute our system of study are: hydrate of structure I or II (H), aqueous liquid (L) and Vapor (V).

In a system of N_c components containing solid hydrate (H), vapor (V) and liquid (L) the thermodynamic equilibrium may be represented by

$$\mu_i^L = \mu_i^V \quad i=1,\dots,N_c \quad (1)$$

for all the N_c components, and by

$$\mu_j^H = \mu_j^L \quad j=1,\dots,N_h \quad (2)$$

for the N_h hydrate forming components including water.

2.2 Thermodynamic Models

2.2.1 Hydrate Phase

A statistical mechanical model (vdWP) was proposed by van der Waals

and Platteeuw (1959). It gives the chemical potential of water in the hydrate phase, μ_w^H , by the following equation

$$\mu_w^H = \mu_w^{MT} - RT \sum_{i=1}^2 v_i \ln \left(1 + \sum_{j=1}^{N_h} C_{ij} f_j \right) \quad (3)$$

where C_{ij} are the Langmuir type constants, v_i are the number of cavities of type i per water molecule in the lattice ($v_1 = 1/23$, $v_2 = 3/23$) and f_j are the fugacities of the various hydrate forming gases.

The Langmuir constants, C_{ij} , account for the gas-water interactions. If it is assumed that the cavities are spherical and that the water molecules which formed the cavity are smeared evenly over the surface of this sphere the Langmuir constants may be obtained from the following equation (John and Holder, 1982).

$$C_{ij} = \frac{4\pi}{\kappa T} \int_0^{R_i} \exp \left(\frac{-W_{ij}(r)}{\kappa T} \right) r^2 dr \quad (4)$$

In the above equation, W_{ij} , is the function for the cell potential at a radial distance r from the center of the cavity and R_i is the cell radius for type i cavity. van der Waals and Platteeuw (1959) used the Lennard-Jones 12-6 spherically symmetric cell potential to represent the binary interaction between a guest molecule and a water molecule of the cavity. McKoy and Sinanoglu (1963) found that better results could be obtained for predicting the hydrate formation conditions by using the Kihara potential function. The cell potential function, W_{ij} , is

calculated by summing the binary interactions of the gas molecule with each of the water molecules whose locations are known by X-ray diffraction studies. Instead of using second virial coefficient data to calculate potential parameters, Marshall et al. (1964) estimated the parameters for methane, nitrogen and argon by fitting experimental hydrate formation pressures. Parrish and Prausnitz (1972) fitted hydrate parameters for fifteen different gases and presented a computer implementable methodology for the prediction of incipient hydrate formation conditions for water-natural gas mixtures. Tester et al. (1972) calculated the integral in Eq. 4 by a Monte Carlo approach for the ice-hydrate-gas system.

For temperatures above 260 K, the Langmuir constants may be obtained alternatively from the following simple empirical correlation, developed by Parrish and Prausnitz (Parrish and Prausnitz, 1972).

$$C_{ij} = \frac{A_{ij}}{T} \exp\left(-\frac{B_{ij}}{T}\right) \quad (5)$$

where A_{ij} and B_{ij} are fitted parameters whose values are given by Parrish and Prausnitz. They reported an accuracy of 0.2 per cent for each hydrate forming gas when using Eq. 5 and comparing the calculated results with those obtained by using Eq. 4.

According to John and Holder (1981; 1982) a degree of spherical asymmetry exists in all cavities. Not only the nearest water molecules but more distant ones also affect the energy of the enclathrated molecule and hence the cell potential. In order to correct for the fact

that actual guest-host interactions depart from the spherical smooth cell potential, and to account for the change of the potential by the water molecules in other cavities, Holder and his co-workers introduced two corrections to the Langmuir constant calculation (John and Holder, 1982; Holder and John, 1983; John and Holder, 1985; John et al. 1985). The corrections account for all nonidealities in the molecular interaction between the enclathrated gas and hydrate lattice molecules. It was suggested that the Langmuir constants be calculated by using the following equation

$$C = C^*Q^* \quad (6)$$

The first constant, C^* , accounts for the change of the potential caused by the second and third shells of water molecules around the cavity of interest. The second constant, Q^* , accounts for the non-sphericity of the cavities and the hydrate forming molecules. This factor was fitted as a function of Kihara parameters. The intention was to keep the Kihara parameters very similar to those obtained by second virial coefficient and viscosity data. The above corrections to the vdWP model are considered promising towards improving the model and hence, the prediction of hydrate formation conditions (Sloan, 1989).

An empirical modification to the vdWP model was suggested by Ng and Robinson (1976). The purpose was to increase the accuracy of the predictions for binary mixtures of natural gas components. They introduced a correction parameter to account for the size differences in

the gas molecules. However, this empirical modification when applied to multicomponent gas mixtures does not give accurate results.

Recently, Istomin (1987) presented a model for gas hydrates taking into account the guest-guest interactions. Results were presented for xenon hydrate at 273 K.

The quantity, μ_w^{MT} , denotes the chemical potential of water in the empty hydrate lattice. This empty lattice is a hypothetical state. The chemical potential μ_w^{MT} is given by the following equation proposed by Holder et al. (1980)

$$\frac{\mu_w^{MT} - \mu_w^{L^{\circ}}}{R T} = \frac{\Delta\mu_w^{\circ}}{R T^{\circ}} - \int_{T^{\circ}}^T \frac{\Delta H_w^{MT-L^{\circ}}}{R T^2} dT + \frac{\Delta V_w^{MT-L^{\circ}} P}{R T} \quad (7)$$

In Eq. 7, $\Delta\mu_w^{\circ}$ is an experimentally determined quantity. It is the chemical potential difference between the empty hydrate and pure liquid water at the reference conditions of $T^{\circ} = 273.15$ K and zero absolute pressure. $\Delta H_w^{MT-L^{\circ}}$ and $\Delta V_w^{MT-L^{\circ}}$ are the enthalpy and volume differences respectively, between the empty hydrate lattice water and the liquid water. The temperature dependence of the enthalpy difference is given by the following equation

$$\Delta H_w^{MT-L^{\circ}} = \Delta H_w^{\circ} + \int_{T^{\circ}}^T [\Delta C_{p_w}^{\circ} + \beta (T - T^{\circ})] dT \quad (8)$$

ΔH_w° , $\Delta C_{p_w}^{\circ}$ are the enthalpy and heat capacity differences between the empty hydrate lattice and liquid water at the reference conditions. The

values for ΔH_w° , $\Delta C_{p_w}^\circ$ and β at the reference conditions have been regressed from hydrate formation experimental data and several different values for these parameters have been reported by various investigators. The parameter values and their literature source are summarized in Table 2.1. It is noted that the values for ΔH_w° are those reported in the literature for the difference between empty lattice and ice minus the heat of fusion of water, which was taken equal to 6011.0 J/mol.

Parrish and Prausnitz (1972) calculated the chemical potential difference, $\mu_w^{MT} - \mu_w^L$, with the aid of the properties of a reference hydrate. This was a tedious calculation procedure. Recently, Anderson and Prausnitz (1986) used Holder's correlation given by Eq. 7.

2.2.2 Vapor Phase

Electrolytes are assumed to be absent from the vapor phase and hence, any of the available equations of state or other suitable model can be used for the vapor. In the present work, the Trebble-Bishnoi equation of state (Trebble and Bishnoi, 1987; 1988) has been employed. This equation can utilize up to four binary interaction parameters and hence, has an increased correlational and predictive capability. The equation and its quadratic mixing rules are given below

$$P = \frac{R T}{v-b} - \frac{a}{v^2 + (b+c)v - (bc+d^2)} \quad (9)$$

where

Table 2.1 Reported Values for the Thermodynamic Reference
Properties of Gas Hydrates

Property	Structure I	Structure II	Reference
	1235 ± 10	-	Holder et al. 1980
$\Delta\mu_w^\circ$	1297	937	Dharmawardhana et al. 1980
(J/mol)	1264	883	Parrish and Prausnitz, 1972
	1299.5 ± 10	-	Holder et al. 1984
	1287	1068	Handa and Tse, 1986
	- 4327	-	Ng and Robinson, 1985
ΔH_w°	- 4622	- 4986	Dharmawardhana et al. 1980
(J/mol)	- 4860	- 5203.5	Parrish and Prausnitz, 1972
	- 4150	-	Holder et al. 1984
	- 5080	- 5247	Handa and Tse, 1986
$\Delta C_{p_w}^\circ$	- 38.13	- 38.13	Parrish and Prausnitz, 1972
(J/mol K)	- 34.583	- 36.8607	Holder and John, 1983
			John et al. 1985
β	0.141	0.141	Parrish and Prausnitz, 1972
(J/mol K ²)	0.189	0.1809	Holder and John, 1983
			John et al. 1985

$$a = \sum_i \sum_j x_i x_j \sqrt{(a_i a_j)} (1 - k_{a_{ij}}) \quad (10)$$

$$b = \sum_i \sum_j x_i x_j \left(\frac{b_i + b_j}{2} \right) (1 - k_{b_{ij}}) \quad (11)$$

$$c = \sum_i \sum_j x_i x_j \left(\frac{c_i + c_j}{2} \right) (1 - k_{c_{ij}}) \quad (12)$$

$$d = \sum_i \sum_j x_i x_j \left(\frac{d_i + d_j}{2} \right) (1 - k_{d_{ij}}) \quad (13)$$

2.2.3 Aqueous Liquid Phase

Although Sander et al. (1986) attempted to include electrolytes in the UNIQUAC model, there is not yet available a general thermodynamic model that will describe an aqueous liquid phase where electrolytes and other molecular species are simultaneously present. Consider, for example, the carbon dioxide-aqueous electrolyte system or the methane-methanol aqueous electrolyte system. Carbon dioxide and methanol have a substantial solubility in the aqueous liquid phase. The development of thermodynamic models for such systems is an open research area.

Therefore, in order to be able to describe the liquid phase two different cases are examined. First, the case where solubility of the gas hydrate forming substances can be ignored is considered. The liquid phase consists of liquid water and dissolved electrolytes. Second, the

case of aqueous solutions of molecular species without electrolytes is considered. Only molecular species are present in the liquid phase together with water.

(a) *Aqueous Electrolyte Solutions*

In this case, the liquid phase is an aqueous solution of electrolytes. In such a solution the solubilities of gases like methane, ethane, propane can be ignored because these gases are sparingly soluble in water and due to the salting out phenomenon they will be less soluble. Therefore, modelling of the liquid phase in this case is achieved by using any of the available electrolyte activity coefficient models. In the present work, Meissner's and Pitzer's models (Meissner and Kusik, 1972; Pitzer and Mayorga, 1973; Zemaitis et al. 1986) for the calculation of the activity of a single electrolyte in an aqueous solution were utilized. The activity of water in such a solution is then calculated by integrating the Gibbs-Duhem equation. In order to calculate the activity of water in a mixed electrolyte solution the predictive method proposed by Patwardhan and Kumar (1986) was used.

(b) *Aqueous solutions without electrolytes*

In this case, the liquid phase is an aqueous solution where molecular species like methanol exist in non-negligible amounts. For modelling the phase, an equation of state or an activity coefficient

model can be used. In this work the Trebble-Bishnoi equation of state was used for all the liquid phase thermodynamic calculations. The equation was also used to model the vapor phase.

2.3 Predictive Methods for Incipient Hydrate Formation Conditions

Incipient gas hydrate formation pressure (or temperature) at a given temperature (or pressure) is that pressure (or temperature) where an infinitesimal amount of hydrate is present. In order to calculate the incipient hydrate formation conditions, it is required to solve Eqns 1 and 2 together with the mass balance equations for each of the components in the vapor and liquid phases. It should be kept in mind that the mass of the hydrate phase is zero (incipient phase). These calculations can, however, be simplified as a result of the nature of the thermodynamic model for the gas hydrate.

A very important feature of the vdWP model, given by Eq. 3, is the fact that the fugacities, f_j , are equal to those in the gas phase. Hence, the isofugacity criteria for the hydrate forming components other than water are implicitly incorporated. As a result, the required equation for water is

$$\mu_w^H = \mu_w^L . \quad (14)$$

2.3.1 Gas Hydrate Formation in Pure Liquid Water

The calculation of the incipient hydrate formation conditions from pure water can be performed easily by the method originally proposed by Parrish and Prausnitz (Parrish and Prausnitz, 1972) and its improved versions (Ng and Robinson, 1976; 1977; Holder et al. 1980; Anderson and Prausnitz, 1986).

Parrish and Prausnitz (1972) were the first to use the vdWP model to develop a computer implementable algorithm for the calculation of the incipient hydrate formation conditions from light hydrocarbon gases. They considered the aqueous liquid phase as an ideal solution

$$\mu_w^L = \mu_w^{L^0} + RT \ln x_w \quad (15)$$

By inserting Eqns 3 and 15 into Eq. 14 and substituting the difference, $\mu_w^{MT} - \mu_w^{L^0}$, by that given with the aid of a reference hydrate the following equation is obtained (Parrish and Prausnitz, 1972)

$$\frac{\Delta V_w^{MT-L^0}}{R T} P + \psi_1(T) - \ln x_w - \sum_{i=1}^2 v_i \ln \left(1 + \sum_{j=1}^{N_h} C_{ij} f_j \right) = 0. \quad (16)$$

In the above equation $\psi_1(T)$ is a temperature function obtained from the correlation for the reference hydrate. Later, Holder suggested the use of Eq. 7 and thus simplified the calculations. At a given temperature the nonlinear Eq. 16 can be solved for pressure to obtain the incipient gas hydrate formation pressure. Eqns 1 are not needed to be solved

because the amount of water in the vapor is considered negligibly small and the mole fraction of water in the aqueous liquid is close to unity.

2.3.2 Gas Hydrate Formation in the Presence of Inhibitors

(a) *Effect of Methanol*

Recently, Anderson and Prausnitz (1986) treated the liquid phase as a real solution and used different models for the activities of water and the other dissolved species. They used the UNIQUAC model along with the Henry's law for CH_4 and N_2 . Molar volumes, partial molar volumes and the fugacity of hypothetical liquid water below the ice point were calculated by empirical correlations.

The incipient hydrate formation pressure is obtained by the following two step procedure:

- (a) At a fixed temperature a pressure is guessed and isothermal - isobaric vapor-liquid equilibrium flash calculations are performed
- (b) The chemical potential of water in the hydrate phase is calculated and checked whether it is equal to that in the liquid (or vapor) phase. If it is equal, then this is the incipient hydrate formation pressure at that temperature. Otherwise, another pressure is selected and the calculations are repeated until the above condition is satisfied.

In other words, the solution is achieved by solving Eqns 1 and Eq. 14 together with the mass balance equation for all the components in the vapor and liquid phase. This solution procedure is possible because: (a) the hydrate phase is incipient and (b) the hydrate thermodynamic model implicitly incorporates the vapor-hydrate equilibrium conditions.

Robinson and Ng (1987) have mentioned a commercial computer program which allows the calculation of the equilibrium hydrate formation conditions. However, the methodology of the calculations has not been described.

Parrish and Prausnitz (1972) and Anderson and Prausnitz (1986) used the Redlich-Kwong equation of state (Redlich and Kwong, 1948) for the vapor phase fugacity calculations. Ng and Robinson (1976; 1977) used the Peng-Robinson equation of state (Peng and Robinson, 1976).

(b) *Effect of Electrolytes*

In this case the chemical potential of water in the liquid phase is given by

$$\mu_w^L = \mu_w^{L^0} + RT \ln a_w, \quad (17)$$

where a_w is the activity of water.

If it is assumed that the mole fraction of the dissolved hydrate forming components in the liquid phase are negligible and that no other

dissolved material is present, then the activity of water can be calculated. Menten et al. (1981) used freezing point depression data for this purpose. This model for the activity of water was coupled with the algorithm of Parrish and Prausnitz for the equilibrium hydrate formation calculations. Using freezing point depression data for calculating the activity of water is not an accurate procedure especially for salt solutions where the molality is above one. In addition, such a method cannot be extended to the case of aqueous mixed electrolyte solutions.

2.4 Flash Calculations in Systems Containing Gas Hydrates

If we want to know the amount of hydrates formed, then the mass balance equations including the hydrate phase have to be solved together with the equilibrium equations. Bishnoi et al. (1989a) were the first to formulate and solve this problem in its general form by including all possible fluid and solid phases. In order to achieve, this the hydrate is treated as a solid solution and the mole fractions are defined appropriately as it is shown in the next paragraphs.

If θ_{ij} is the fraction of cavity of type i occupied by gas component j then

$$\theta_{ij} = \frac{C_{ij} f_j}{N_h + \sum_{k=1} C_{ik} f_k} \quad (18)$$

The hydrate phase composition on a water-free basis can be

calculated by use of

$$\zeta_j^* = \frac{\sum_{i=1}^2 v_i \theta_{ij}}{2 N_h} \quad (19)$$

$$\sum_{i=1}^2 v_i \sum_{k=1}^2 \theta_{ik}$$

The solid hydrate phase, is a solid solution. Hence, the mole fraction of a component j in the hydrate is given by

$$\zeta_j = \frac{\zeta_j^*}{1 + n_{wg}} \quad (20)$$

where n_{wg} is the ratio of water to gas molecules in the hydrate. This ratio is given by the following equation

$$n_{wg} = \frac{1}{2 N_h} \quad (21)$$

$$\sum_{i=1}^2 v_i \sum_{k=1}^2 \theta_{ik}$$

Hence, by combining Eqns 19, 20 and 21 we obtain

$$\zeta_j = \frac{\sum_{i=1}^2 v_i \theta_{ij}}{2 N_h} \quad (22)$$

$$\sum_{i=1}^2 v_i \sum_{k=1}^2 \theta_{ik} + 1$$

Eq. 22 was used to define the equilibrium distribution ratios for the components present in the hydrate in order to adapt Gupta's methodology (Gupta, 1989) for performing simultaneously the phase equilibrium, mass balance and stability calculations in a multiphase, multicomponent system containing gas hydrates. The additional benefit of performing flash calculations is the fact that an in depth understanding of the phase behavior of such complex systems is gained. In Figure 2.1 the equilibrium phase fractions for a condensate-water system at 278 K are shown (Bishnoi et al. 1989a).

2.5 Interaction Parameter Estimation for Equations of State

Most of the phenomenological models in science and engineering are nonlinear in their adjustable parameters. The best estimates of these parameters can be obtained by a method which correctly treats the statistical behavior of the measurement random errors of the observed quantities. As a result of the random measurement errors, the estimated parameters will be known with a certain degree of uncertainty. Furthermore, because of the measurement errors and the model inadequacies, it is not possible to represent the experimental data exactly using a model. A parameter estimation method which correctly utilizes all the available information will give the best fit of the model to the data and minimize the parameter uncertainty.

Traditionally, Least Squares (LS) estimation has been used to obtain the parameters. Statistically it is the correct method to use

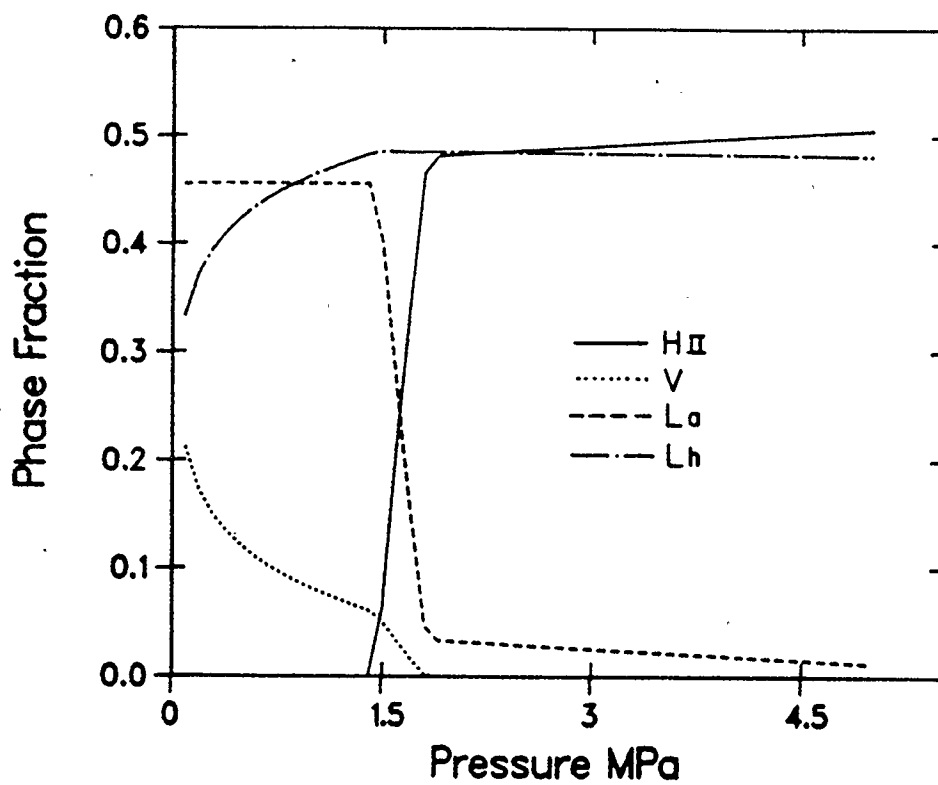


Figure 2.1 Equilibrium Phase Fractions for a Condensate-Water System at 278 K (Bishnoi et al. 1989a).

when the errors in the measurements are normally distributed with zero mean and constant variance. However, the error variances are not the same for each of the measured variables, and may differ from experiment to experiment significantly. A method that takes into account the errors in the measurements is based on the principle of maximum likelihood. Its general form as parameter estimator was introduced by Fisher (1922). It states that the parameters should be chosen so as to make the experimental observations appear to be the most likely when taken as a whole. In order to apply the method, a probability density function should be chosen for the variables. Usually the distribution of a measured variable about its true value is closely approximated by the normal distribution.

Equations of state are extensively used for the calculation of high pressure phase equilibria and/or properties of fluid mixtures. The incorporation of binary interaction parameters in the mixing rules improves substantially their correlational flexibility. In Figure 2.2 the vapor liquid equilibrium predictions for the methane-methanol system are shown. The dotted line is calculated with all the binary interaction parameters equal to zero. As seen from the figure, the calculated liquid mole fractions differ substantially from the experimental values. However, by introducing an interaction parameter, a tremendous improvement is accomplished. The solid line represents the predicted values using this interaction parameter. Binary vapor-liquid equilibrium (VLE) data are usually required for the adjustment of the interaction

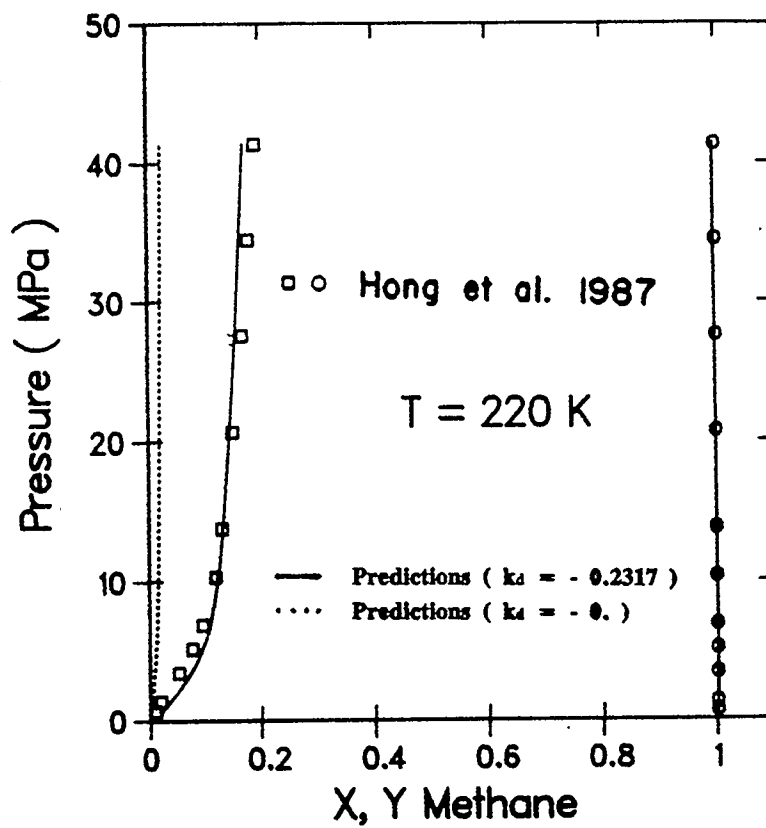


Figure 2.2 Vapor Liquid Equilibrium Calculations for the Methane-Methanol System.

parameters. These VLE data are the measurements of the temperature, T , the pressure, P ; the liquid phase mole fraction, x , and the vapor phase mole fraction, y , of one of the components. All the measurements are taken at equilibrium.

Least squares (LS) and maximum likelihood (ML) estimation methods have been widely used for the estimation of the parameters needed by activity coefficient models (Sutton and MacGregor, 1977; Anderson et al., 1978; Neau and Peneloux, 1981; Kemeny et al., 1982; Salazar-Sotelo et al., 1986). One important underlying assumption in applying ML estimation is that the model is capable of representing the data without any systematic deviation. This assumption is reasonably satisfied when correlating low pressure vapor liquid equilibrium (VLE) data using excess Gibbs free energy models. On the other hand, the equations of state predict the properties of mixtures of polar components with variable degree of success. In this case the magnitude of the variation in the experimental error could be significantly less than the systematic deviation due to thermodynamic model inadequacies. In such cases ML estimation should be used with caution. This is the reason why mostly least squares has been used for the estimation of binary interaction parameters for equations of state. Skjold-Jorgensen (1983) formulated the problem of parameter estimation for an equation of state using ML estimation methods, however, computational results were not presented.

Sometimes, when an equation of state or any other thermodynamic model is used to perform vapor-liquid equilibrium calculations,

erroneous liquid-liquid phase separation is predicted if the interaction parameters were obtained from the regression of the VLE data. This is a consequence of the inadequacy of the thermodynamic model. Schwartzenruber et al. (1987) while correlating propane-methanol VLE data encountered this problem. They were the first to propose a procedure for the calculation of interaction parameters which would not yield prediction of erroneous liquid-liquid phase splitting. In their approach, all but one interaction parameters were fitted to the VLE data. The remaining parameter was obtained by solving the equation which gives the limits of stability for the binary liquid. This solution procedure guarantees the stability of the liquid phase. However, the estimated interaction parameters are not optimal in the sense of corresponding to the constrained minimum of the optimality criterion.

2.5.1 Problem Statement for Binary VLE Data Regression

It is assumed that a set of N VLE experiments have been performed and at each of these experiments, four state variables have been measured. These measurements are the liquid, \hat{x} , and vapor, \hat{y} , mole fractions of one of the components, the temperature, \hat{T} , and the pressure, \hat{P} , of the system all taken at equilibrium. If x , y , T , P are the corresponding "true" but unknown values of the state variables, they are related to the measurements by the following equations.

$$\hat{x}_i = x_i + \varepsilon_{x,i} \quad i=1,\dots,N \quad (23a)$$

$$\hat{y}_i = y_i + \varepsilon_{y,i} \quad i=1,\dots,N \quad (23b)$$

$$\hat{T}_i = T_i + \varepsilon_{T,i} \quad i=1,\dots,N \quad (23c)$$

$$\hat{P}_i = P_i + \varepsilon_{P,i} \quad i=1,\dots,N \quad (23d)$$

where $\varepsilon_{.,i}$ are the corresponding errors in the measurements. The thermodynamic model (EOS or activity coefficient model) is a phenomenological model nonlinear in the interaction parameters. It can be viewed as a functional relationship among the above true state variables, a set of unknown parameters, \mathbf{k} , and a set of "precisely" known parameters, \mathbf{u} , such as the pure component EOS parameters and critical properties. However, it should be noted that the assumption of precisely known pure component critical properties may not always be valid. The elements of the parameter vector \mathbf{k} are the binary interaction parameters. Given the above information and having a thermodynamic model, the objective is to determine the parameter vector \mathbf{k} by matching the data with the model predictions by satisfying some optimality criterion. This criterion is a measure of the ability of the thermodynamic model to correlate the experimental data. In other words, it is a performance index. It is a scalar function of the parameter vector \mathbf{k} and hence, it is usually denoted by $S(\mathbf{k})$.

2.5.2 Estimation Methods

(a) *ML Parameter and State Estimation (Error in Variables Method)*

According to the phase rule for a binary two phase system at each experimental point only two of the above four state variables are independent. Arbitrarily, one can select two as independent and use the thermodynamic model and the equilibrium equations to solve for the other two variables which become the dependent ones. For experiment i , let η_{ij} ($j=1,2$) be the independent variables (e.g. $\eta_{i1}=x_i$ and $\eta_{i2}=T_i$). The dependent variables ξ_{ij} can be obtained from the equilibrium relationships using the thermodynamic model, and in principle can be written as

$$\xi_{ij} = h_j(\eta_{i1}, \eta_{i2}; \mathbf{k}; \mathbf{u}); \quad j = 1, 2 \quad (24)$$

In this case the ML estimate of \mathbf{k} is obtained by minimizing the following objective function (Box, 1970; Britt and Luecke, 1973)

$$\sum_{i=1}^N \sum_{j=1}^2 \left[\frac{[\eta_{ij} - \hat{\eta}_{ij}]^2}{\sigma_{\eta_{ij}}^2} + \frac{[h_j(\eta_{i1}, \eta_{i2}; \mathbf{k}; \mathbf{u}) - \hat{\xi}_{ij}]^2}{\sigma_{\xi_{ij}}^2} \right] \quad (25)$$

The above quadratic optimality criterion can be derived from the ML function by assuming (a) the experiments are independent, (b) the errors in the measurements of the state variables are normally distributed with

zero mean and known variance-covariance $\Sigma_i = \text{diag}(\sigma_{x,i}^2, \sigma_{T,i}^2, \sigma_{y,i}^2, \sigma_{P,i}^2)$, (c) the elements of the covariance matrix Σ_i are known *a priori*, and (d) the thermodynamic model is capable of representing the data without any systematic deviation.

In the case where the elements of the covariance matrix are not known, Eq. (25) should be modified by replacing σ 's with their estimates $\hat{\sigma}$'s and by adding an extra term in the optimality criterion.

Anderson et al. (1978) and Salazar-Sotelo et al. (1986) are among the researchers who have recently calculated activity coefficient model interaction parameters using this criterion. Unless limited experimental data are used, the dimensionality of this problem is extremely large and hence, difficult to treat with standard nonlinear least squares iterative procedures. Schwetlick and Tiller (1985), Salazar-Sotelo et al. (1986) and Valko and Vajda (1987) examined and exploited the structure of this problem from a computational viewpoint and proposed efficient algorithms for its solution.

(b) *Simplified Error in Variables Method*

The *error in variables method* can be simplified to weighted LS estimation if the independent variables are assumed to be known precisely. On statistical grounds this assumption is reasonable if the experimental error in the independent variables is much smaller when compared to that of the dependent ones. On thermodynamic grounds the selection of the independent variables should be based on the VLE

behavior of the system. Systems with a sparingly soluble component, such as methane-methanol, are poor candidates for anything except isothermal-isobaric flash calculations, because of the large derivatives of the pressure with respect to the liquid mole fraction. For systems with azeotropic behavior bubble point pressure calculations should be performed at a specified liquid mole fraction and temperature.

If we further assume that the variances of the errors in the measurement of the dependent variables are known *a priori*, the following objective functions can be formulated:

$$S_{Tx}(\mathbf{k}) = \sum_{i=1}^N \left[\frac{(P_i^{\text{calc}} - \hat{P}_i)^2}{\sigma_{P,i}^2} + \frac{(y_i^{\text{calc}} - \hat{y}_i)^2}{\sigma_{y,i}^2} \right] \quad (26)$$

and

$$S_{TP}(\mathbf{k}) = \sum_{i=1}^N \left[\frac{(x_i^{\text{calc}} - \hat{x}_i)^2}{\sigma_{x,i}^2} + \frac{(y_i^{\text{calc}} - \hat{y}_i)^2}{\sigma_{y,i}^2} \right] \quad (27)$$

The calculation of y_i^{calc} and P_i^{calc} in the case of S_{Tx} and that of x_i^{calc} and y_i^{calc} in the case of $S_{TP}(\mathbf{k})$ are obtained by solving the following two equilibrium equations

$$f_j^L = f_j^V \quad j=1,2 \quad (28)$$

at each experimental point.

The above two optimality criteria constitute least squares estimation procedures known as weighted least squares (WLS). By further

assuming that the variances of the measurement errors of the dependent variables are constant, the simple LS estimation procedures are obtained.

(c) *ML Parameter Estimation (Implicit Formulation Method)*

If we wish to avoid the computationally demanding state estimation, we have to change the optimality criterion and impose additional distributional assumptions. In this case the residuals in the optimality criterion, instead of representing the errors in the state variables, are suitable implicit functions of the four state variables dictated by the isofugacity criterion.

The errors in the measurements of all four state variables are taken into account by the error propagation law (Fabries and Renon, 1975) In this case the necessary assumptions are: (a) the experiments are independent, (b) the variance-covariance matrix, Σ , of the errors in the measurement of the state variables is known *a priori*, (c) the residuals employed in the optimality criterion are normally distributed and (d) the thermodynamic model is capable of representing the data without any systematic deviation.

2.6 Research Objectives

The specific research objectives of the thesis are now identified. Since, the incipient hydrate formation pressure depends strongly on the

activity of water, a procedure to calculate it accurately over a wide range of electrolyte concentration will be utilized. The calculation of the activity of water will be incorporated into a method for predicting the incipient hydrate formation conditions. The procedure should be extended to mixed electrolytes. It is desired that this method should not have any adjustable parameters other than those available in the literature and be easily implementable on the computer.

In the case of aqueous solutions without electrolytes it is preferred to use only one thermodynamic model for the fluid phases. This will make the computations less complicated. It will avoid the dependence on many parameters and will offer the benefits of using one thermodynamic model for the calculation of high pressure vapour liquid equilibrium. The method should not contain any adjustable parameters but rather use published parameter values.

A new apparatus which will be used to obtain equilibrium data for hydrate forming systems will be fabricated. Experimental data for gas hydrate formation from natural gas components in the presence of mixed electrolytes will be mainly obtained. Such data are not available and will be useful for testing predictive methods for the calculation of hydrate formation conditions.

The hydrocarbon-alcohol-water systems are of great interest in gas hydrates research. Binary interaction parameters are needed by an equation of state in order to improve its correlative ability particular for these physical systems. The Trebble Bishnoi equation of state can utilize up to four such parameters and hence, has a significant

correlational flexibility. We need to develop computationally efficient interaction parameter estimation procedures which will be based on statistics. VLE data will be used for the regression. However, the estimation procedures will be extended to the case where three phase vapor-liquid-liquid equilibrium data are also available.

In addition, we require that when these parameters are used in the equation of state, the predicted phase behavior is consistent with the experimentally observed. The latter consideration is important because erroneous liquid phase splitting is often predicted by the equation of state as a result of its inadequacy to represent the phase behavior over a wide range of conditions. Computationally efficient parameter estimation procedures should be developed to eliminate this problem.

The system methane-water will be examined in order to see if the limits of supersaturation can be calculated from thermodynamic considerations. For that purpose the stability limits for the methane-water system will be calculated using an equation of state. In addition tangent plane analysis for studying hydrate equilibrium will also be performed.

3. PREDICTION OF THE INCIPIENT HYDRATE FORMATION CONDITIONS IN AQUEOUS ELECTROLYTE SOLUTIONS

In this chapter a methodology, developed in the present work, for the prediction of the incipient hydrate formation conditions in aqueous solutions of single or mixed electrolytes is presented. In addition, the methodology is used to predict the hydrate formation conditions and the results are compared with all the available data in the literature. The experimental data obtained in the present work will be compared with the predictions based on the methodology, in chapters 5 and 6.

3.1 Methodology

Eqns 1 and 2 are the phase equilibrium conditions for a hydrate - vapor - aqueous liquid system of N components of which only N_h components exist in the hydrate phase. For a mixture of light hydrocarbon gases with an aqueous electrolyte solution this set of equations may be reduced to the following equation

$$\mu_w^H = \mu_w^L \quad (29)$$

In writing Eq. 29 the amount of water vapor present in the gas phase is considered negligible. In addition, it is assumed that the electrolytes are present only in the liquid solution. Since the salts do not enter the hydrate lattice, the statistical thermodynamics model of van der

Waals and Platteeuw is valid, and the chemical potential of water in the hydrate is given by Eq. 3. The chemical potential of water in the solution is given by Eq. 17. It is now assumed that the mole fractions of the dissolved light hydrocarbon gases are negligibly small, as is the case with methane, ethane and propane. The activity of water can then be calculated by using the activity of a dissolved salt and the Gibbs-Duhem equation as given later. The chemical potential of pure water is related to the chemical potential of water in the empty hydrate lattice by Eq. 7. By inserting Eq. 3 and Eq. 17 into Eq. 29 and subsequently substituting for the term, $\mu_w^{MT} - \mu_w^L$, from Eq. 7 (Holder's correlation) we obtain the following equation

$$\frac{\Delta V_w^{MT-L}}{R T} P + \psi(T) - \ln a_w - \sum_{i=1}^2 v_i \ln \left(1 + \sum_{j=1}^{N_h} C_{ij} f_j \right) = 0. \quad (30.)$$

In the above equation $\psi(T)$ is a temperature dependent function given by the following equation,

$$\psi(T) = \frac{1}{R} \left[\frac{\Delta \mu_w^0}{T^0} + \frac{\beta}{2} (T^0 - T) + \psi_{11} \ln \left(\frac{T^0}{T} \right) + \psi_{12} \left(\frac{1}{T} - \frac{1}{T^0} \right) \right], \quad (31)$$

where

$$\psi_{11} = \Delta C_{p_w}^0 - \beta T^0 \quad (32)$$

$$\psi_{12} = \Delta H_w^0 - \Delta C_{p_w}^0 T^0 + \frac{\beta}{2} (T^0)^2 \quad (33)$$

At a fixed temperature Eq. 30 can be solved in order to obtain the hydrate formation pressure. The Langmuir constants, C_{ij} , are obtained from the correlation suggested by Parrish and Prausnitz and is given by Eq. 5. The fugacities, f_j are computed by using the Trebble-Bishnoi equation of state.

The presence of the salts alters significantly the state of the liquid phase. During the dissolution in water, electrolytes dissociate fully or partially into their ions and an electrolyte solution results. For aqueous electrolyte solutions the structure and properties depend on the nature and magnitude of ion-water and ion-ion interactions. In addition, water-water interactions can also play a role which decreases as the concentration of the salt increases.

The interaction between ions and water is stronger than the interaction between a dissolved gas and water. As a result, the liquid crystalline structure of water having cavities becomes *impaired* and gas solubility drops. This is the salting out phenomenon. For the creation of structural cells from water molecules, in order to form hydrates, substantially greater supersaturation of the solution is required.

3.2 Activity of Water

The activity of water in the liquid phase is calculated by assuming that it is influenced only by the presence of electrolytes. A number of models are available for calculating the activity of single salts in

aqueous solutions (Meissner and Kusik ,1972; Pitzer, 1973; Pitzer and Mayorga, 1973; Zemaitis, 1986). Recently, a method has been proposed to account for the overall non-ideal effects of electrolytes in mixed salt solutions and calculate the activity of water (Patwardhan and Kumar, 1986). These models have been used to develop expressions for the activity of water as given below.

3.2.1 Single Electrolyte Solutions

For an aqueous solution of a single electrolyte, the Gibbs-Duhem equation is written as follows (Lewis and Randall, 1961)

$$x_w d \ln a_w + x_{el} d \ln a_{el} = 0. \quad (34)$$

where

$$a_{el} = a_{\pm}^{\nu} = (m_{\pm} \gamma_{\pm})^{\nu} \quad (35)$$

In Eq. 35, a_{el} is the activity of the electrolyte, ν is the stoichiometric number of moles of ions in one mole of salt and is given by, $\nu_+ + \nu_-$, γ_{\pm} is the mean ionic activity coefficient and m_{\pm} is the geometric mean of the ion molalities. By writing the ratio of the mole fractions in terms of the molality, m , and since, $d \ln m_{\pm} = d \ln m$ (Lewis and Randall, 1961), the Gibbs-Duhem equation is written as follows

$$d \ln a_w = - \frac{18}{1000} v dm - \frac{18}{1000} m v d \ln (\gamma_{\pm}) \quad (36)$$

The molality, m , of the solution is related to the ionic strength, I , of the solution by the following equation

$$I = \frac{1}{2} (m_+ z_+^2 + m_- z_-^2) = \frac{1}{2} m z_+ z_- v \quad (37)$$

By integrating Eq. 36 and substituting m from Eq. 37, the following expression for the activity of water is obtained

$$\ln a_w = - \frac{36 I}{1000 z_+ z_-} - \frac{36}{1000 z_+ z_-} \int_1^{\gamma_{\pm}} I d \ln \gamma_{\pm} \quad (38)$$

where z_+ , z_- are the charges of the ions. The above equation is general and can be used with any of the available activity coefficient models for electrolyte solutions. In the present work the model proposed by Pitzer (Pitzer, 1973; Pitzer and Mayorga, 1973) and the model proposed by Meissner and Kusik (Meissner and Kusik, 1972; Zemaitis et al. 1986) are used. These models are very well documented and suitable for molalities exceeding one molal. When Pitzer's activity coefficient model is used, Eq. 38 takes the following form after integration

$$\ln a_w = - \frac{18 v m}{1000} (1 + z_+ z_- \rho_1 + m \rho_2 + m^2 \delta_2) \quad (39)$$

where

$$\rho_1 = - \frac{A_\phi I^{0.5}}{1 + 1.2 I^{0.5}} \quad (40)$$

$$\rho_2 = \delta_0 + \delta_1 \exp(-2 I^{0.5}) \quad (41)$$

A_ϕ is the Debye-Huckel coefficient and δ_0 , δ_1 , δ_2 are the adjustable parameters for Pitzer's activity coefficient model. When using Meissner's activity coefficient model, Eq. 36 is integrated numerically by using Simpson's composite rule.

3.2.2 Mixed Electrolyte Solutions

Patwardhan and Kumar (1986) derived the following predictive equation for the activity of water in mixed electrolyte solutions

$$\ln a_w = \sum_{k=1}^{ns} \left[\frac{m_k}{m_k^0} \right] \ln a_{w,k}^0 \quad (42)$$

In the above equation, m_k is the molality of electrolyte k in the mixed solution, m_k^0 is the molality of a solution containing only electrolyte k , which has the same ionic strength as that of the mixed solution and $a_{w,k}^0$ is the activity of water in this single salt solution. It is noted that the equation does not contain any additional adjustable parameters. It is valid over the entire concentration region encountered in practice

and has a predictive accuracy of 2 percent.

In the present work the activity of water in the liquid phase is calculated using Eq. 42. The activities of water in single electrolyte solutions, $a_{w,k}^{\circ}$, required in the equation are calculated from either Eq. 39 or Eq. 36.

3.3 Results and Discussion

At a given temperature, the incipient hydrate formation pressure is calculated by solving Eq. 30 which is nonlinear in pressure. The various parameters required in the equation are taken from Parrish and Prausnitz (1972).

Figure 3.1 shows the experimental and calculated inhibiting effect of sodium chloride on methane gas hydrate formation. The solid lines in the figure are the predictions. The experimental data are from Roo et al. (1983) except the values at 273.20, 283.20 and 290.20 K for pure water which have been cited from Holder et al. (1980). As seen the calculated results are in excellent agreement with the experimental data. The activity of water was calculated using Eq. 39 which is based on Pitzer's model for the activity of the electrolyte. The calculations were also done with using Eq. 36 where the mean ionic activity of the electrolyte, γ_{\pm} , is calculated from Meissner's model. It was, however, found that the calculations based on Pitzer's model gave overall smaller deviations from the experimental data. This is expected because Meissner's model is not suitable for molalities exceeding 4 m. The

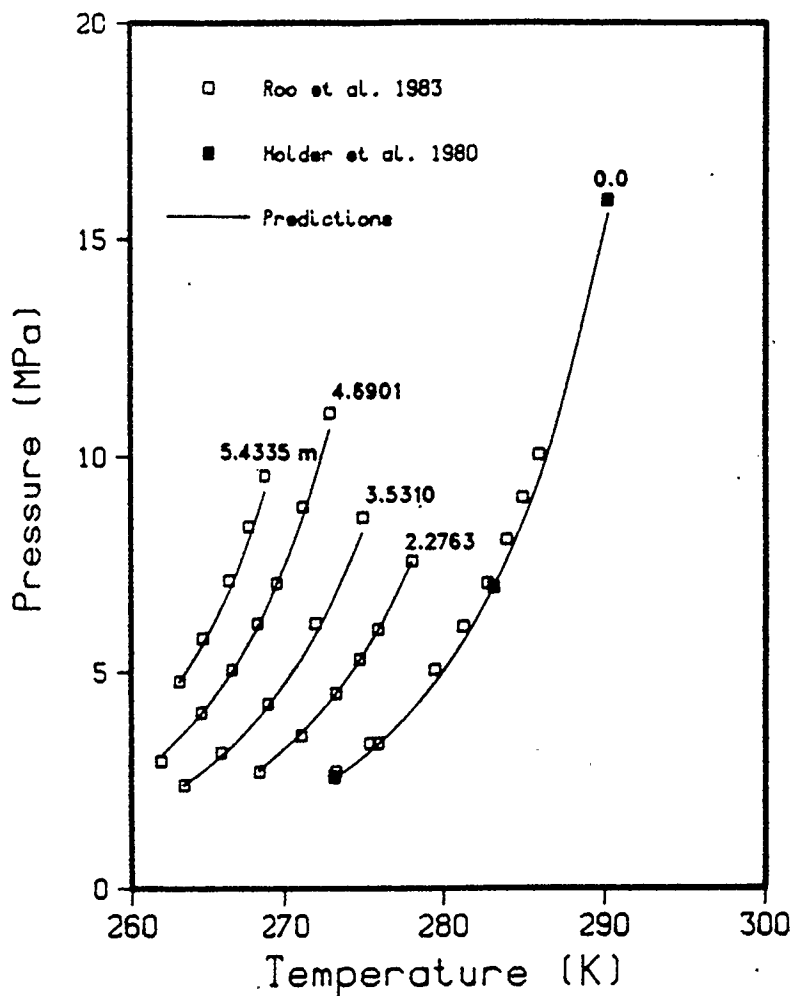


Figure 3.1 Experimental and Predicted Pressures for Methane Hydrate Formation in Aqueous Sodium Chloride Solution.

maximum deviation of the predictions shown in Figure 3.1 is 6.2 per cent and the root mean square deviation is 3.3.

The strong inhibiting effect of the electrolyte can be seen by comparing the hydrate formation pressures with those at zero salt concentration at any temperature. The pressures differ by almost 2 MPa at 273.3 K for the 2.2763 m solution. The profound effect of electrolytes is seen mathematically from Eq. 30 where a non linear term, $RT \ln a_w$, is added to the equation describing the formation from pure water. It was noticed during the calculations that the pressure predictions are very sensitive to the calculated values of the activity of water.

Figure 3.2 shows the inhibiting effect of sodium chloride on another hydrocarbon hydrate, the propane hydrate. The maximum per cent deviation between the predicted and the experimental values is 5.9 and the per cent RMSD is 3.0. The data at 2.5 weight per cent and some of the data at 0.0 weight per cent are from Kubota et al. (1984). The remaining data at 0.0 wt % are cited from Byk and Fomina ((168), whereas at the other salt concentrations are from Knox et al. (1961). It should be mentioned that Knox et al. and Kubota et al. performed these studies as part of their efforts to investigate the process of water desalination via gas hydrate formation. The activity of water was calculated from Eq. 39 or Eq. 36 with Meissner's model. By using Pitzer's model (Eq. 39) for the calculation of the activity of water slightly better predictions were obtained.

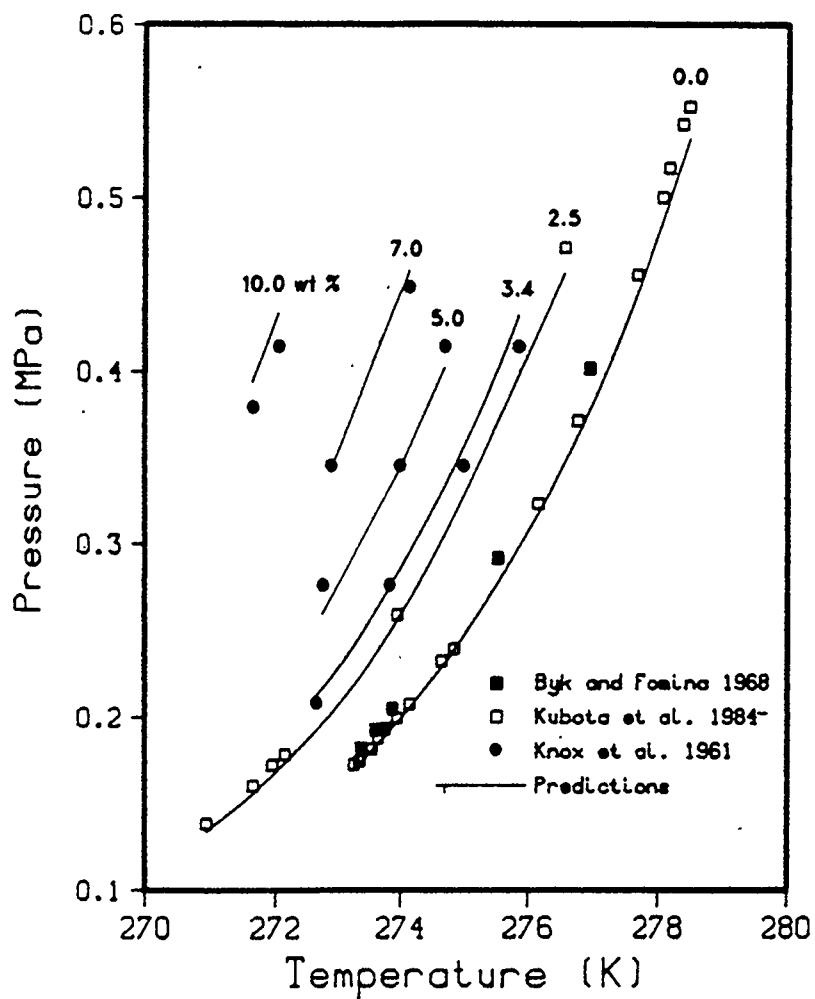


Figure 3.2 Experimental and Predicted Pressures for Propane Hydrate Formation in Aqueous Sodium Chloride Solution.

In addition to the above, the method was used to predict the inhibiting effect of potassium chloride and calcium chloride on cyclopropane hydrate formation. Experimental data on these systems have been reported by Menten (1979). The predicted values and the experimental data are in very good agreement and are shown in Figure 3. The solid lines represent the predictions using Pitzer's model. The use of Meissner's model for the calculation of the activity of water resulted in slightly worse predictions. In Figure 3.3, the maximum per cent deviations are 7.2 and 3.5 for the potassium chloride and the calcium chloride solutions respectively. In addition, the per cent RMSD's are 4.1 and 2.4.

Cyclopropane forms structure II hydrates below 274.61 K and structure I above this temperature without the presence of the salts. This behavior can also be seen from the predictions at 0.0 M by the change in the slope of the curve. Menten (Menten, 1979) also reported that structure II forms from 0.1 M calcium chloride solution at 273.71 K. The prediction at 273.71 K for this solution also gave the formation of structure II hydrate.

As it was mentioned in the beginning of this chapter, the comparison of the experimental data obtained in this work with the predictions based on the above methodology will be presented in chapters 5 and 6. As it will be seen there, the method is also very successful in predicting the incipient hydrate formation conditions in aqueous solutions of mixed electrolytes. Such data were not available when the methodology was developed.

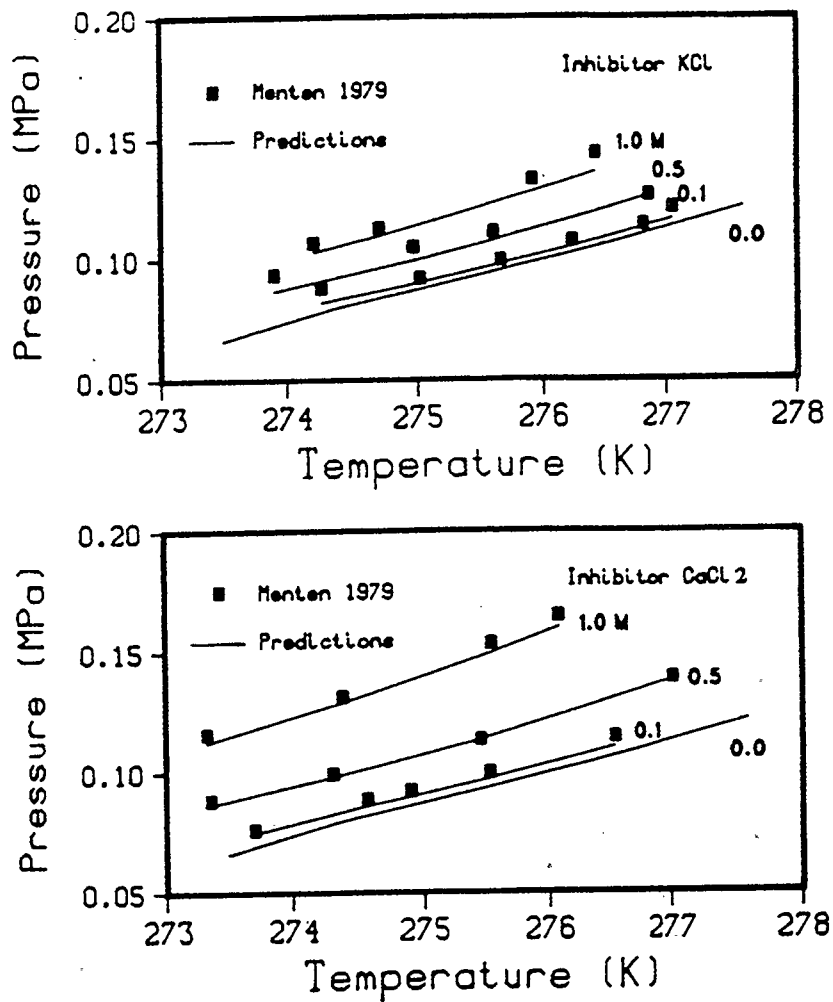


Figure 3.3 Experimental and Predicted Pressures for Cyclopropane Hydrate Formation in Aqueous KCl and CaCl₂ Solutions.

From the above analysis it is evident that the proposed methodology provides a valuable tool for the investigation of the gas hydrate formation conditions in environments such as sea or ground water. In addition, it can facilitate feasibility studies for water desalination, gas storage via gas hydrate formation and natural gas recovery.

4. PREDICTION OF THE INCIPIENT HYDRATE FORMATION CONDITIONS IN THE PRESENCE OF METHANOL

In this chapter a methodology to calculate the incipient hydrate formation conditions in the presence of methanol will be presented. The equations given here were solved by Anderson and Prausnitz (1986). However, as it was mentioned earlier, we had undertaken this work with the objective to utilize only an equation of state for the description of the fluid phases instead of three different models that they had used. As it will be seen, the use of an equation of state is simple and was found to give satisfactory results. It should be mentioned that the method is not limited to methanol and can be used for any other molecular species.

4.1 Methodology

In a system of N_c components containing solid hydrate (H), vapor (V) and liquid (L), the thermodynamic equilibrium in terms of fugacities may be represented by,

$$f_i^L = f_i^V \quad , \quad i = 1, \dots, N_c \quad (43)$$

for all the N_c components, and by

$$f_j^H = f_j^L \quad , \quad j = 1, \dots, N_h \quad (44)$$

for the N_h hydrate forming components including water. However, since the vapor (V)-hydrate (H) equilibrium conditions for the hydrate forming substances other than water are implicitly incorporated in the hydrate thermodynamic model, Eq. 44 reduces to the following equation

$$f_w^H = f_w^L \quad (45)$$

In the above equations, the fugacities in the vapor and the liquid phases may be calculated using a suitable thermodynamic model. In the present work, however, the Trebble-Bishnoi equation of state (Trebble and Bishnoi, 1988) is used. The equation of state interaction parameters for additional systems are shown in Table 4.1. The sources of the experimental data that were used to obtain the parameters by the regression methods of chapters 2 and 8 are also shown in the table. The introduction of methanol in a liquid water-hydrocarbon mixture alters the prevailing structure in the aqueous phase. Methanol-water interactions are stronger than the interactions between water and the dissolved gases because the water and methanol molecules are interlinked by hydrogen bonds. These bonds and the structure formed in the solution are very much dependent on the concentration. As a result, the formation of gas hydrates occurs to a lower extent than in the case of pure water. In other words the probability of hydrate formation is reduced because of a breakdown in the structural organization of water.

Table 4.1 Binary Interaction Parameters for the Trebble-Bishnoi EOS

<i>Binary System</i>	<i>Interaction Parameter*</i>	<i>Data or Parameter Source</i>
$C_2H_6 - H_2O$	$k_d = -0.2611 \pm 0.3 \%$	Hayduk, 1982
$C_3H_8 - H_2O$	$k_d = -0.2969 \pm 1.4 \%$	Hayduk, 1986
$CO_2 - H_2O$	$k_d = -0.1652 \pm 1.1 \%$	Houghton et al. 1957 Stewart and Munjal, 1970
$N_2 - CH_3OH$	$k_d = -0.3819 \pm 0.4 \%$	Weber et al. 1984
$CH_4 - CH_3OH$	$k_d = -0.2945 \pm 2.3 \%$	Trebble, 1988b
$C_2H_6 - CH_3OH$	$k_b = -0.3188 \pm 8.0 \%$ $k_d = -0.9099 \pm 6.7 \%$	Ma and Kohn, 1964 Ohgaki et al. 1976
$C_3H_8 - CH_3OH$	$k_a = 0.1612 \pm 6.1 \%$ $k_d = -0.3250 \pm 7.5 \%$	Trebble, 1988b
$CO_2 - CH_3OH$	$k_a = 0.0608 \pm 2.4 \%$ $k_d = -0.1083 \pm 2.8 \%$	Weber et al. 1984

* The interaction parameters other than those shown for each binary system are zero.

It is noted that methanol is excluded from the hydrate lattice. Hence, the model of van der Waals and Platteeuw is valid and used in the present work to describe the fugacity of water in the hydrate phase. The fugacity of water in the hydrate is written as following

$$f_w^H = f_w^{MT} \exp \left(\frac{\mu_w^H - \mu_w^{MT}}{R T} \right) \quad (46)$$

The fugacity of water in the empty lattice, f_w^{MT} , is obtained from the difference in the chemical potential of water in the empty lattice, μ_w^{MT} , and that of pure liquid water, $\mu_w^{L^o}$, using the following equation

$$f_w^{MT} = f_w^{L^o} \exp \left(\frac{\mu_w^{MT} - \mu_w^{L^o}}{R T} \right) \quad (47)$$

In Eq. 47 the fugacity of pure water, $f_w^{L^o}$, is calculated from the equation of state even when the temperature is below the ice-point temperature and pure liquid water is a hypothetical state.

4.1.1 Computational Procedure

Since we seek the incipient hydrate formation conditions, the computational scheme is formulated as shown in Figure 4.1 For a given gas, water and methanol mixture, in order to calculate the incipient hydrate formation pressure (or temperature) at a given temperature (or pressure), the isothermal-isobaric flash calculations are performed at

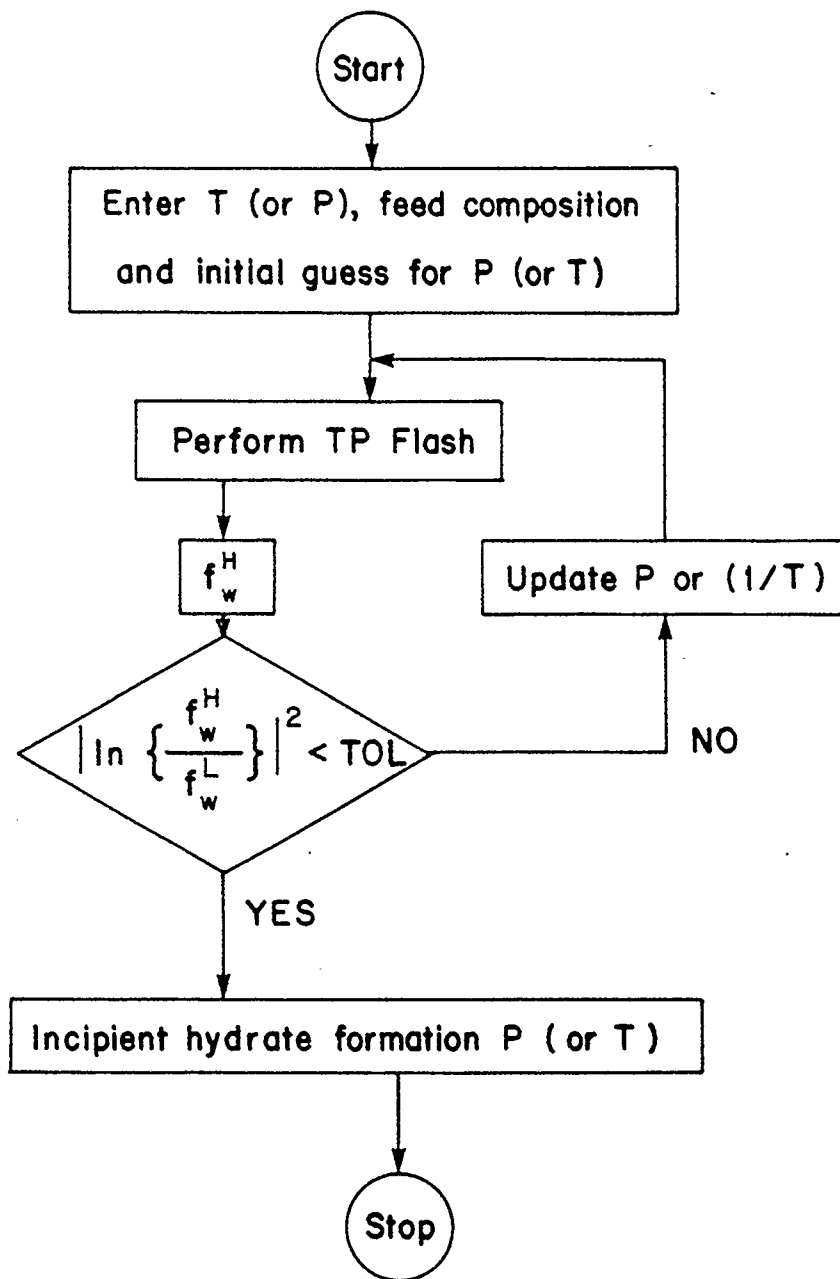


Figure 4.1 Computational Flow Diagram

an assumed pressure (or temperature). At these conditions of pressure and temperature, the fugacity of water in the hydrate is now calculated. If this fugacity is equal to the fugacity of water computed by the flash calculations, the assumed pressure (or temperature) is the hydrate formation pressure (or temperature). The tolerance (TOL) for this comparison is the same as that used for checking the convergence of the flash calculations (10^{-12}). When the incipient hydrate formation temperature is sought at a given pressure, the inverse of temperature is updated by the Secant method.

4.2 Results and Discussion

The accuracy of the predictions of gas hydrate formation conditions depends on various parameters which are needed by the thermodynamic models, and on assumptions associated with these models. For the gas hydrate thermodynamic model, there is uncertainty in the values of the reference thermodynamic parameters. Several researchers have reported different values which were summarized in Table 2.1. In the present work, for structure I hydrates the following values were used for the thermodynamic reference properties: $\Delta\mu_w^\circ=1289.5$ (J/mol), and $\Delta H_w^\circ=-4327.0$ (J/mol). The corresponding values used for structure II hydrates are 893.0 (J/mol) and -4986.0 (J/mol). In addition, for both the structures the following parameter values were used: $\Delta C_{p_w}^\circ=-38.13$ (J/mol K) and $\beta=0.141$ (J/mol K²). The above set of parameters was selected because it gave the smallest average absolute deviation of the predicted values

from all the available experimental data for single hydrate forming components. These parameters were also used for the predictions for gas mixtures.

(a) *Gas Hydrate Formation From Single Gases*

Figures 4.2 to 4.4 show the inhibiting effects of methanol on gas hydrate formation from CH_4 , C_3H_8 and CO_2 respectively. The results for C_2H_6 are shown in Figure 1.2. The experimental data on the inhibiting effects are from Robinson and his co-workers (Ng and Robinson, 1983; Ng and Robinson, 1984; Ng et al., 1985, Ng et al., 1987). The sources of the experimental data at zero per cent methanol are shown in the figures. The concentration of methanol is in weight percent in the liquid phase. As seen from the figures the predictions agree very well with the experimental data. Small discrepancies are only observed for carbon dioxide.

(b) *Gas Hydrate Formation from Gas Mixtures*

In Figure 4.5 the predictions and the experimental data for a CH_4 - C_2H_6 gas mixture are shown for methanol concentrations of 0, 10 and 20 weight percent in the liquid phase. Methane and ethane are similar molecules and their binary interaction parameters with methanol have been regressed from the vapor-liquid experimental data at approximately the same temperature conditions as those for the hydrate experiments. As

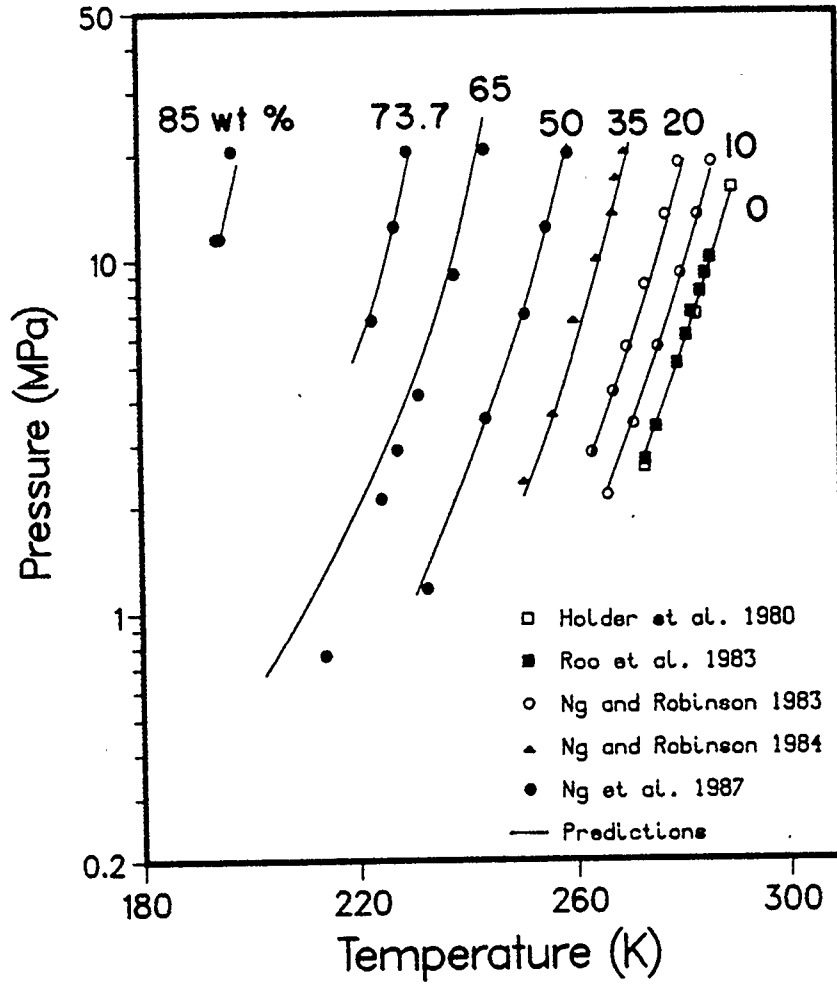


Figure 4.2 Inhibiting Effect of Methanol on Methane Hydrate Formation

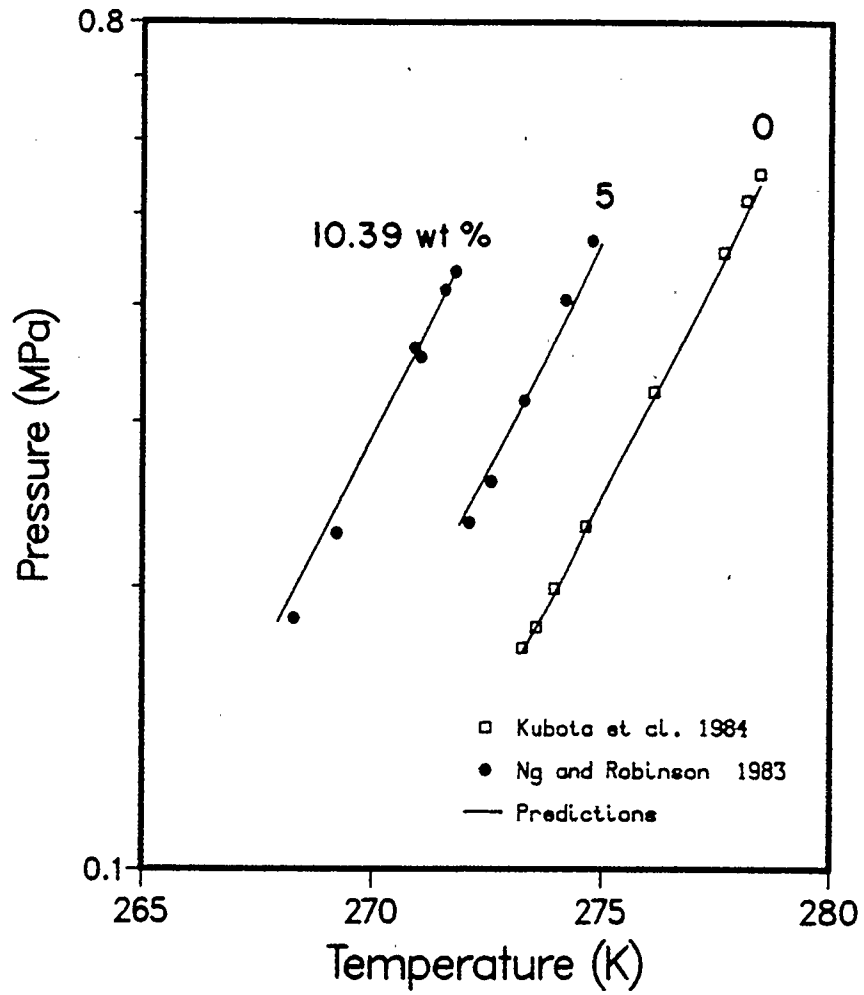


Figure 4.3 Inhibiting Effect of Methanol on Propane Hydrate Formation

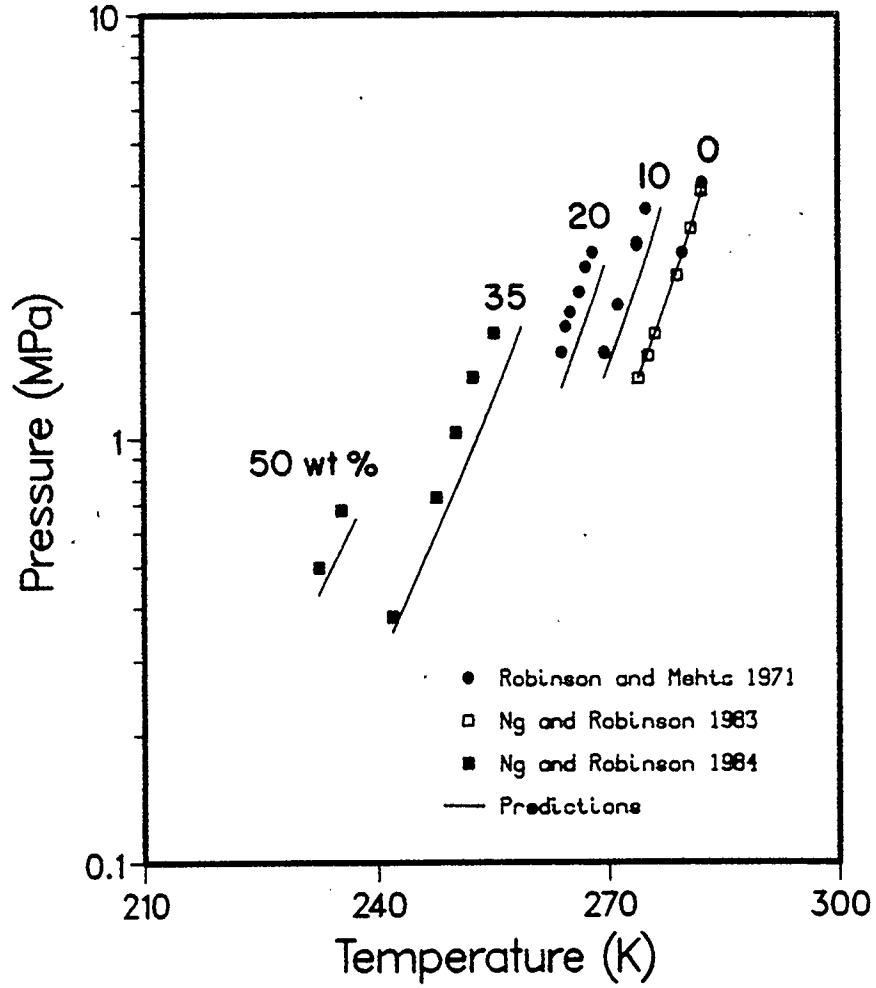


Figure 4.4 Inhibiting Effect of Methanol on CO₂ Hydrate Formation

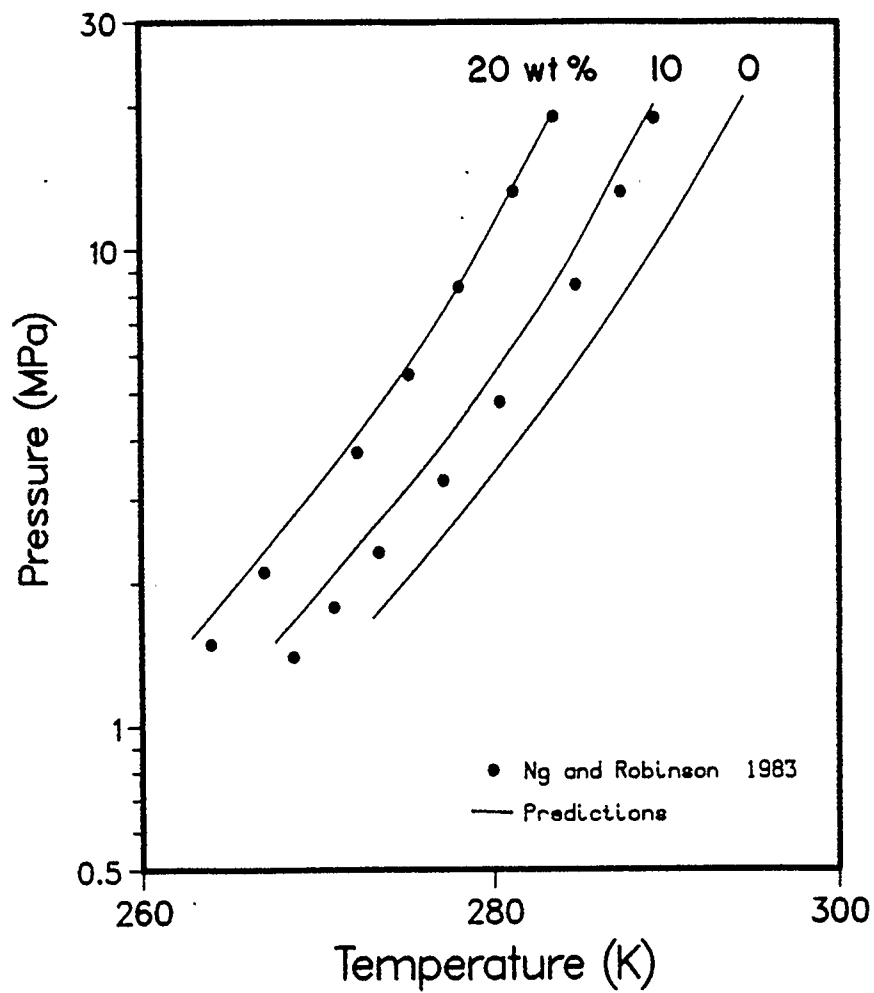


Figure 4.5 Inhibiting Effect of Methanol on Hydrate Formation from a Mixture of 89.51 mole % Methane and 10.49 mole % Ethane

seen from the figures the calculated pressures for incipient hydrate formation at the experimental temperatures agree well with the experimental values. The results for a $\text{CH}_4\text{-C}_3\text{H}_8$ gas mixture are shown in Figures 4.6 and 4.7. As seen from the figures for methanol concentrations up to 35 percent the agreement between the experimental and the predicted values is very good and similar to that for the methane-ethane mixture. However, for a solution containing 50 percent methanol, the predicted hydrate formation pressures are consistently smaller than the experimental data. It should be mentioned here that the interaction parameters for the propane-methanol system have been regressed from the vapor-liquid equilibrium data that were obtained at temperatures above 313.15 K. Similar agreement between experimental values and predictions is observed for a $\text{CH}_4\text{-CO}_2$ gas mixture, as seen in Figures 4.8 and 4.9. In Figure 4.9 the maximum deviation in predicted hydrate point pressure (at fixed temperature) is about 50.0 percent whereas the maximum deviation in predicted hydrate point temperature (at fixed pressure) is about 4.7 K. Anderson and Prausnitz reported errors of 5.0 K in predicting the hydrate point temperature for multicomponent systems, but they do not report the methanol concentration where these observations were made and for what gas mixtures. We observed these deviations only when the methanol concentration is 50 weight percent in the liquid phase.

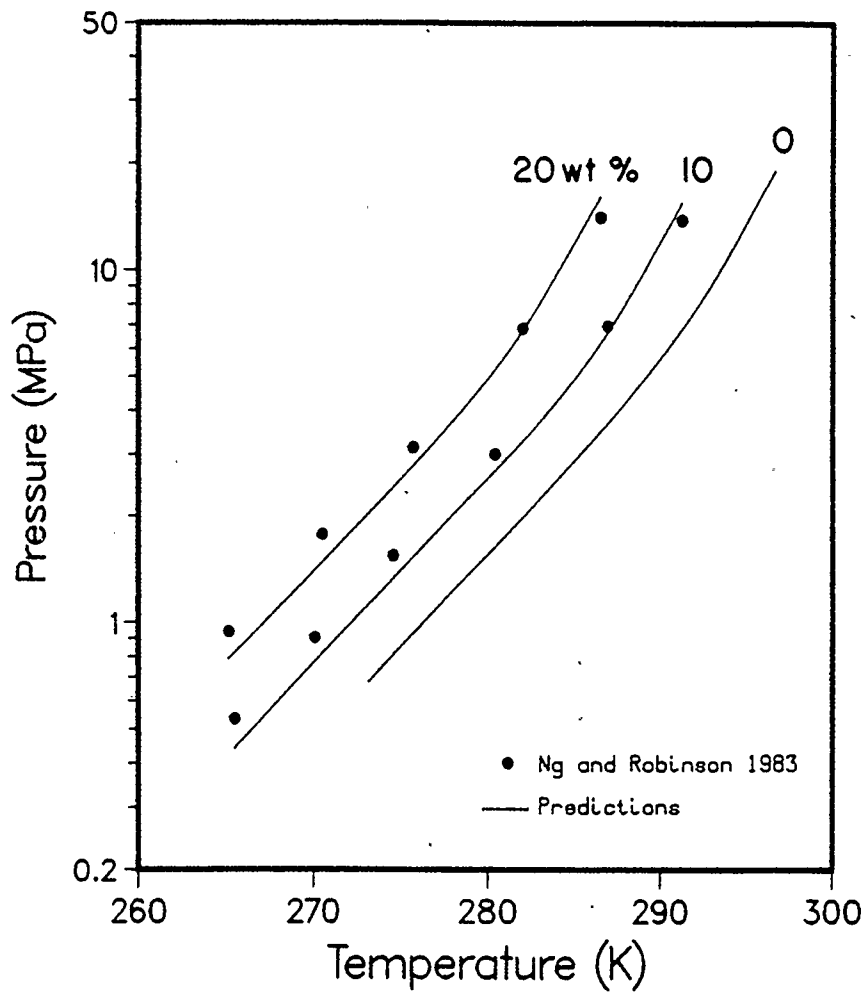


Figure 4.6 Inhibiting Effect of Methanol on Hydrate Formation from a Mixture of 95.01 mole % Methane and 4.99 mole % Propane

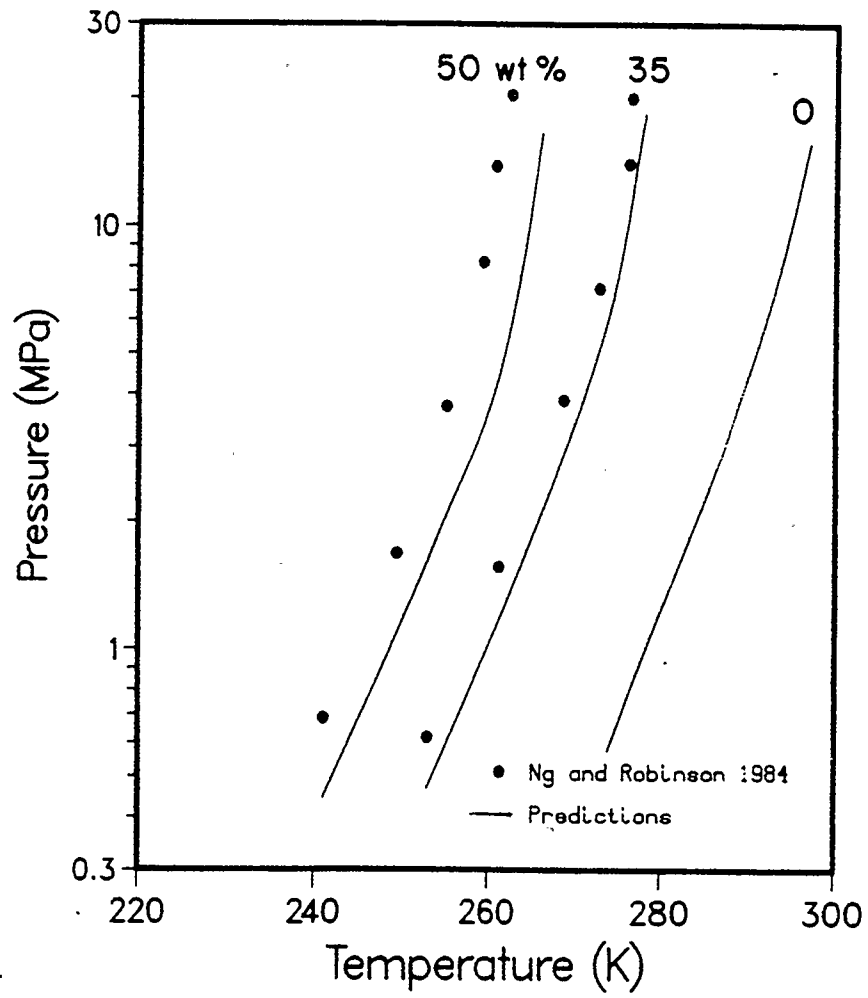


Figure 4.7 Inhibiting Effect of Methanol on Hydrate Formation from a Mixture of 91.12 mole % Methane and 8.88 mole % Propane

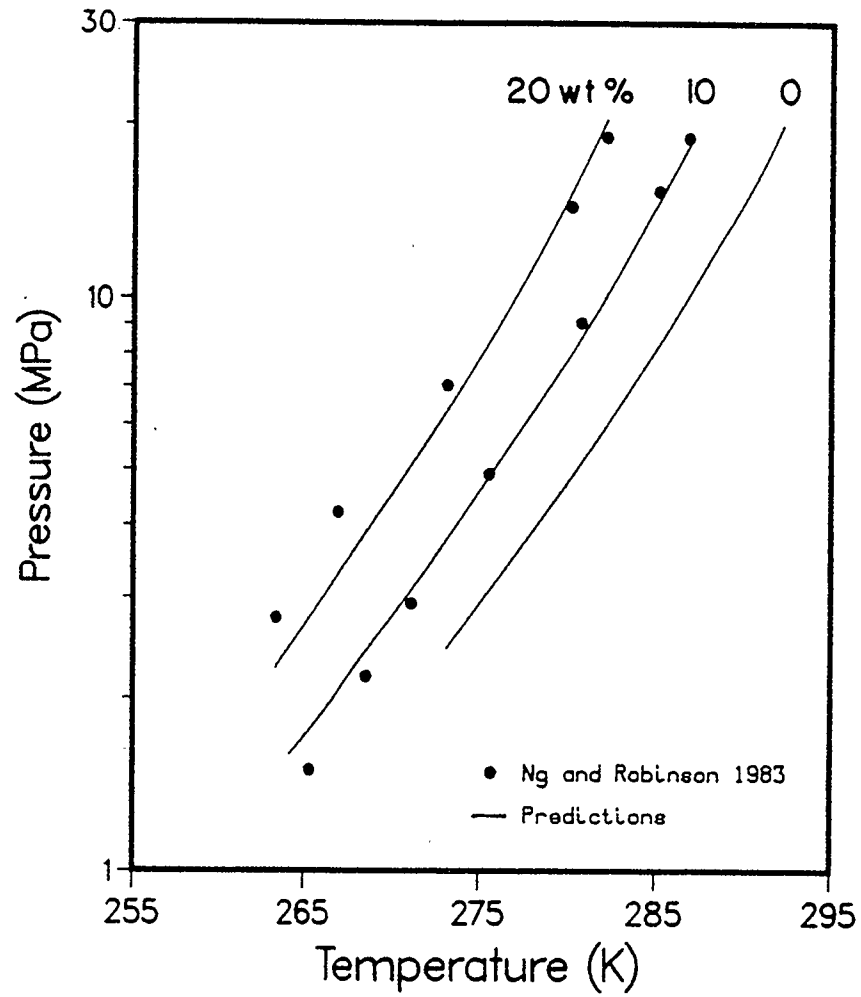


Figure 4.8 Inhibiting Effect of Methanol on Hydrate Formation from a Mixture of 90.09 mole % Methane and 9.91 mole % CO_2

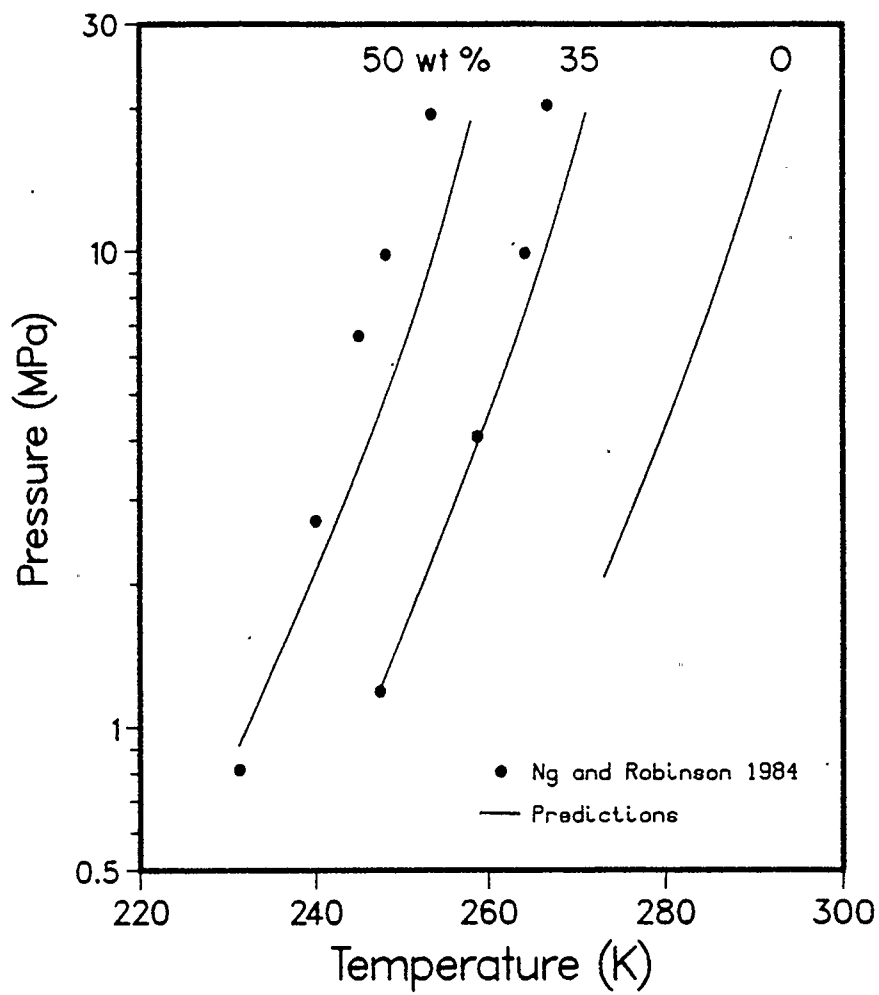


Figure 4.9 Inhibiting Effect of Methanol on Hydrate Formation from a Mixture of 69.75 mole % Methane and 30.25 mole % CO₂

Figures 4.10 and 4.11 show the results for the two multicomponent gas mixtures of compositions given in Table 4.2. The methanol concentration is 10 and 20 percent. In addition, the predictions without the methanol are shown in the figures. There is very good agreement between the experimental and the predicted values for the Natural Gas I as seen in Figure 4.10. The gas mixture of Figure 4.11 contains CO_2 in addition to the hydrocarbon gases. The predictions at 20 weight percent methanol for this mixture are not as good as those for Natural Gas I.

(c) *Equilibrium Phase Compositions*

Equilibrium compositions in the hydrating region have been measured by Robinson and his co-workers. The composition of the vapor and liquid phases at equilibrium in such regions can be calculated by performing isobaric-isothermal flash calculations. The results of such calculations and the experimental data are shown in Table 4.3 for the $\text{CO}_2\text{-H}_2\text{O-CH}_3\text{OH}$ system and in Tables 4.4 and 4.5 for two multicomponent mixtures. As seen from the tables, the calculated compositions of the vapor and the aqueous liquid phases compare very well with the experimental values. Such calculations were also done for systems of water and methanol with methane, ethane and propane. These calculated results together with the experimental measurements are given in Tables 4.6, 4.7 and 4.8.

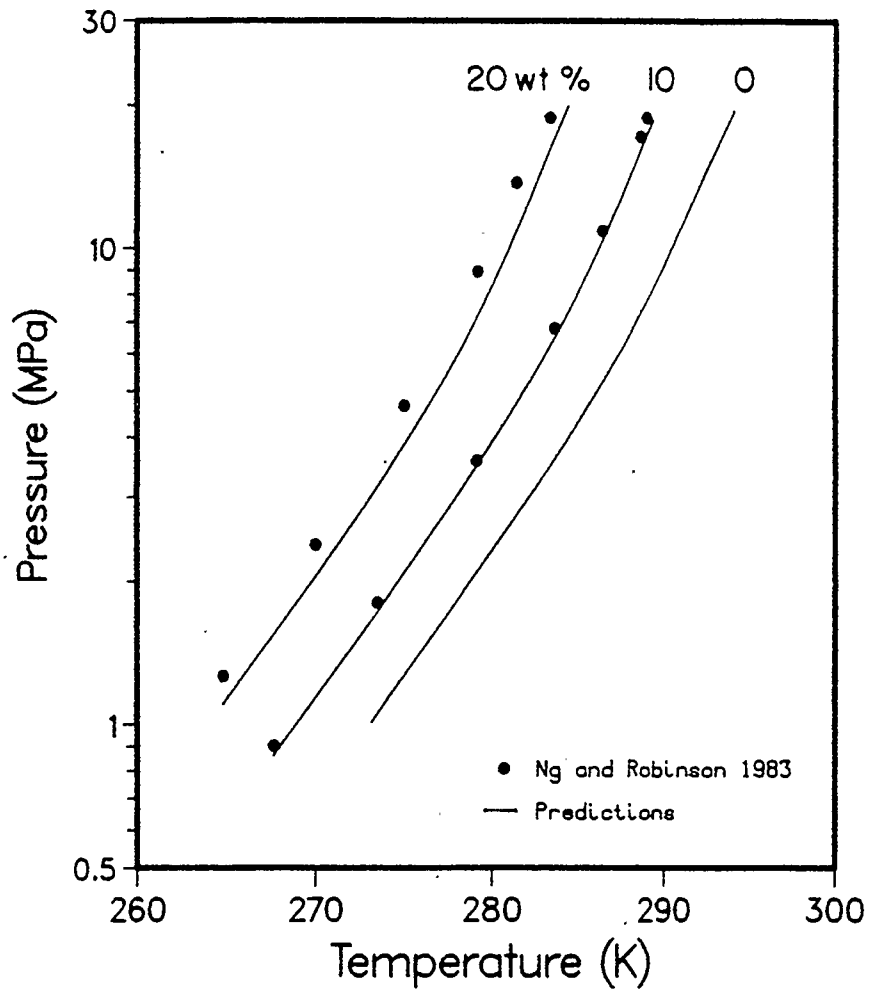


Figure 4.10 Inhibiting Effect of Methanol on Hydrate Formation from Natural Gas Mixture I

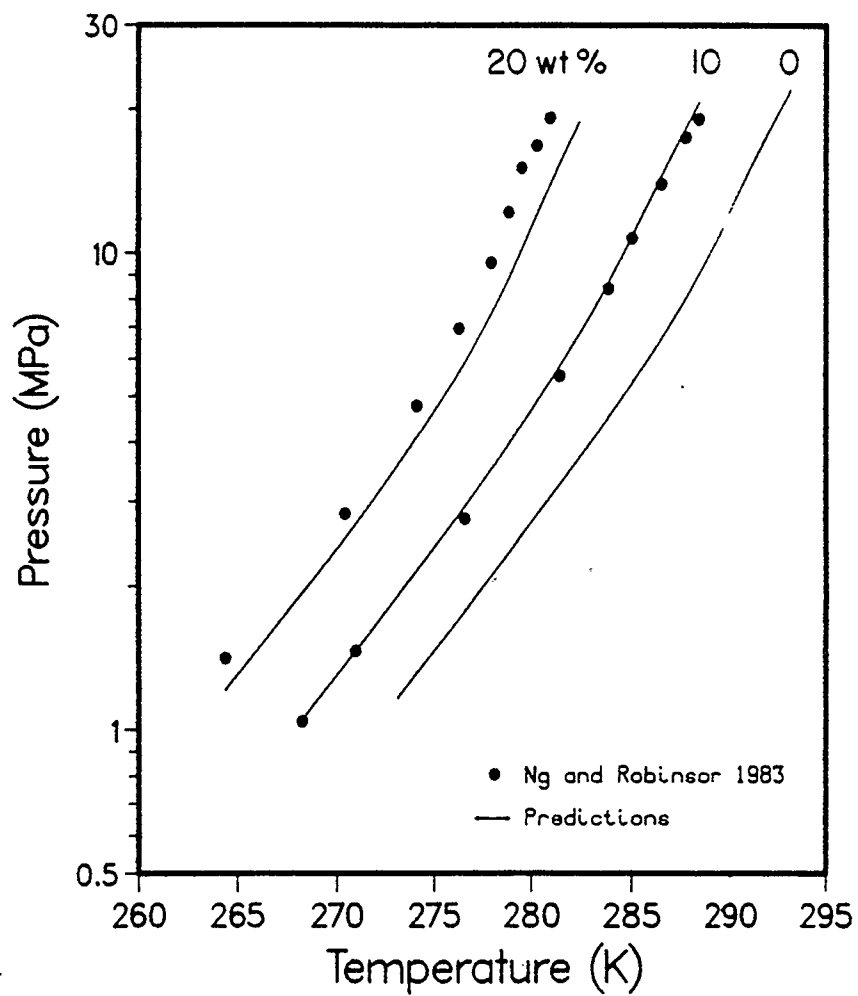


Figure 4.11 Inhibiting Effect of Methanol on Hydrate Formation from Natural Gas Mixture II

Table 4.2 Molar Composition of the Natural Gas Mixtures

<i>Component</i>	<i>Natural Gas I</i>	<i>Natural Gas II</i>
N_2	7.0	5.96
CH_4	84.13	71.60
C_2H_6	4.67	4.73
C_3H_8	2.34	1.94
n-C ₄	0.93	0.79
n-C ₅	0.93	0.79
CO_2	-	14.19

Table 4.3 Equilibrium Phase Compositions for the CO₂-H₂O-CH₃OH System

<i>M o l e F r a c t i o n s</i>					
<i>Component</i>	<i>Feed</i>	<i>L i q u i d</i>		<i>V a p o r</i>	
		Exper.*	Calcul.	Exper.*	Calcul.
		Temperature = 267.55 K		Pressure = 2.47 MPa	
H ₂ O	0.8474	0.8517	0.8688	0.00024	0.00022
CH ₃ OH	0.1192	0.1193	0.1222	0.00040	0.00045
CO ₂	0.0334	0.0270	0.0090	0.99936	0.99933

* Ng and Robinson (1983)

Table 4.4 Equilibrium Phase Compositions for a Multicomponent Gas-Methanol-Water System

<i>Component</i>	<i>Feed</i>	<i>M o l e F r a c t i o n s</i>			
		<i>L i q u i d</i>		<i>V a p o r</i>	
		<i>Exper.*</i>	<i>Calcul.</i>	<i>Exper.*</i>	<i>Calcul.</i>
		Temperature = 288.85 K		Pressure = 16.71 MPa	
H ₂ O	0.85020	0.93337	0.93717	0.00028	0.00038
CH ₃ OH	0.05310	0.05830	0.05839	0.00077	0.00133
N ₂	0.00570	0.00020	0.00000	0.06219	0.06140
CH ₄	0.06875	0.00280	0.00227	0.74194	0.71833
C ₂ H ₆	0.00453	0.00010	0.00005	0.05196	0.04838
C ₃ H ₈	0.00187	0.00002	0.00001	0.02174	0.02004
n-C ₄	0.00075	0.00000	0.00000	0.00872	0.00808
n-C ₅	0.00075	0.00000	0.00000	0.00950	0.00808
CO ₂	0.01435	0.00521	0.00211	0.10290	0.13398

* Ng and Robinson (1983)

Table 4.5 Equilibrium Phase Compositions for a Multicomponent Gas-Methanol-Water System

<i>Component</i>	<i>Feed</i>	<i>Mole Fractions</i>			
		<i>Liquid</i>		<i>Vapor</i>	
		<i>Exper.*</i>	<i>Calcul.</i>	<i>Exper.*</i>	<i>Calcul.</i>
Temperature = 269.25 K		Pressure = 2.11 MPa			
H ₂ O	0.83370	0.87527	0.87552	0.00032	0.00022
CH ₃ OH	0.11700	0.12080	0.12285	0.00059	0.00049
N ₂	0.00291	0.00009	0.00000	0.06357	0.06091
CH ₄	0.03503	0.00107	0.00070	0.74828	0.71910
C ₂ H ₆	0.00231	0.00010	0.00002	0.04908	0.04790
C ₃ H ₈	0.00095	0.00003	0.00001	0.02022	0.01961
n-C ₄	0.00039	0.00000	0.00000	0.00982	0.00816
n-C ₅	0.00039	0.00000	0.00000	0.00823	0.00816
CO ₂	0.00732	0.00264	0.00090	0.09989	0.13545

* Ng and Robinson (1983)

Table 4.6 Equilibrium Phase Compositions for the CH₄-H₂O-CH₃OH System

<i>M o l e F r a c t i o n s</i>					
<i>Component</i>	<i>Feed</i>	<i>L i q u i d</i>		<i>V a p o r</i>	
		Exper.*	Calcul.	Exper.*	Calcul.
Temperature = 280.65 K Pressure = 9.09 MPa					
H ₂ O	0.8497	0.93871	0.93895	0.00009	0.00016
CH ₃ OH	0.0531	0.05854	0.05864	0.00009	0.00038
CH ₄	0.0972	0.00275	0.00241	0.99982	0.99946
Temperature = 268.15 K Pressure = 4.20 MPa					
H ₂ O	0.8330	0.87490	0.87539	0.00005	0.00010
CH ₃ OH	0.1168	0.12281	0.12273	0.00013	0.00033
CH ₄	0.0502	0.00229	0.00188	0.99982	0.99957
Temperature = 280.45 K Pressure = 18.57 MPa					
H ₂ O	0.7732	0.87260	0.87333	0.00008	0.00012
CH ₃ OH	0.1084	0.12250	0.12222	0.00026	0.00167
CH ₄	0.1184	0.00490	0.00445	0.99966	0.99821

* Ng and Robinson (1983)

Table 4.7 Equilibrium Phase Compositions for the Ethane - Water - Methanol System.

<i>Component</i>	<i>Feed</i>	<i>M o l e F r a c t i o n s</i>			
		<i>L i q u i d</i>		<i>V a p o r</i>	
		<i>Exper.*</i>	<i>Calcul.</i>	<i>Exper.*</i>	<i>Calcul.</i>
		Temperature = 270.05 K		Pressure = 0.470 MPa	
H ₂ O	0.9352	0.94074	0.94116	0.00076	0.00101
CH ₃ OH	0.0584	0.05877	0.05877	0.00076	0.00079
C ₂ H ₆	0.0064	0.00049	0.00007	0.99848	0.99820
		Temperature = 266.45 K		Pressure = 0.786 MPa	
H ₂ O	0.8680	0.87605	0.87661	0.00037	0.00046
CH ₃ OH	0.1220	0.12317	0.12320	0.00152	0.00086
C ₂ H ₆	0.0100	0.00078	0.00019	0.99811	0.99868

* Ng and Robinson (1984)

Table 4.8 Equilibrium Phase Compositions for the Propane - Water - Methanol System.

<i>M o l e F r a c t i o n s</i>					
<i>Component</i>	<i>Feed</i>	<i>L i q u i d</i>		<i>V a p o r</i>	
		Exper.*	Calcul.	Exper.*	Calcul.
		Temperature = 269.35 K		Pressure = 0.23 MPa	
H ₂ O	0.9359	0.94094	0.94122	0.00141	0.00187
CH ₃ OH	0.0584	0.05868	0.05873	0.00207	0.00141
C ₃ H ₈	0.0057	0.00038	0.00005	0.99652	0.99672

* Ng and Robinson (1983)

4.3 Methanol Dehydration Unit

As it was shown above, the composition of the equilibrium phases in systems containing methanol and water can be calculated with good accuracy. This makes the proposed methodology suitable for calculating the amount of methanol required to achieve a desired inhibiting effect. For example, consider that the dry Natural Gas II, shown in Table 4.1, is saturated with water at 302.55 K (29.4 °C) and 6.995 MPa. It is desired to cool it down to 277.55K (4.4 °C). The process to achieve this is shown in Figure 4.12. Methanol is injected prior to the cooling and the liquid water containing methanol is separated from the gas after the chiller. The pressure drops in the chiller and the piping are negligibly small. In order to find the amount of methanol, required in the process, that will depress the hydrate formation temperature to 277.55 K (4.4 °C) at 6.995 MPa, the computation scheme shown in Figure 4.1 is used to iterate on the amount of methanol. The results of these calculations for one million moles of the dry gas are shown in Table 4.9.

It is noted from Table 4.9 that Stream 4 contains 19.91 wt percent methanol. One can also obtain this concentration of methanol in the aqueous liquid phase using Figure 4.11 corresponding to the incipient hydrate formation conditions of 277.55 K (4.4 °C) and 6.995 MPa.

The amount of methanol lost in Stream 3 in the gas phase, as seen in Table 4.6, is about 88 % of the injected methanol. It is further noted that the amount of methanol required is 830 moles. If the Hammerschmidt method is used, the amount of methanol required is 230

moles. This difference emphasizes the need to account properly for the losses in the vapor phase.

The proposed method is a very useful design tool. It can be incorporated in a process simulator in order to perform calculations in situations similar to that shown in Figure 4.12.

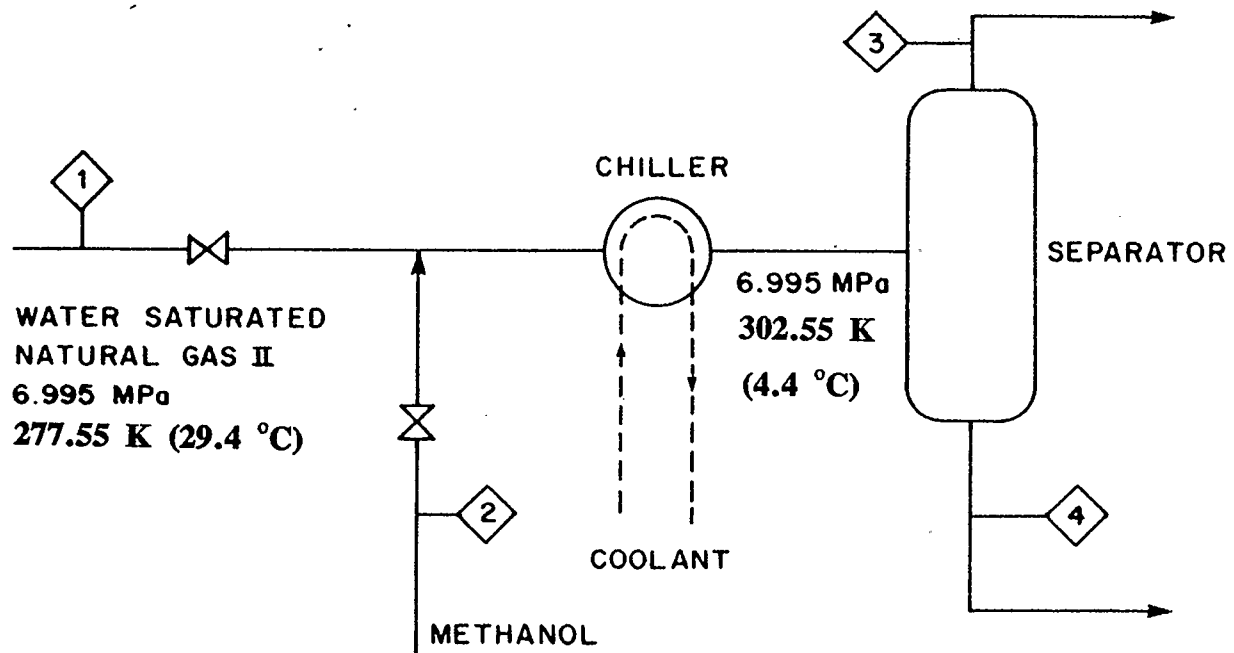


Figure 4.12 Methanol Dehydration Unit

Table 4.9 Water and Methanol Flows per One Million Moles of Dry
Natural Gas II

<i>Moles in Stream</i>				
<i>Component</i>	1	2	3	4
H ₂ O	1000	-	285	715
CH ₃ OH	-	830	730	100

5. EXPERIMENTAL APPARATUS AND PROCEDURE

In this chapter the experimental apparatus which was designed and constructed is presented. However, before that, background information on the previous experimental studies will be presented. Particularly, the presentation concerns the methods followed by various researchers for performing hydrate equilibrium experiments. A part of this background information includes an experimental procedure developed in our laboratory by using the apparatus for gas hydrate kinetics studies.

5.1 Background on Gas Hydrate Experimental Methods

During the first century following the discovery of gas hydrates in 1810, only experimental studies were conducted. The objectives of these studies were to identify (a) the molecules which form gas hydrates and (b) the conditions under which this phenomenon takes place. A thorough account for all the work during the first century following the discovery of gas hydrates can be found in two monographs (Berecz and Balla-Achs, 1983; Sloan, 1989). Tremendous experimental work, mainly for natural gas components and their mixtures was conducted in both the industry and the academia during the last fifty years. The research was a direct result of the necessity to know the conditions under which a natural gas pipeline and other processing facilities could be plugged due to gas hydrate formation.

The experimental methods for the determination of the pressure and temperature conditions at which gases and water form hydrates can be categorized as visual and non-visual depending upon the ability of the experimenter to observe the formation and decomposition of the gas hydrate crystals. Most of the experimental studies were carried out in equilibrium cells with windows which allowed for visual observation. The experiments were performed under isothermal or isobaric conditions. In the present work the experiments will be performed in a visual cell under isothermal conditions.

5.1.1 Visual Methods

The visual methods have the advantage that the phase change can be visually confirmed. However, there is a pressure limit up to which a cell with windows can be used.

Isobaric Operation (Temperature Search Method)

A windowed cell containing water and immersed into a temperature controlled bath is pressurized with the gas mixture having the desired composition. The most standard procedure is to pressurize the cell up to the working pressure at a temperature above the hydrate forming conditions. The pressure is maintained constant by the exchange of gas or liquid with an external source. Mixing of the contents in the cell is achieved by rocking, agitation or magnetic stirring. Nucleation of the

hydrates is induced by cooling the cell to a temperature well below (5-10 K) the expected equilibrium conditions. Once the hydrates are formed the cell is heated slowly up to the point where all the hydrates have dissociated. The temperature is kept at a degree or so higher than this decomposition point in order to ensure complete hydrate dissociation. Subsequently, the temperature is lowered slightly to recrystallize the hydrate. Nucleation is achieved easily now because of the enhanced degree of structurilization of the water. Only a small amount of hydrate is allowed to form, and the temperature is raised again until the new hydrate crystals at the window of the cell begin to dissociate. The temperature and the pressure at this point are considered equilibrium values.

The most recent examples of researchers who applied this technique are Wu et al. (1976); Ng and Robinson (1985) and Holder and Hand (1982). Their apparati have evolved from that constructed by Deaton and Frost (1937) and those developed by Katz and his coworkers (Wilcox et al. 1941; Kobayashi and Katz 1949). It should be noted that the essential features of these apparati remain unchanged until today.

Isothermal Operation (Pressure Search Method)

John and Holder (1982) while studying the methane-n-butane system followed a procedure whereby hydrates are formed, the temperature is fixed and the pressure is adjusted to a value about 50 kPa greater than the equilibrium hydrate formation pressure for methane at that

temperature. The pressure is then reduced by 100 kPa, and sufficient time is allowed for the system to equilibrate (approximately 24-36 hours). The equilibrium pressure is noticed and a gas sample is obtained in a sampling bulb and then analyzed chromatographically. Due to sampling, a pressure drop of about 100 kPa occurs and the system, is allowed to reach a new equilibrium point. Hence, one can obtain a sequence of isothermal pressure-composition measurements.

Earlier, Bond and Russell (1949) had followed similar procedures. They studied hydrogen sulfide hydrate formation in pure water or in the presence of methanol. In the case of pure water, the pressure is released until a considerable amount of hydrate has decomposed. The pressure at this point is somewhat lower than the equilibrium pressure. Standing at constant temperature the system, containing liquid water with dissolved hydrogen sulfide, solid hydrate and gaseous H_2S , shows a slow increase in pressure. After the pressure has become constant, additional H_2S is bled off to cause a slight reduction in pressure. The system is allowed to stand. Generally, it is observed that the pressure again rises to the same constant pressure that was first observed. This constant, reproducible pressure is taken to be the equilibrium pressure.

When they performed experiments in the presence of methanol, hydrogen sulfide was withdrawn at intervals and the pressure increase on standing was observed, as with pure water. As this continued, the hydrate slowly disappeared. The pressure observed at the point where the last trace of solid hydrate disappeared was taken as the equilibrium pressure for the solution at the given temperature. The above procedures

required 2 to 4 hours to determine an equilibrium point with pure water and about 4 to 6 hours for the experiments with methanol.

Vysniauskas and Bishnoi (1983; 1985) designed a constant volume cylindrical cell with marine-type windows to study the kinetics of hydrate formation. High agitation rates were accomplished by magnetic stirring. The cell is immersed into a temperature controlled bath. This equipment offers the advantage of very good mixing and quick elimination of the hysteresis phenomena by selecting a high agitation rate.

Based on my experience from the experimental and theoretical kinetic studies that I had conducted earlier (Englezos, 1986), a procedure, similar to that by Bond and Russell, was formulated in order to provide equilibrium hydrate formation data for single gases using the apparatus of Vysniauskas and Bishnoi. The equipment can not be used for studying gas mixtures because it is a constant volume cell with no provision for sampling. A number of experimental data for methane hydrate formation in the presence of NaCl and NaCl + KCl were obtained.

The experimental apparatus which was originally designed by Vysniauskas and Bishnoi (1983) and later modified by Dholabhai (1989) is shown in Figure 5.1. The cell is shown in Figure 5.2. Only a part of the assembly is used for the equilibrium studies. A detailed description of the apparatus can be found in the following references (Vysniauskas and Bishnoi, 1983; Dholabhai, 1989).

An Experimental Procedure Using the Kinetics Apparatus

The cell is charged with 250 ml of distilled and de-ionized water or the electrolyte solution and the agitation is started. The temperature is kept constant throughout the experiment. The cell is twice pressurized with methane gas which is subsequently discharged. After that, the cell is pressurized again with methane gas to a pressure well above the expected equilibrium hydrate formation pressure at the system temperature. A pressure difference of about 1.2 to 1.5 MPa is usually adequate to induce the nucleation of the hydrate crystals quickly. A value for the equilibrium pressure can be estimated using the method presented in chapter 3. Once the hydrates have been formed the pressure is slowly decreased by releasing the gas. The system is left at a pressure somewhat below the expected equilibrium pressure. The amount of hydrate crystals is usually very small at this point.

The temperature and the pressure are monitored with the aid of the data acquisition system. If for a period of 3 to 4 hours the temperature and the pressure remain steady while a very small amount of hydrates is present this pressure is taken as the equilibrium pressure at this temperature. If no hydrates are present that means that the equilibrium pressure is higher. In this case, hydrates are formed again as before and the pressure is left to stabilize at a value of 0.1 MPa above the previously set pressure.

The electrolyte solutions were prepared by weighing the suitable amounts of electrolytes and dissolving them into a known volume of water

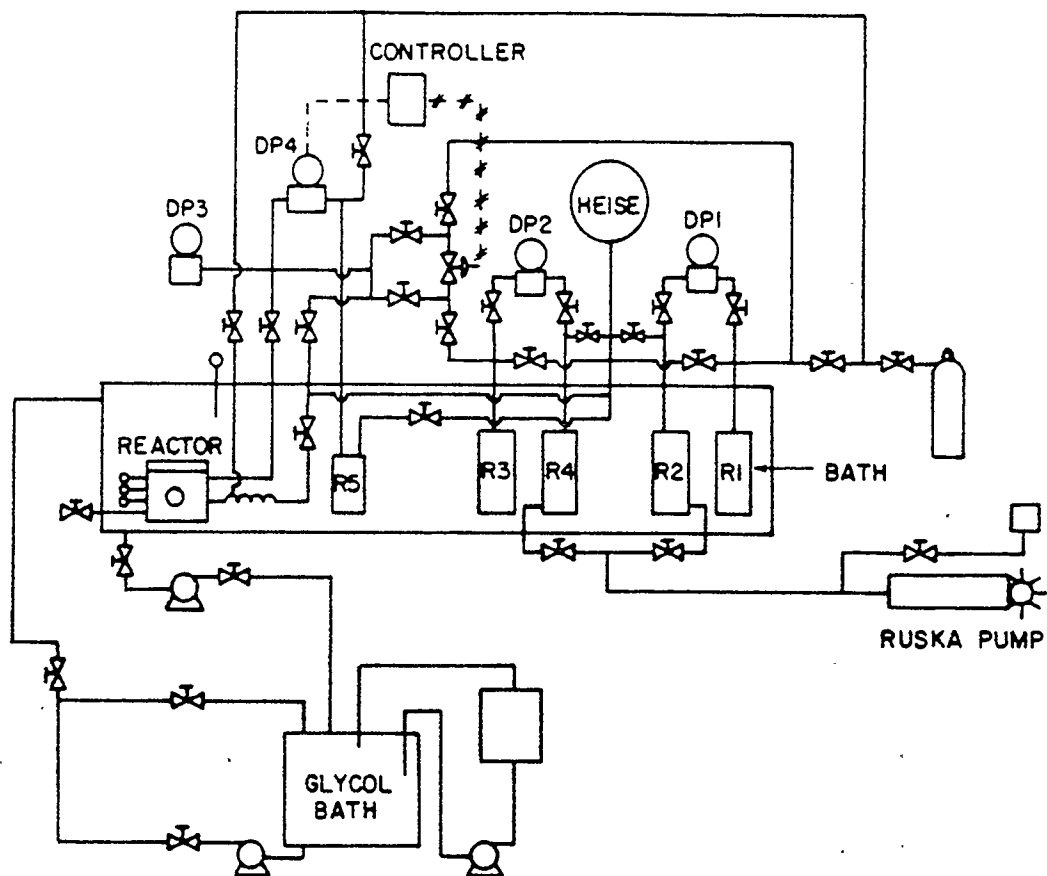


Figure 5.1 The Experimental Apparatus for Hydrate Kinetic Studies

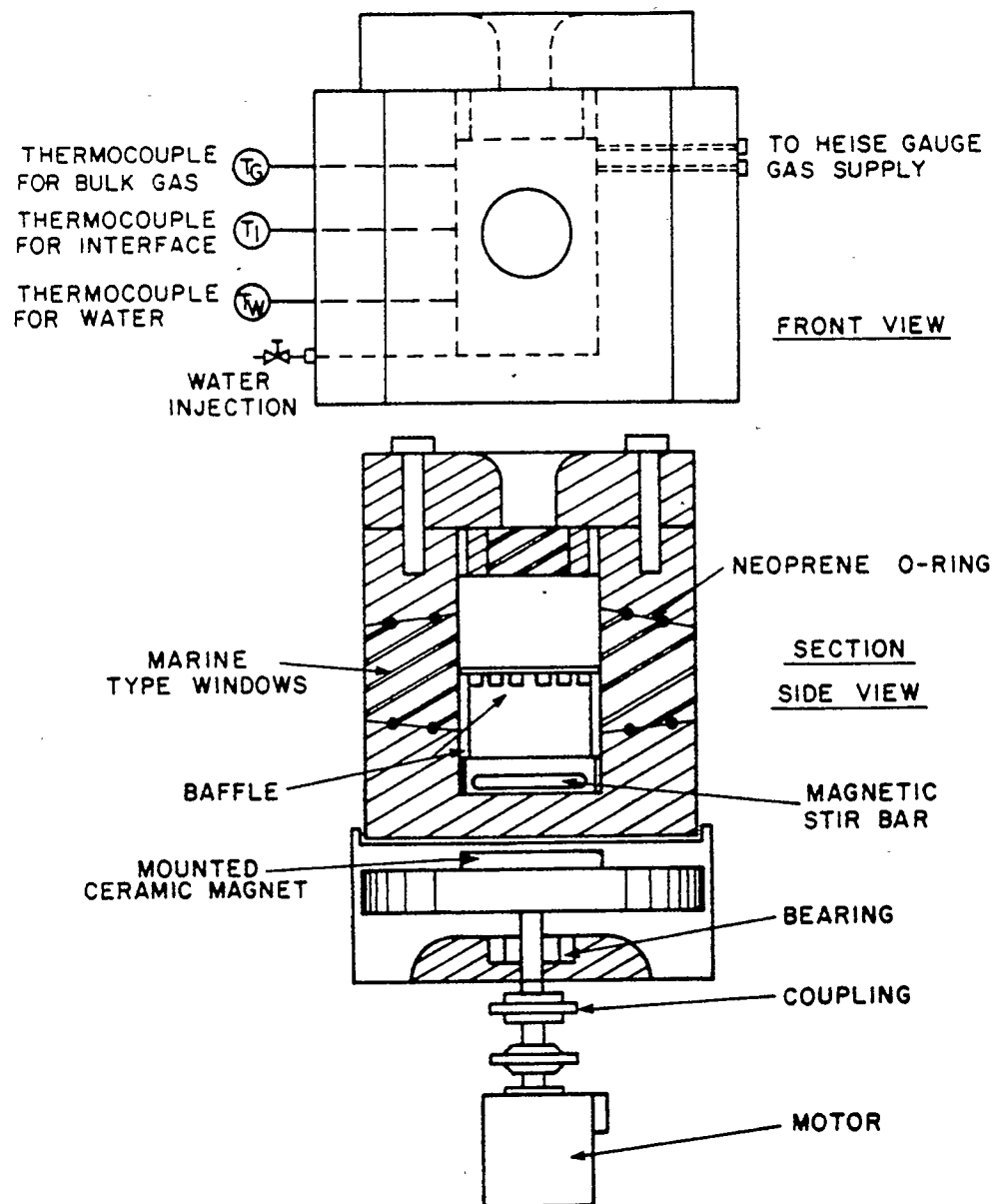


Figure 5.2 The Constant Volume High Pressure Cylindrical Cell

A Mettler balance with a resolution of 0.01 g was used. The pressure is believed to be known within ± 0.025 MPa whereas the temperature within ± 0.05 °C (Dholabhai et al. 1990).

5.1.2 Non-visual Methods

During hydrate formation or decomposition in an isochoric cell there is a pressure drop associated with the process. Marshall et al. (1964) developed a method based on this phenomenon. The method was automated by Schroeter et al. (1983). The cell is filled with water and pressurized with gas to a pressure above the equilibrium conditions at the given temperature. The system is cooled until hydrates are formed. At this point there is a significant pressure drop due to hydrate formation. Subsequently, the system is heated. The cooling and heating processes are computer controlled. During the experiment the pressure-temperature hysteresis curves associated with formation and decomposition are observed and stored. The equilibrium conditions are taken to be the point where the heating and cooling P-T curves intersect. The cell contents are mixed by rocking and the mixing process is further enhanced by placing two stainless steel balls inside.

5.1.3 Experimental Data Using the Kinetics Apparatus

Six methane hydrate formation experiments in the presence of 3 wt per cent NaCl and seven in the presence of a mixture of 3 wt per cent

NaCl and 3 wt per cent KCl were performed. The results are shown in Table 5.1 and Figure 5.3. Also shown in the figure are the experimental data of Roo et al. (1983) at 11.75 wt % NaCl and 0.0 wt %. In the figure, the solid lines represent the calculated hydrate formation pressures using the method presented in chapter 3. The activity of water was calculated by using Pitzer's model for the single electrolyte solutions and the method of Patwardhan and Kumar (1986) for the mixed solution of NaCl and KCl. As seen from the figure, the experimental data for 3 wt % NaCl and 3 wt % NaCl + 3 wt % KCl are consistent with those for pure water and 11.75 wt % NaCl solutions, and the corresponding predictions.

The agreement between the experimental data and the predictions is very good. The maximum per cent deviation between the experimental and the calculated hydrate formation pressures is 5.56 per cent in the case of hydrate formation in pure water and 1.60 in the cases of hydrate formation in the 11.75 wt % NaCl solution. The maximum per cent deviations for the experimental data of this work are 0.58 in the case of the 3 wt per cent NaCl solution and 2.60 per cent for the mixed salt solution. The largest deviations, although not significant in absolute numbers, are observed in the case of hydrate formation in pure water. Deviations of this magnitude are expected for hydrate formation predictions in view of the uncertainties for the thermodynamic parameters of hydrates as it was mentioned in chapter 4. There is no specific reason for the fact that the predictions in the presence of salts are found to be better.

Table 5.1 Experimentally Determined Methane Hydrate Formation Pressures in the Presence of Aqueous Solutions of Sodium Chloride and Potassium Chloride

<i>Electrolyte</i>	<i>Temperature (K)</i>	P_{exp} (MPa)
NaCl (3 wt %)	272.69	2.753
	274.36	3.243
	276.49	3.993
	277.23	4.303
	278.34	4.807
	279.35	5.361
NaCl (3 wt %) + KCl (3 wt %)	271.35	2.704
	273.04	3.192
	275.19	3.873
	276.17	4.346
	277.20	4.746
	277.75	5.106
	279.21	5.857

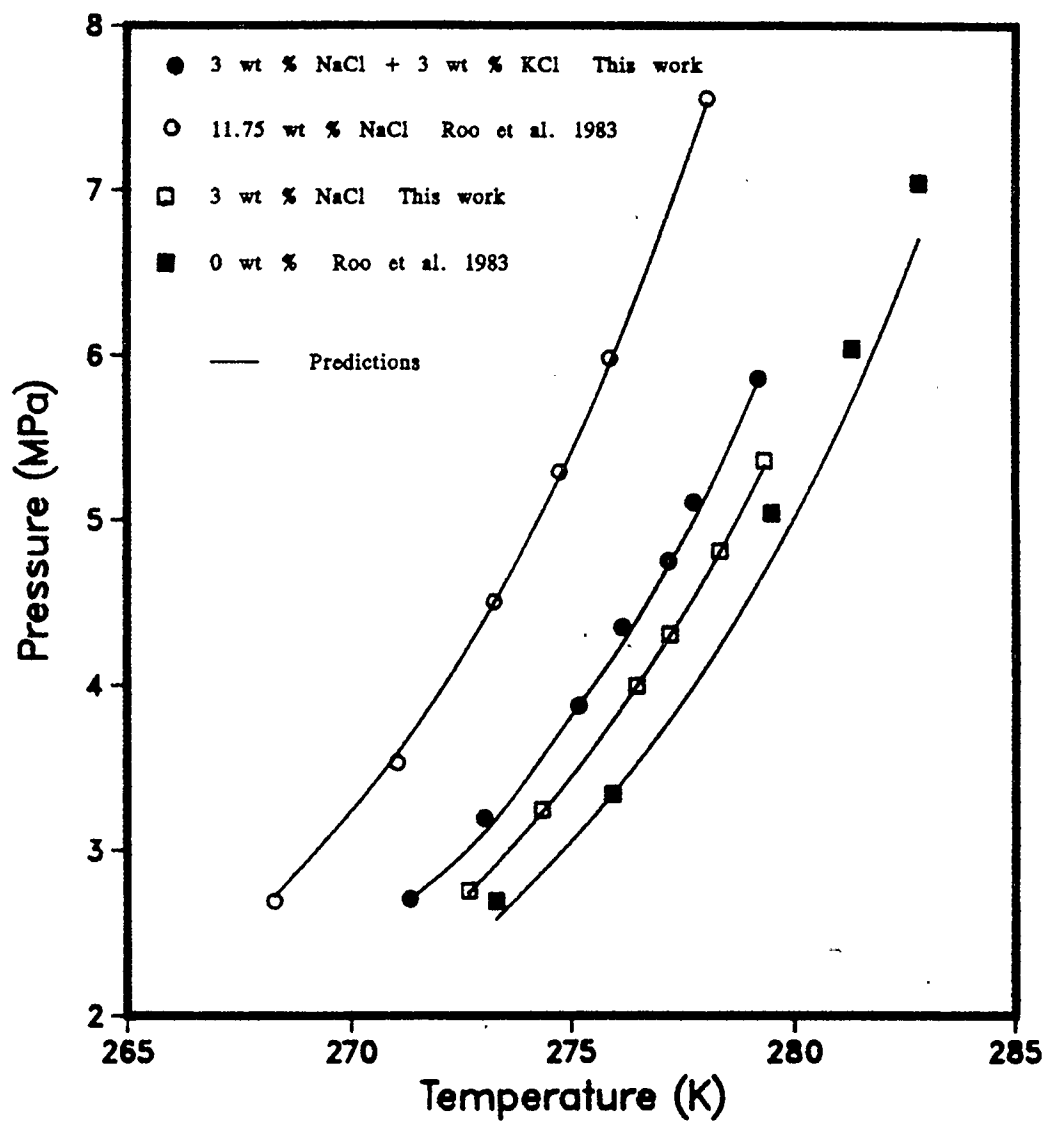


Figure 5.3 Experimental and Predicted Pressures for Methane Hydrate Formation in Aqueous Solutions of NaCl and a Mixture of NaCl and KCl.

5.2 Design of a New Experimental Apparatus

From an experimental viewpoint the important aspects relating to equilibrium in a hydrate forming system which should be taken into account when designing an apparatus are the mixing of the phases, the desire to observe the phase changes visually and the hysteresis phenomenon. The location of the pressure-temperature point of hydrate formation depends on the history of the liquid phase (Vysniauskas and Bishnoi, 1983).

Keeping in mind these aspects and based on the experience gained with the equipment for the gas hydrate kinetic studies, a new experimental apparatus for the collection of equilibrium hydrate formation data from single gases or gaseous mixtures was designed and fabricated. The equilibrium cell has windows which permit visual observation of its contents.

5.2.1 Apparatus

The block diagram of the experimental apparatus is shown in Figure 5.4 whereas the detailed schematic of the apparatus is shown in Figure 5.5. The heart of the apparatus is the equilibrium cell which is immersed into a temperature controlled bath. A mixture of ethylene glycol and water (50-50 weight per cent) is used as the refrigeration/heating fluid. The temperature in the bath can be maintained at ± 0.1 K over a long period of time. The refrigerator is

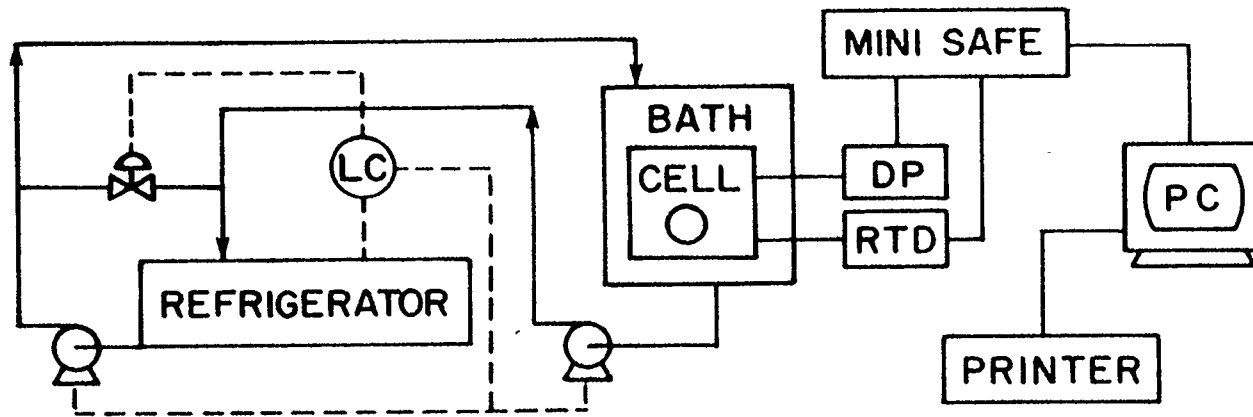
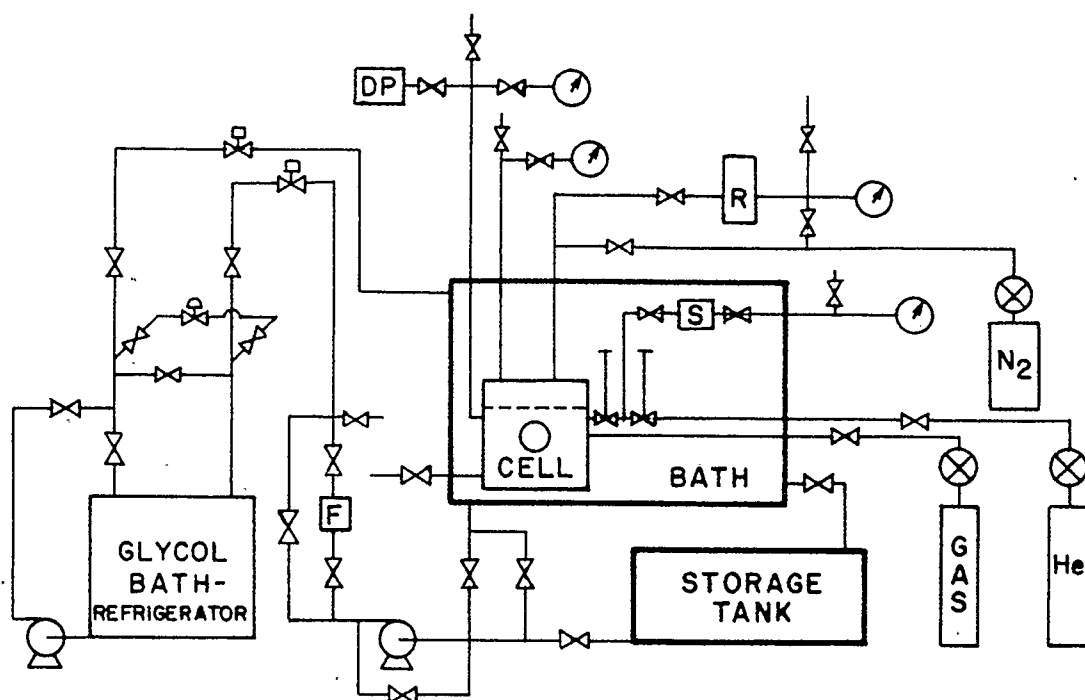


Figure 5.4 Block Diagram of the Experimental Apparatus



LEGEND

DP DP CELL
 R NITROGEN RESERVOIR
 S SAMPLING BOMB
 F FILTER
 ⋈ ON / OFF VALVE

⊙ PRESSURE GAUGE
 ⊗ PRESSURE REGULATOR
 ⊠ SOLENOID VALVE
 ⊞ PNEUMATIC DIAPHRAGM
 CONTROL VALVE

Figure 5.5 Schematic of the Experimental Apparatus

the model 2425 by Forma Scientific, Inc. It has a capacity of 189.3 Liters. The two pumps for the circulation of the glycol-water mixture are the ECJ1 (next to the refrigerator) and ECD1 models by Eastern Centrichem. Copper tubing (1/2") is used for the circulation of the glycol. There is a level control system which prevents the overflow or drainage of the refrigerator tank. In addition, two solenoid valves are used to interrupt the flow when there is a power failure.

The pressure and temperature are monitored with the aid of the miniSAFE data acquisition system, available by Control Microsystems and connected to a Zenith personal computer. The Crosstalk software package is used to establish communication between the PC and the miniSAFE data acquisition system

5.2.2 The Equilibrium Cell

The cell is a variable volume high pressure vessel. The volume of the cell is changed by a floating piston. Sealing of the piston is achieved by using two neoprene o-rings. Two cross sections at an angle of 90 ° are shown in Figures 5.6 and 5.7. The lid of the cell is closed using eight 1/2" stainless steel bolted studs. A neoprene o-ring is used to seal the lid. The cell is equipped with two marine type windows made of plexiglas. They are also sealed using neoprene o-rings.

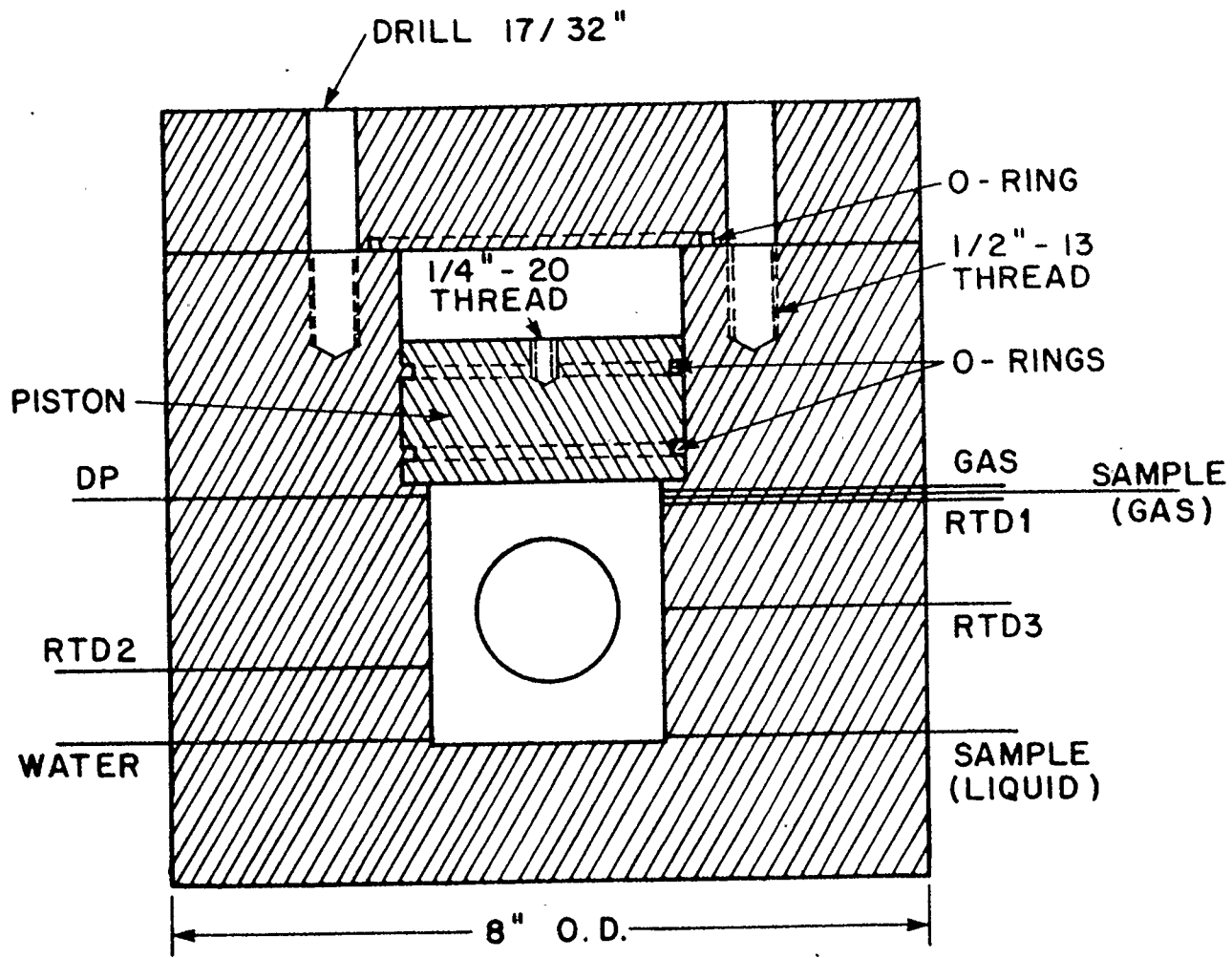


Figure 5.6 A Cross Section of the Equilibrium Cell

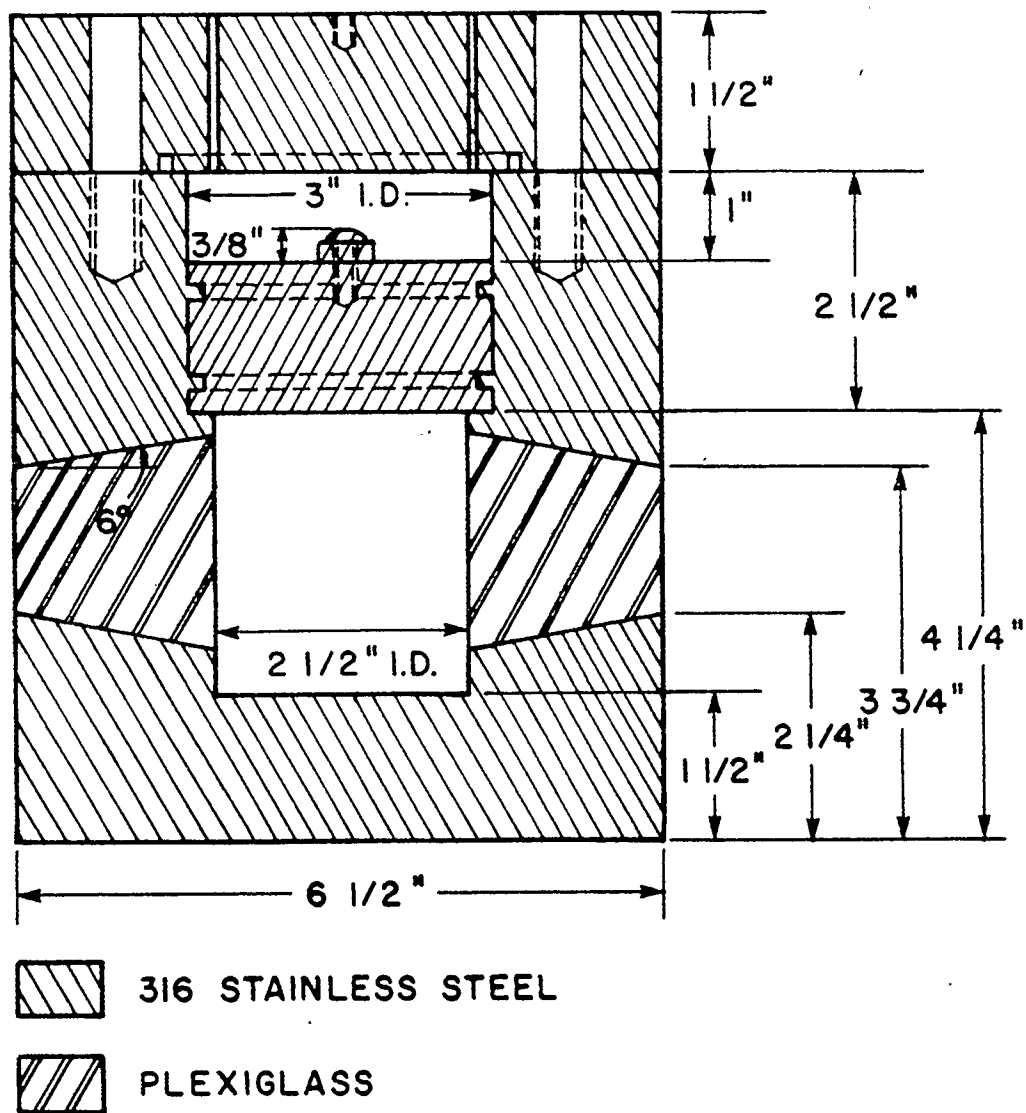


Figure 5.7 A Cross Section of the Equilibrium Cell

Stirring of the cell contents is accomplished by a magnetic stir bar coupled to a set of ten magnets mounted outside and underneath the cell. The magnets are enclosed in an aluminum housing. A DC motor equipped with an rpm controller provides rotation of the magnets with the aid of the 0.5" shaft. The dimensions of the magnets are $7/8 \times 1 \ 7/8 \times 3/8$ in inches and were obtained by Tormag Engineering Products Ltd. The stirring mechanism assembly is shown in Figure 5.8.

The temperature of the cell contents is monitored with omega platinum resistance thermometers. The pressure is measured with two instruments. A Rosemount differential pressure transducer is connected with the data acquisition system. Also, a 0-15 MPa Bourdon tube Heise pressure gauge is used. Nitrogen gas is used to drive the piston in order to change the volume of the cell.

A standard Rosemount platinum resistance thermometer, model 162 CE, with an accuracy better than $0.03 \text{ }^{\circ}\text{C}$ was used for the calibration of the resistance thermometer probes (RTD's). The resistance of the standard thermometer was measured by the Guildline 9577 Precision Digital Voltmeter and converted to temperature by using a calibration table for this thermometer. The table was supplied by the Instrumentation Laboratory of the Department of Electrical Engineering at the University of Calgary. A triple point apparatus for water was used in order to compare the three RTD's against the standard thermometer. Since it was found that the three RTD's were giving temperatures different than zero (0.08, 0.16 and 0.22 respectively) the RTD conditioning box was adjusted

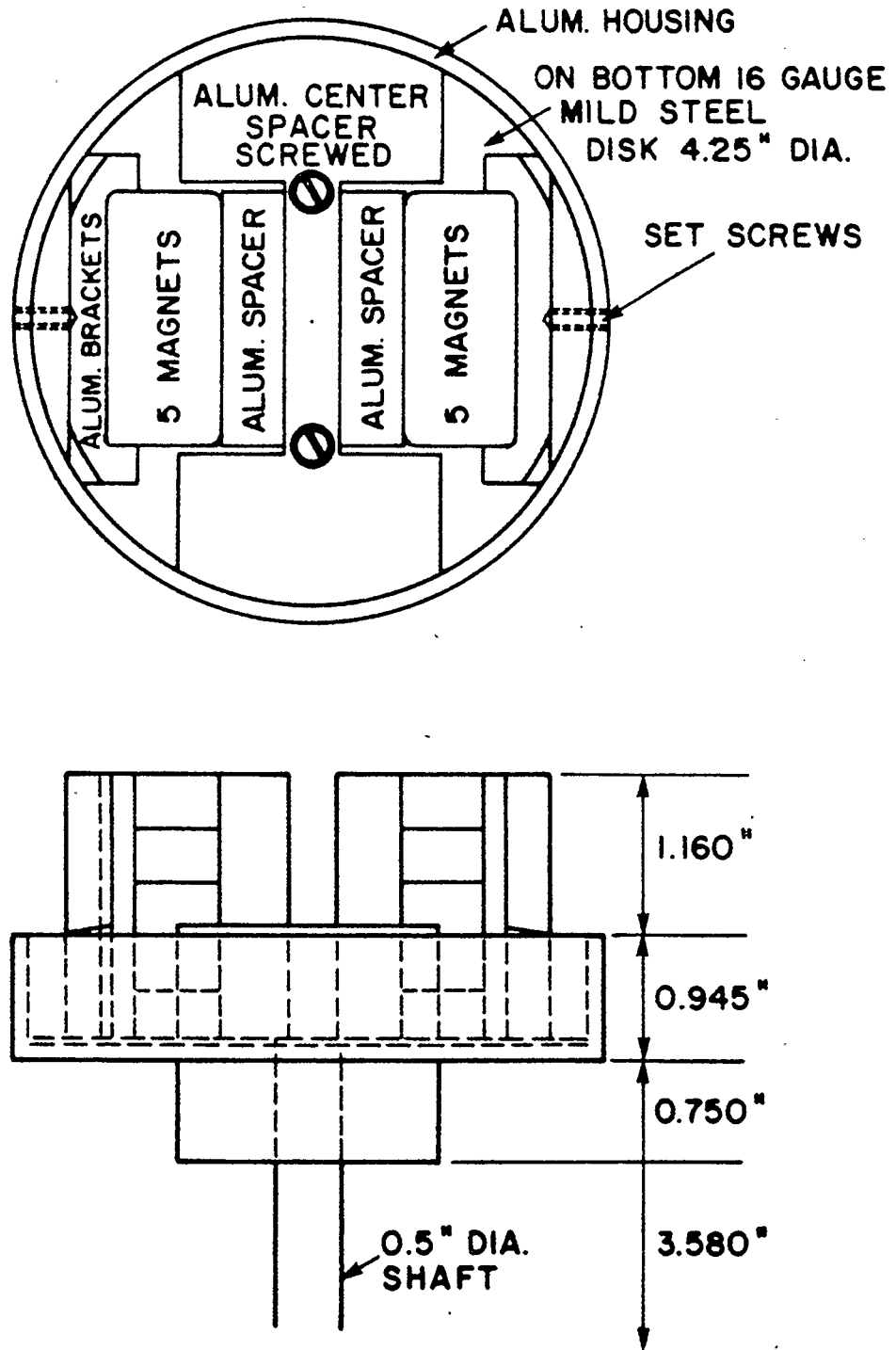


Figure 5.8 The Stirring Mechanism Assembly

so that the three RTD's read 274.15 K. The comparison of the three RTD's and the standard thermometer was also done at two other temperatures (-265.15 and 282.40K). These temperatures were obtained by placing the RTD's and the standard thermometer in the constant temperature glycol bath. A straight line was fitted to the measurements for each RTD. The maximum estimated standard deviation was 0.055. The RTD's have an accuracy of ± 0.05 K and the drift was found to be less than ± 0.01 K. Hence, the temperature measurements are believed to be within ± 0.06 K.

The Chandler Dead-Weight Tester was used for the calibration of the differential pressure transducer and the Heisse gauge. This standard pressure measurement device has an accuracy of 0.1 % of indicated pressure. The calibration was done for the 0-500 psi pressure range, hence the maximum inaccuracy of the Dead-Weight Tester is 3.447 kPa. The DP transducer has an accuracy of ± 2 % of span, or ± 8.62 kPa. It includes combined effects of linearity, hysteresis and repeatability. Forty measurements were compared against the Dead Weight Tester and the results were fit to a straight line. The pressure is believed to be known within ± 10.0 kPa. The resolution of the 12-bit data acquisition system is calculated to be 1.05 kPa for the pressure measurements and 0.005 °C for the temperature measurements.

5.3 Experimental Procedure

Using the Mettler balance the electrolyte solution is prepared and an amount of approximately 115 cm³ is charged into the cell. Once

constant temperature has been achieved, the hydrate forming gas is supplied to the cell and discharged twice. Subsequently, the cell is pressurized with the gas to a pressure slightly above (20-30 kPa) the calculated equilibrium pressure. Stirring is now commenced, and the system is allowed to stay there until the temperature is stable. Usually, the temperature is selected to be the temperature at which the highest experimental hydrate formation pressure will be obtained. Only the temperature measurement of the probe RTD3 is used.

Once the temperature is constant, hydrate nucleation is induced by increasing the pressure in the gas phase. This is achieved without the introduction of new gas from the cylinder but with the use of the nitrogen driven piston. Hydrates are usually formed in a few minutes. Subsequently, they are decomposed by decreasing the pressure. This induced nucleation is repeated once more. The purpose is to achieve an enhanced degree of structurilization of the aqueous liquid phase and eliminate the hysteresis phenomenon. For each solution under study this is performed only at the first experimental temperature.

After the complete decomposition of the hydrate crystals for the second time, the cell is again pressurized to a pressure somewhat above the equilibrium pressure and then the hydrate formation is induced by increasing the pressure using the nitrogen driven piston. After a small amount of hydrates is formed, the pressure is decreased by releasing the nitrogen gas thus moving the piston upwards. The system is then left at these conditions. The pressure and temperature are monitored and printed every five minutes. If for a period of three to four hours the

temperature and pressure remain steady while there is a very small amount of hydrates present, then this pressure is taken as the equilibrium pressure at this constant temperature. If no hydrates are present, it means that the equilibrium pressure is higher. In this case, nucleation of hydrates is induced again. However, the pressure is now set at a value higher (30-40 kPa) than the previously set. The experiment is ended once the pressure and temperature are stable with the hydrate phase present.

5.4 The Validity of the Experimental Apparatus and the Procedure

In order to establish the validity of the experimental set up, six experiments were performed for the ethane-water system and the results were compared with the data available in the literature. In Figure 5.10 the literature data from two sources together with the experimental data obtained in the present work are shown. The calculated hydrate formation pressures using the method presented in chapter 3 are also shown in the figure. The numerical values of the measured data are given in chapter 6. As seen from the figure there is very good agreement among all the experimental data and the predictions are slightly above the data. The maximum deviation of the experimental data obtained in our equipment and the predictions is 2.74 per cent. The maximum deviations between the predictions and the data of Deaton and Frost and the data of Holder and Hand are 3.33 and 2.56 per cent respectively.

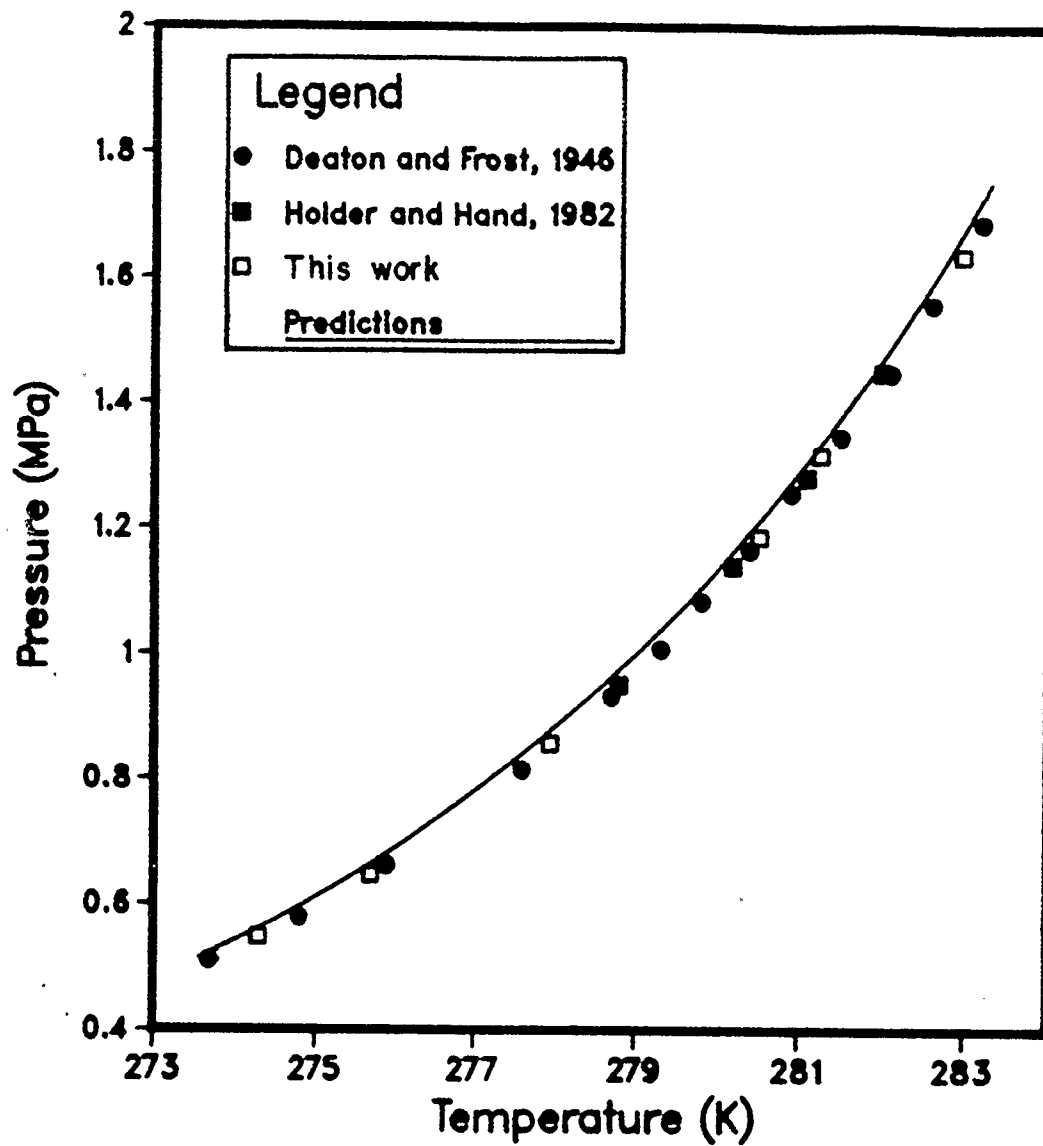


Figure 5.9 Comparison of the Experimental Data Obtained in this Work and the Data of Other Workers

6. EXPERIMENTAL RESULTS

As it was mentioned in chapters one and two there were no experimental equilibrium hydrate formation data in the presence of mixed electrolytes at the time when this study was initiated. Also, experimental data for the main natural gas components were reported only for methane and propane in the presence of single electrolytes. The experimental data for methane hydrate which were presented in the previous chapter and the data obtained by Dholabhai (1989) were the first hydrate formation data in the presence of mixed electrolytes. Since there were no data available for ethane hydrate, it was decided to study this hydrocarbon hydrate.

6.1 Experimental Data with the New Experimental Apparatus

Six ethane hydrate formation experiments in pure water were performed in order to compare the results with the data obtained by other researchers. These data together with the data from two other sources are given in Table 6.1. A graphical representation was also given in Figure 5.9. It was found that the new experimental apparatus and the procedure of performing the experiments gives results which are consistent with the data from other laboratories. After these experiments a series of experiments with electrolytes were performed. The electrolytes which are mostly encountered in sea or ground water were used. These are NaCl, KCl and CaCl₂. First, experiments were

performed with single salt solutions of each one of these salts. Then, experiments were performed with binary salt solutions at one concentration. The NaCl-KCl binary was also examined at a second concentration. One ternary solution and a four-component mixture were also studied. The fourth electrolyte was KBr. The selected concentrations were small enough so that the molalities were within the suggested range for using the electrolyte activity coefficient model and no precipitation of salt could happen. The salt concentrations however were large enough to be relevant to industrial applications and to test the predictive method. A sample of each aqueous solution was taken in a flask and immersed into the bath in order to verify the absence of any salt precipitation at the experimental temperature.

All the experimental data are given in Tables 6.2 to 6.4. In Figures 6.1 to 6.3 these results together with the results for hydrate formation in pure water are given in graphical form. In these figures the solid lines represent the predictions using the method presented in chapter 3. It is seen that the predictions agree very well with the experimental data. In Figure 6.1 the maximum and smallest absolute deviations between the experimental and the calculated hydrate formation pressures are 7.07 and 0.76 per cent respectively. The average absolute deviation is 3.19 per cent. In Figure 2 these quantities are 4.58, 0.22 and 2.13 per cent and in Figure 3 they are 2.78, 0.08 and 1.53 per cent. It is concluded that the predictive method of chapter 3 can represent very well the experimental hydrate formation data in the presence of single or mixed electrolytes and hence it is useful for process design.

Table 6.1 Experimental Data on Ethane Hydrate Formation Pressures in Pure Water

<i>Temperature</i> (K)	<i>Experimental Pressure (MPa)</i>		
	This Work	Deaton and Frost, 1946	Holder and Hand, 1982
273.70	-	0.510	-
274.30	0.548	-	-
274.8	-	0.579	-
275.70	0.647	-	-
275.90	-	0.662	-
277.60	-	0.814	-
277.95	0.856	-	-
278.70	-	0.931	-
278.80	-	-	0.950
279.30	-	1.007	-
279.80	-	1.083	-
280.20	-	-	1.140
280.40	-	1.165	-
280.53	1.186	-	-
280.90	-	1.255	-
281.10	-	-	1.280
281.27	1.136	-	-
281.50	-	1.345	-
282.00	-	-	1.450
282.10	-	1.448	-
282.60	-	1.558	-
282.98	1.637	-	-
283.2	-	1.689	-

Table 6.2 Experimental Data on Ethane Hydrate Formation
Pressures in Aqueous Solutions of Single Salts

<i>Electrolyte</i>	<i>Temperature (K)</i>	P_{exp} (MPa)
NaCl (20 wt %)	271.90	1.825
	270.55	1.499
	268.80	1.196
	267.10	0.942
	265.36	0.736
KCl (12.295 wt %)	269.51	0.495
	272.00	0.683
	274.68	0.956
	276.73	1.277
	278.40	1.577
CaCl ₂ (15 wt %)	267.17	0.573
	269.21	0.736
	271.29	0.967
	273.28	1.249
	275.20	1.613

Table 6.3 Experimental Data on Ethane Hydrate Formation
Pressures in Aqueous Solutions of Mixed Salts

<i>Electrolyte</i>	<i>Temperature (K)</i>	P_{exp} (MPa)
NaCl (9.934 wt %) +	269.20	0.846
KCl (9.934 wt %)	271.28	1.130
	273.14	1.401
	275.09	1.851
NaCl (10.0 wt %) +	266.87	0.519
CaCl ₂ (5.0 wt %)	269.90	0.748
	272.17	1.010
	273.86	1.266
	276.13	1.728
CaCl ₂ (5.0 wt %) +	268.08	0.500
KCl (10.0 wt %)	270.07	0.637
	272.32	0.853
	274.05	1.030
	276.43	1.454

Table 6.4 Experimental Data on Ethane Hydrate Formation Pressures in Aqueous Solutions of Mixed Salts

<i>Electrolyte</i>	<i>Temperature (K)</i>	P_{exp} (MPa)
NaCl (10.0 wt %) + KCl (5.0 wt %)	267.13	0.488
	269.35	0.650
	271.94	0.920
	274.46	1.282
	276.53	1.694
NaCl (6 wt %) + CaCl ₂ (3 wt %) + KCl (5 wt %)	269.01	0.558
	270.55	0.661
	273.55	0.986
	275.90	1.357
	278.43	1.969
NaCl (5 wt %) + CaCl ₂ (3 wt %) + KCl (5 wt %) + KBr (3 wt %)	269.35	0.616
	271.00	0.765
	273.55	1.061
	276.30	1.499
	278.77	2.188

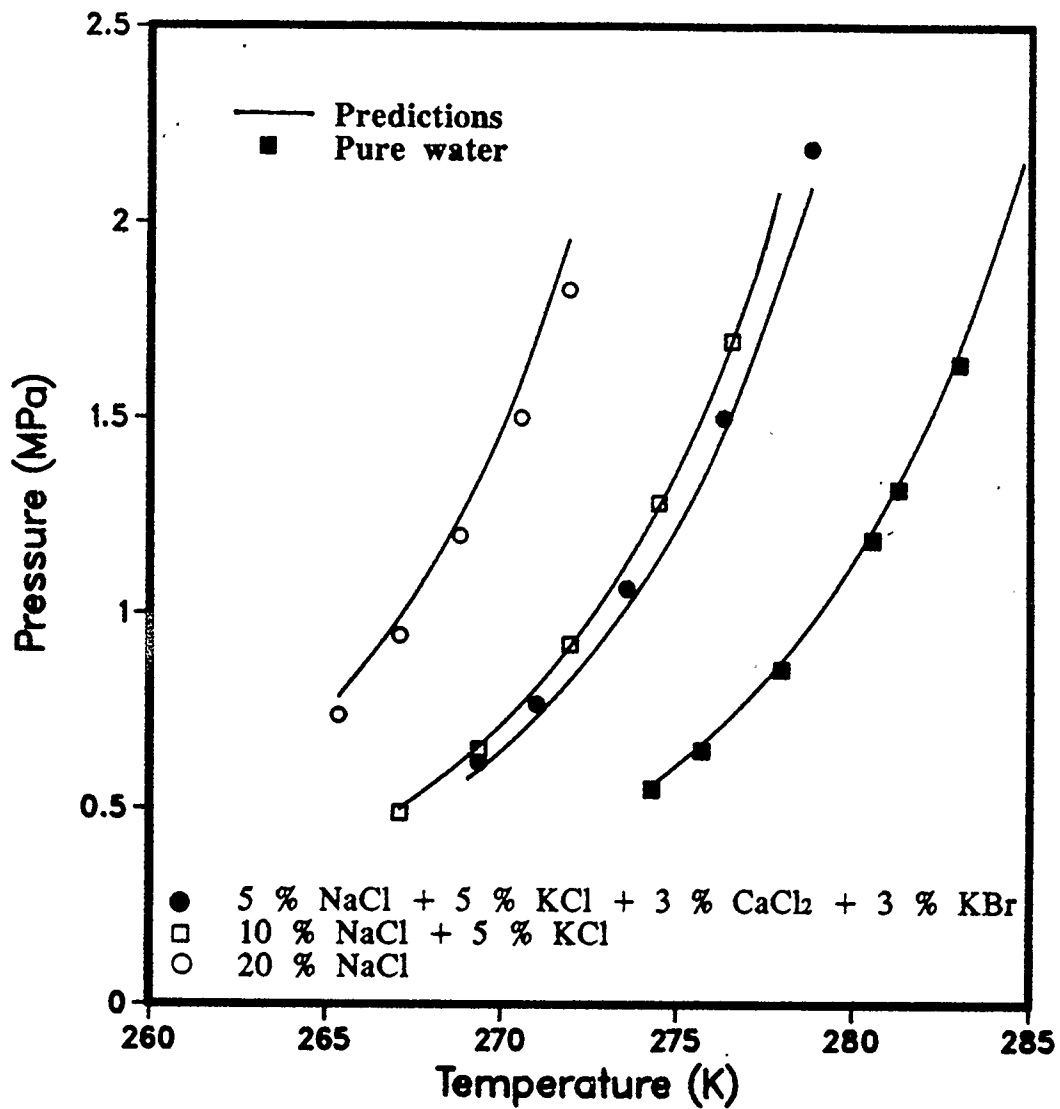


Figure 6.1 Experimental Data and Predicted Ethane Hydrate Formation Pressures in Aqueous Salt Solutions

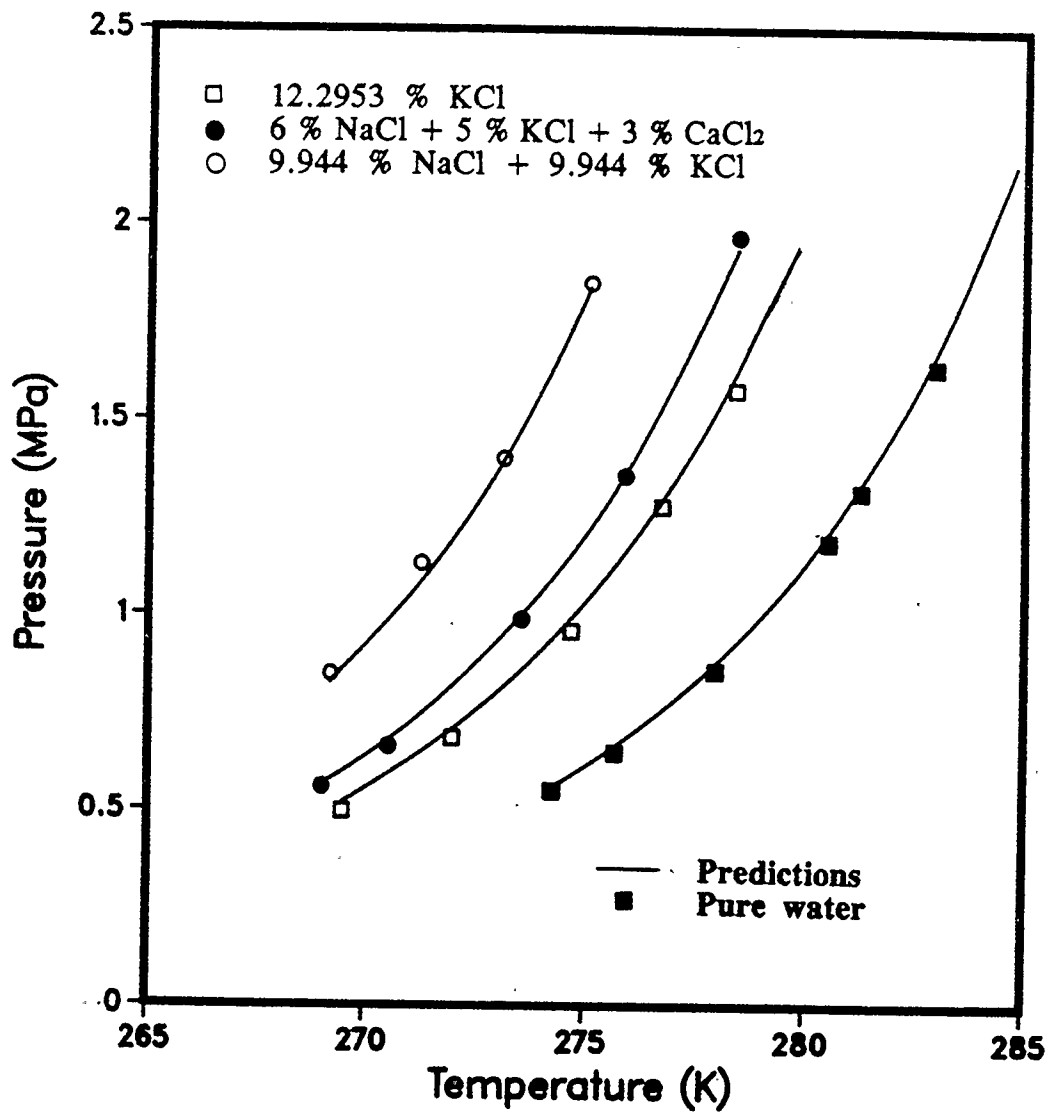


Figure 6.2 Experimental Data and Predicted Ethane Hydrate Formation Pressures in Aqueous Salt Solutions

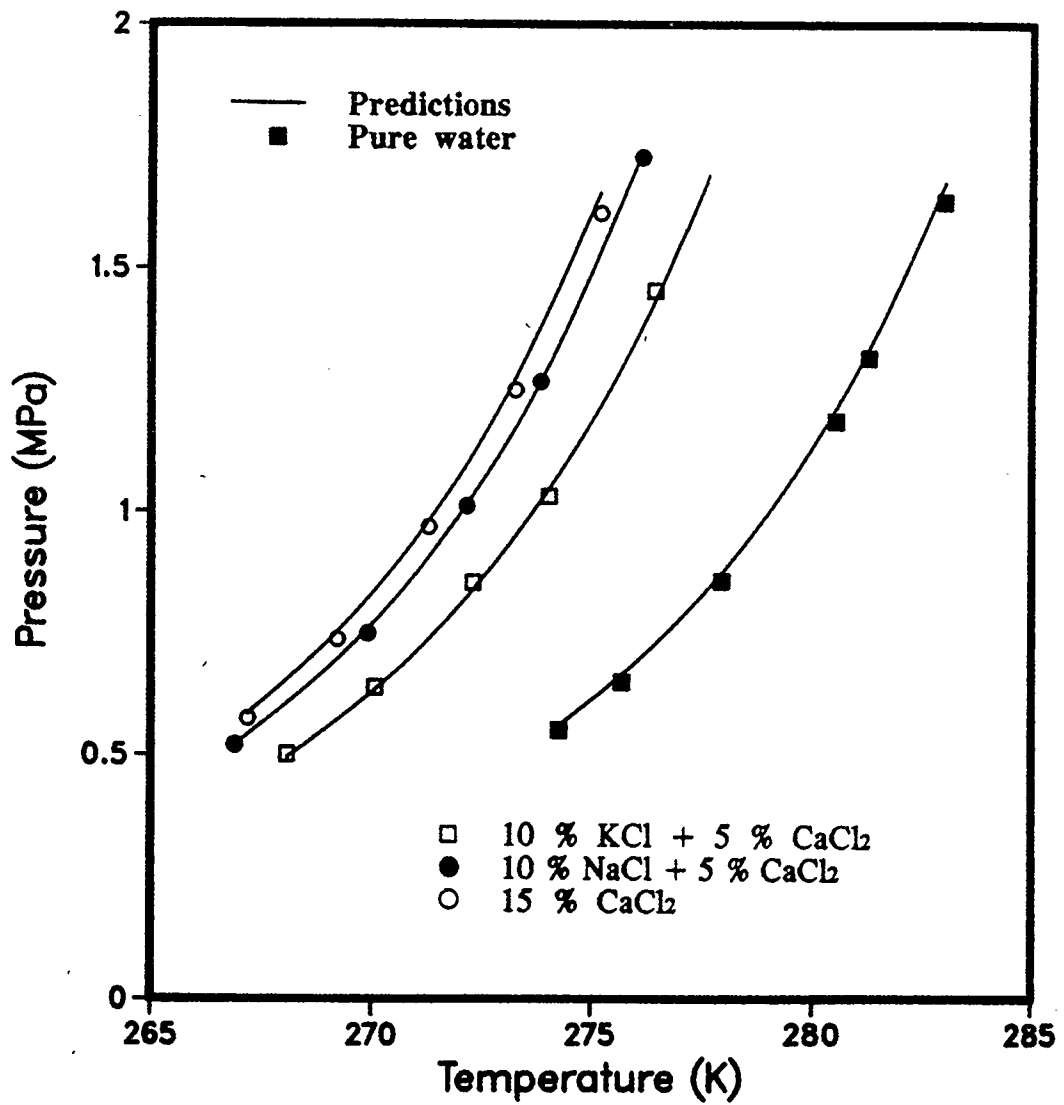


Figure 6.3 Experimental Data and Predicted Ethane Hydrate Formation Pressures in Aqueous Salt Solutions

7. GIBBS FREE ENERGY ANALYSIS OF THE CH₄ - H₂O SYSTEM

In this chapter the methane-water system is examined with respect to methane hydrate nucleation. First, the limits of thermodynamic stability for the liquid phase are calculated and compared with the experimentally measured amount of methane gas dissolved at the time when hydrates are formed. Second, the vapor-liquid-hydrate phase behavior is determined graphically with the aid of the tangent plane criterion. These studies provide a better insight of the hydrate formation process and the starting point for the thermodynamic analysis of the hydrate nucleation process.

7.1 Solubility of Methane in Water, Supersaturation and Nucleation

While studying the kinetics of methane hydrate formation it was observed that methane gas could be dissolved in the liquid water to a point beyond that corresponding to calculated gas-liquid equilibrium. In other words the aqueous liquid phase was supersaturated with methane before the hydrate nuclei appeared. This phenomenon is depicted in Figure 7.1. The figure represents the consumption of methane in a typical hydrate formation kinetic experiment. In such an experiment methane gas is brought into contact with liquid water at isobaric and isothermal conditions and the amount of gas consumed is measured with time. The concentration of the gas at the nucleation point, point B in the figure, is higher than that corresponding to the metastable

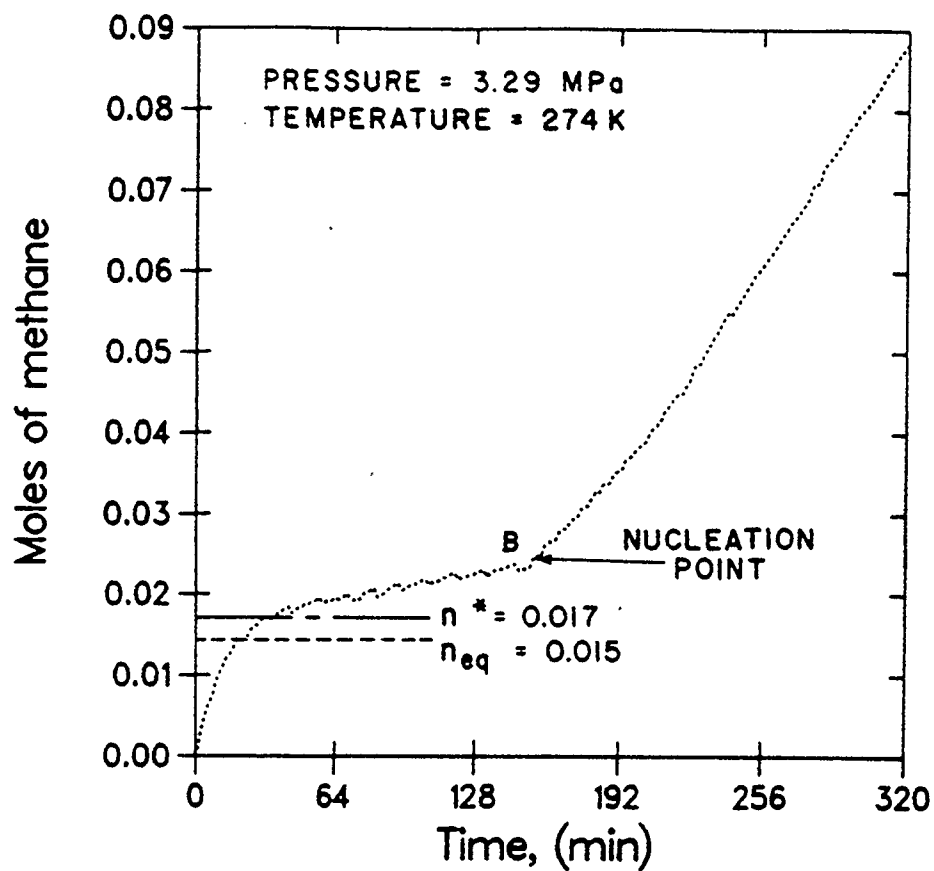


Figure 7.1 Experimental Gas Consumption Curve for Methane Hydrate Formation in a Semi-batch Reactor Containing 300 cm³ of Distilled and De-ionized Water.

vapor-liquid equilibrium as calculated by Henry's law or the Trebble-Bishnoi equation of state.

The metastable vapor-liquid equilibrium conditions are indicated by the calculated number of moles, n^* . The conditions are metastable because at this temperature and pressure hydrate formation occurs and hence, one cannot perform a vapor-liquid equilibrium experiment to measure n^* . The thermodynamic limits of the mole fractions of methane just before the nuclei appear are called limits of supersaturation. In the figure the number of moles, n_{eq} , represent the calculated amount of methane dissolved in the liquid phase in equilibrium with the vapor at the same temperature (274 K) and the corresponding equilibrium methane hydrate formation pressure which is 2.88 MPa.

Crystallization of a solute from a solution is a well known process. An essential requirement for crystallization from solution is the establishment of sufficient supersaturation. Gas hydrate formation is a crystallization process and hence, it is not surprising that supersaturation phenomena are observed. The question is whether these limits of supersaturation can be calculated.

Since we know the amount of water we can calculate the mole fraction of the dissolved methane corresponding to the number of moles of gas at the nucleation point and compare it with the calculated mole fraction at the metastable vapor-liquid equilibrium conditions. The experimentally determined mole fractions of methane at nucleation are shown in Table 7.1 together with the calculated mole fractions of methane by the Trebble-Bishnoi equation of state.

Table 7.1 Experimental Mole Fractions of Methane at Nucleation, Two Phase Equilibrium Mole Fractions and Limits of Stability

T (K)	P (MPa)	Mole Fraction of Methane		
		Experimental Nucleation point x 10	Trebble-Bishnoi EOS x 10	Spinodal point x 10
274	3.29	0.0140	0.0102	0.3266
"	3.49	0.0127	0.0108	0.3259
"	3.74	0.0150	0.0115	0.3259
276	3.66	0.0143	0.0107	0.3366
"	4.86	0.0162	0.0137	0.3364
279	5.39	0.0242	0.0139	0.3521
"	5.79	0.0191	0.0148	0.3513
"	6.39	0.0199	0.0160	0.3512
282	8.36	0.0233	0.0186	0.3675

Experimental data on the solubility of methane at pressures slightly lower than the incipient hydrate formation pressure are reported by Bishnoi et al. (1985, 1986) and are given in Table 7.2 together with the values calculated by the Trebble-Bishnoi equation of state. The equation of state consistently predicts lower solubilities for methane. If we account for this deviation and correct the calculated values for the mole fraction of methane in Table 7.1 the resulting mole fractions will still be smaller than the mole fractions at nucleation.

A good starting point to calculate the limits of supersaturation is to examine whether the observed limits of supersaturation are related with the limits of stability or spinodal points for the methane-water liquid mixture. Therefore the objective is to calculate the stability limits and compare them with the limits of supersaturation. This is examined in the next section.

7.1.1 Limits of Stability for the Methane-Water System

For a binary system the limits of stability are found by solving the following nonlinear equation

$$\left(\frac{\partial \ln f_1^L}{\partial x_1} \right)_{T,P} = 0. \quad (48)$$

The partial derivative in Eq. 48 was calculated analytically by using the Trebble-Bishnoi equation of state. The calculated limits of

Table 7.2 Experimental and Calculated Solubilities of Methane
In Water

T (K)	P (MPa)	Mole Fraction of Methane	
		Experimental x 10	Trebble-Bishnoi EOS x 10
274	2.85	0.0107	0.0089
276	3.37	0.0114	0.0099
279	4.55	0.0138	0.0121
282	6.35	0.0170	0.0150

stability for the methane-water system are shown in the last column of Table 7.1. These calculated values differ substantially from the experimental nucleation points. Hydrate nuclei appear at mole fraction for the dissolved methane smaller by an order of magnitude than the mole fractions at which the equation of state suggests that the liquid will split. It is noted, however, that the stability limits announce the appearance of another liquid phase which is not possible for the methane-water system at these conditions. Therefore, although the equation of state is suggesting that there is a limit to the dissolution of methane gas in liquid water the calculated stability limits should not be confused with the limits of supersaturation. It is also seen from Table 7.1 that at isothermal conditions the stability limits decrease slightly with pressure and that the experimental nucleation points do not suggest any pressure relationship. It was also found that the calculated stability limits increase linearly with temperature at the same pressure.

The supersaturation phenomenon for a hydrate forming system may be attributed to the tendency of the liquid water molecules to form a quasi-crystalline structure. Due to hydrogen bonding clusters of water molecules are formed and enclose the methane gas molecules thus depleting methane in the bulk liquid phase and create a "vacancy" for more methane molecules to be dissolved. These clusters when they reach a critical size become stable and appear as hydrate nuclei.

7.2 Gibbs Free Energy Analysis for the Phase Behavior

Tangent plane analysis is performed for the delineation of the phase behavior of the methane-water system. The Trebble-Bishnoi equation of state is used to calculate the Gibbs free energy change of mixing in the gaseous and liquid states. The van der Waals-Platteeuw model is used for the hydrate phase calculations. Gibbs free energy analysis of phase behavior, using an equation of state has been reported previously by Heidemann (1974) and Baker et al. (1982).

7.2.1 Gibbs Free Energy Change of Mixing

The Gibbs free energy change of mixing for the methane-water system in its gaseous or liquid state is given by

$$\Delta G_{\text{mx}} = R T \left[x_1 \ln (f_1/f_1^{\circ}) + x_2 \ln (f_2/f_2^{\circ}) \right] \quad (49)$$

where f_1° is the fugacity of pure methane in its gaseous state, f_2° is that of pure water in its liquid state, both at the temperature and pressure of the system and f_1 , f_2 are the component fugacities in the gaseous or liquid mixture.

The hydrate is treated as a solid solution and hence, the Gibbs free energy is given by the following equation

$$G^H = x_1^H \mu_1^H + x_2^H \mu_2^H \quad (50)$$

where the chemical potential of the gas in the hydrate is given by

$$\mu_1^H = \mu_1^o + R T \ln (f_1^H/f_1^o) \quad (51)$$

The standard state is pure methane gas at the temperature and pressure of the system. The chemical potential of water in the hydrate is given by Eq. 1 which in this case is written as following

$$\mu_2^H = \mu_2^{MT} + R T \sum_{i=1}^2 v_i \ln (1-\theta_i) \quad (52)$$

The Gibbs free energy change of mixing for the hydrate is given by

$$\Delta G^{mx} = G^H - x_1^H \mu_1^o - x_2^H \mu_2^o \quad (53)$$

Substituting Eqns 50, 51 and 52 into 53 we obtain the following equation

$$\Delta G^{mx} = R T x_1^H \ln (f_1^H/f_1^o) + x_2^H \left[\mu_2^{MT} - \mu_2^o + R T \sum_{i=1}^2 v_i \ln (1-\theta_i) \right] \quad (54)$$

The chemical potential differences, $\mu_2^{MT} - \mu_2^o$ is given by Eq. 7. The fugacity of the gas in the hydrate is related to the fraction of type 1 and 2 cavities occupied by the gas and with the Langmuir constants C_1 and C_2 as following

$$f_1^H = \frac{\theta_1}{C_1(1-\theta_1)} \quad (55)$$

$$\theta_2 = \frac{f_1^H C_2}{1 + f_1^H C_2} \quad (56)$$

The Trebble-Bishnoi equation of state was used for calculating the liquid and gas phase fugacities required in Eq. 49. The values of f_1^H , required in Eq. 54, were calculated by varying θ_1 from 0. to 1. and using Eq. 55. Equation 56 was then used to calculate the values of θ_2 . The ratio of water molecules to one gas molecule in the hydrate is given by $46/(2\theta_1+6\theta_2)$. This expression was used to calculate the mole fraction x_1^H from θ_1 to θ_2 . The values of the Langmuir constants are calculated from the correlation of Parrish and Prausnitz (1972).

7.2.2 Results and Discussion

In Figure 7.2 the Gibbs free energy change of mixing for methane-water at 0.82 MPa and 274 K is shown. In the vicinity of pure liquid water and pure gaseous methane the gas and liquid curves have minima. In figures 7.3 and 7.4 these minima can be seen together with the curves corresponding to the Gibbs free energy of mixing at two additional pressures. In Figure 7.2 the curve for the Gibbs free energy of mixing for the solid hydrate is extended up to a methane mole fraction of about 0.148 which is the methane mole fraction for the

hydrate having all the cavities occupied. This curve also goes through a minimum, indicated by the letter C, in the vicinity of the above mentioned mole fraction. This minimum lies above the tangent AB thus indicating that the gas-liquid equilibrium is a true equilibrium state according to the tangent plane criterion (Baker et al. 1982; Michelsen, 1982). By increasing the pressure the curve for the hydrate shifts, as seen in Figure 7.5. At about 2.88 MPa there is a common tangent line connecting the gas, liquid and the hydrate mixing curves as illustrated in Figure 7.6. Hence, the pressure of 2.88 MPa is the three phase equilibrium pressure at 274 K, within the accuracy of the parameters used in the thermodynamic model for the hydrate. At pressures higher than the equilibrium pressure the hydrate curve shifts in such a way that the minimum C lies below the tangent AB indicating that the gas-liquid equilibrium is unstable because there is an accessible state with lower Gibbs free energy. This is shown in Figure 7.7.

Therefore, the position of the point C with respect to the tangent AB indicates at various pressures indicates whether the hydrate is an accessible stable phase or not. The univariant three phase vapor-liquid-hydrate equilibrium for the methane-water system is identified by the fact that the minimum in the hydrate curve falls on the common tangent between the gas and the liquid. Extension of such an analysis to multicomponent systems is complex to be represented geometrically. However, for multicomponent hydrate forming systems the flash calculations scheme of Bishnoi et al. (1989) provides the information towards this direction.

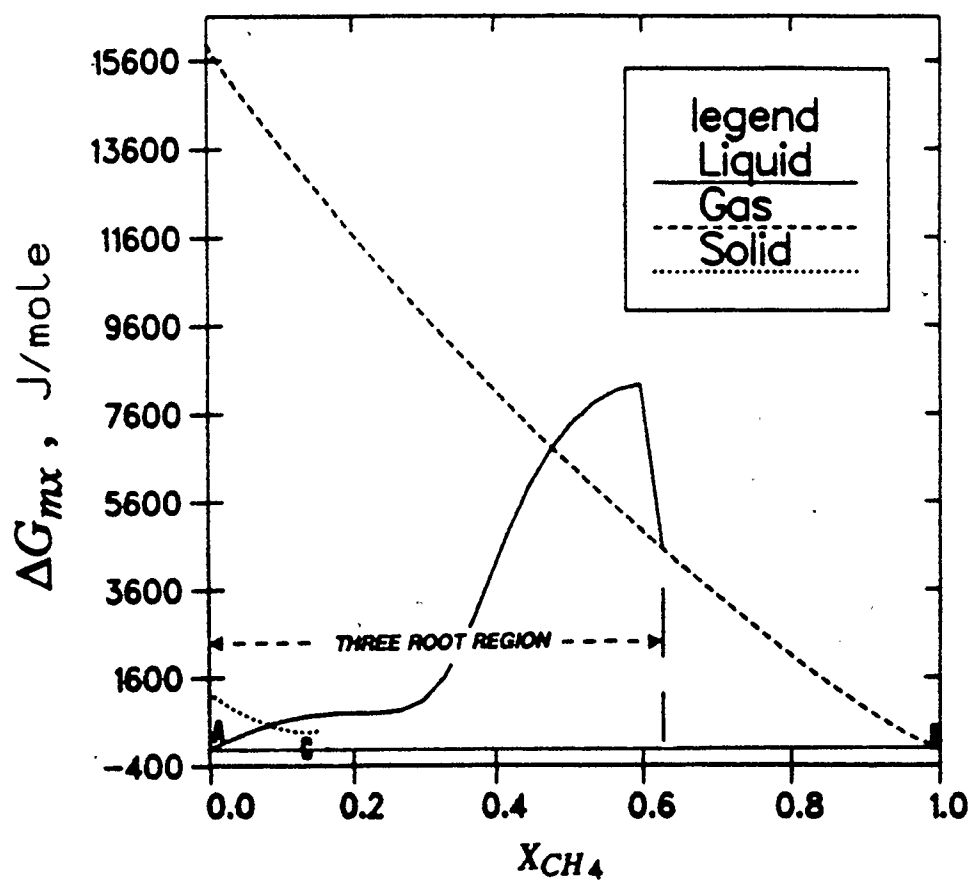


Figure 7.2 Gibbs Free Energy Change of Mixing for Methane-Water at 0.82 MPa and 274 K.

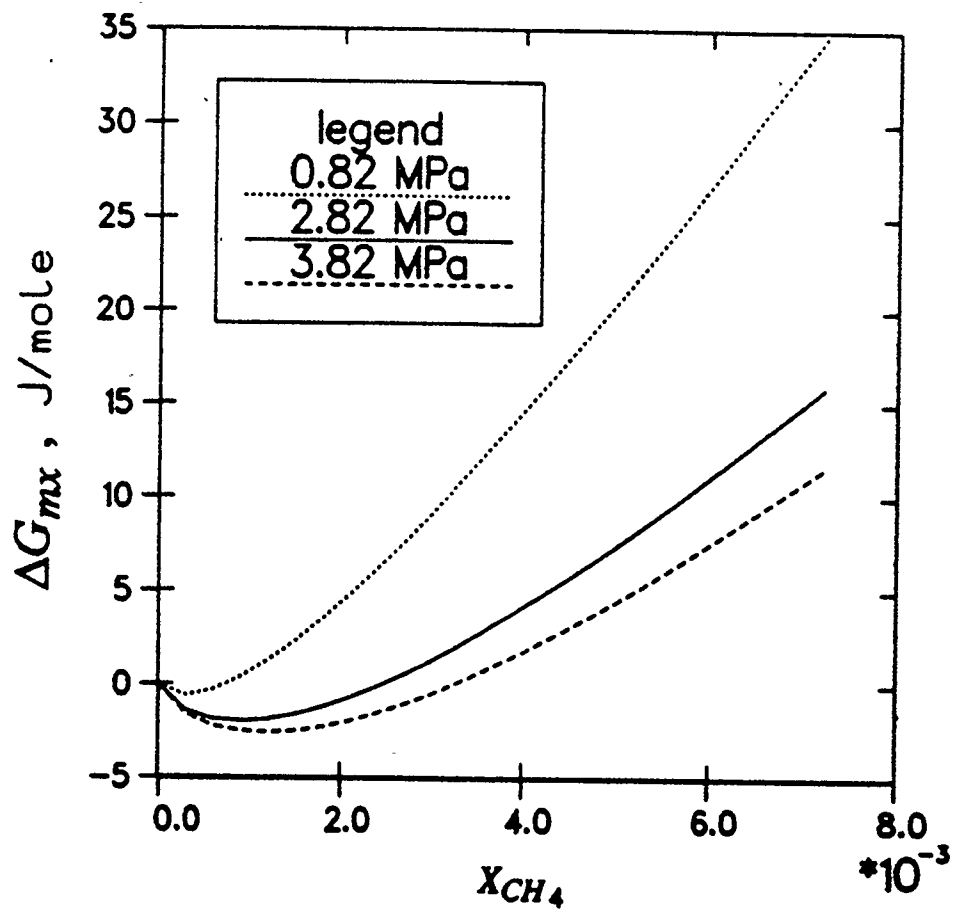


Figure 7.3 Gibbs Free Energy Change of Mixing for Methane-Water in Liquid Phase, in the Vicinity of Zero Methane Mole Fraction.

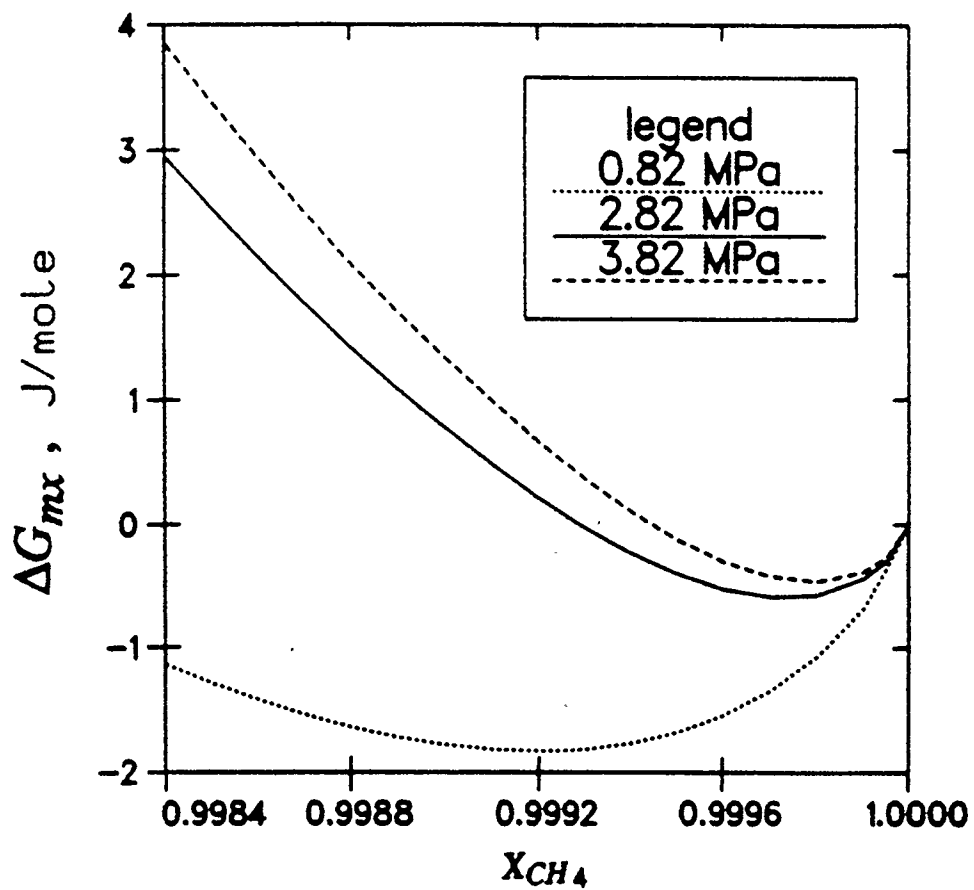


Figure 7.4 Gibbs Free Energy Change of Mixing for Methane-Water in Vapor Phase, in the Vicinity of Unity Methane Mole Fraction

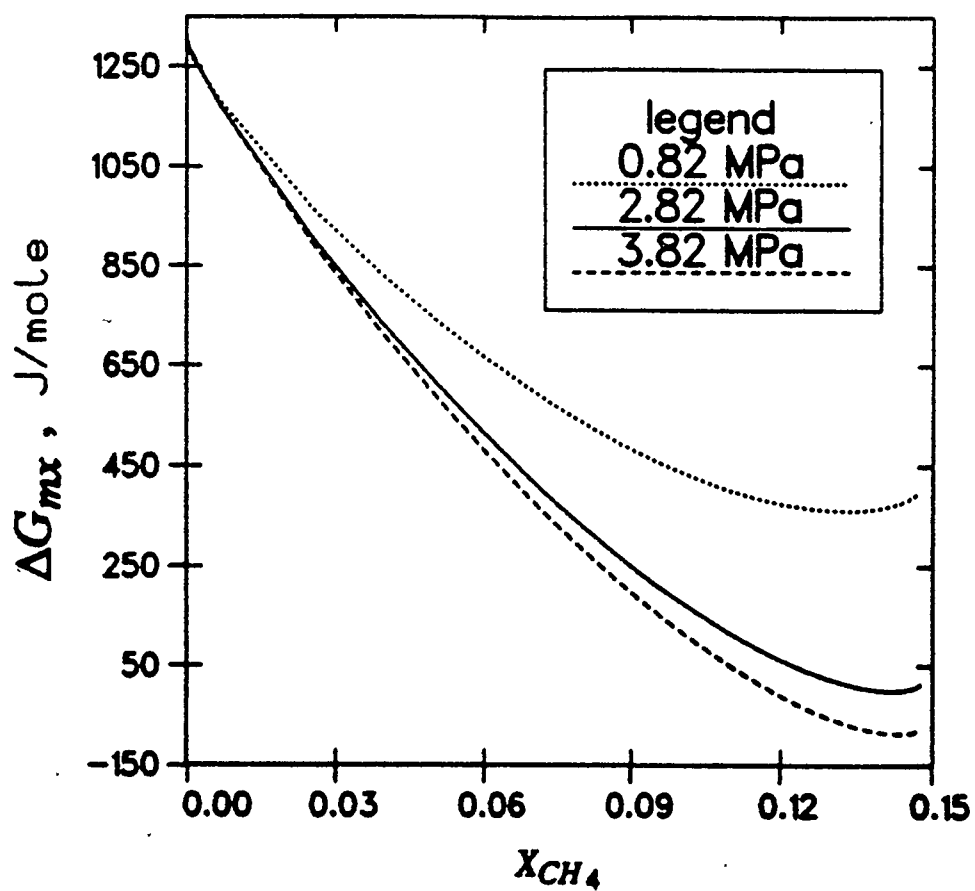


Figure 7.5 Gibbs Free Energy Change of Mixing for Methane-Water in Hydrate Phase

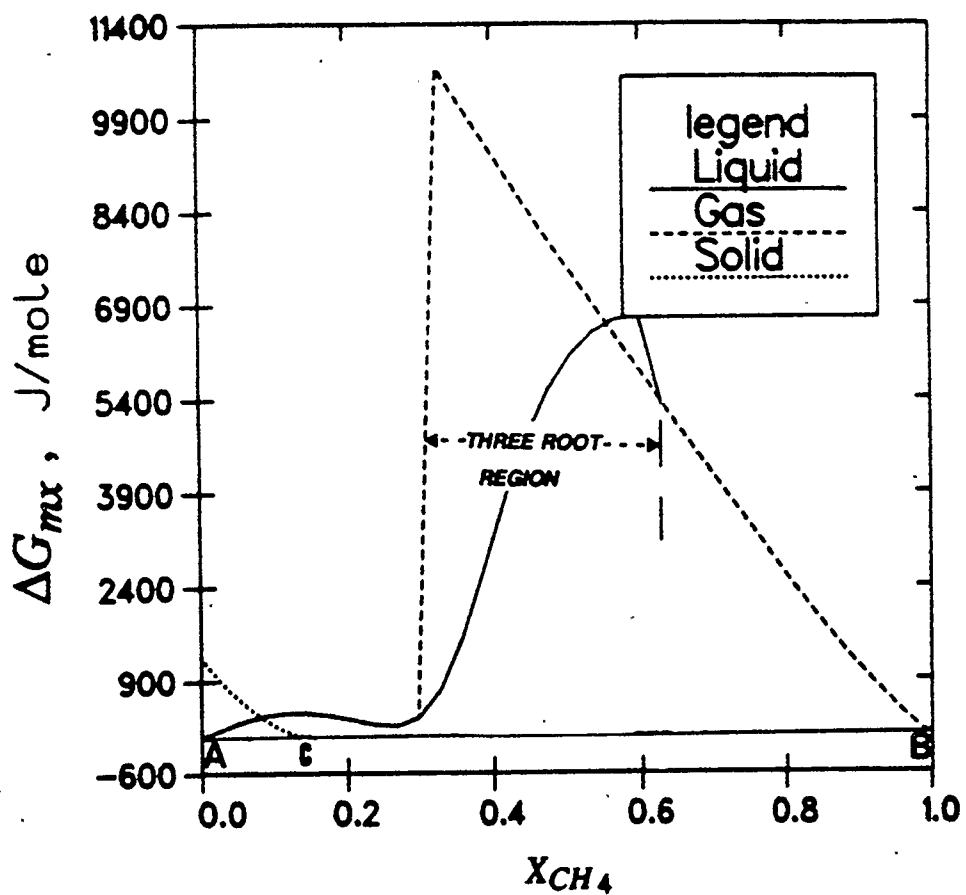


Figure 7.6 Gibbs Free Energy Change of Mixing for Methane-Water at 2.88 MPa and 274 K.

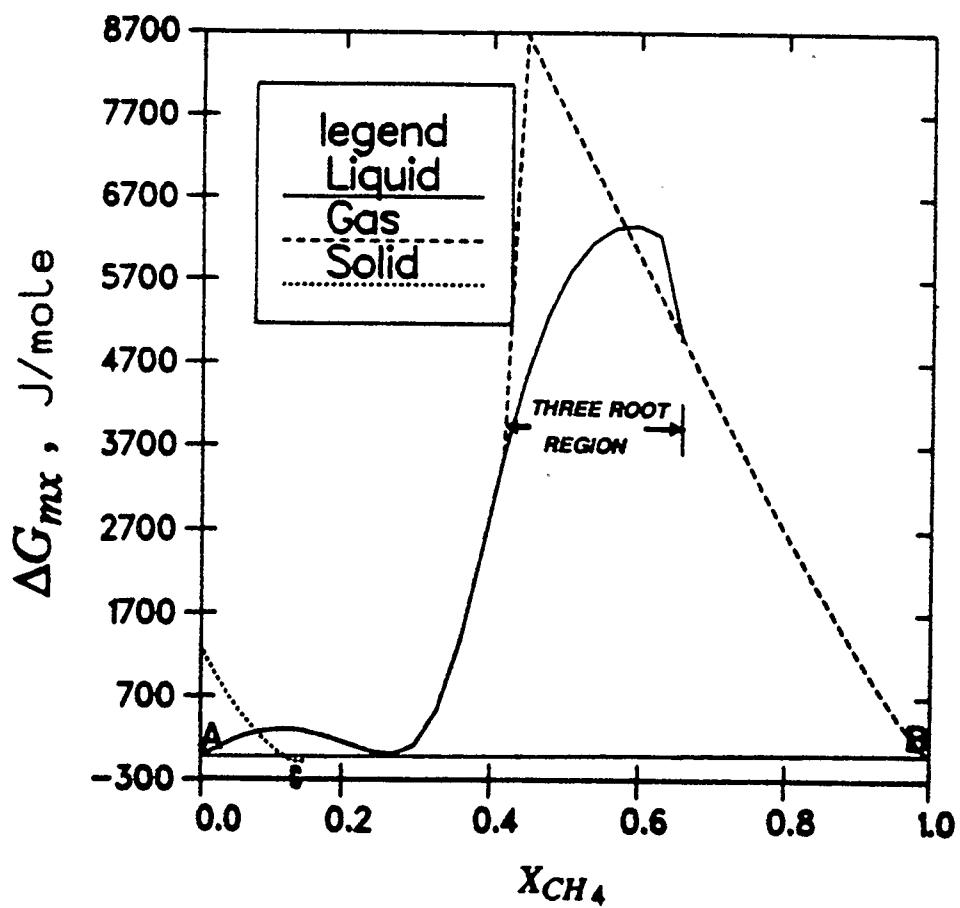


Figure 7.7 Gibbs Free Energy Change of Mixing for Methane-Water at 3.82 MPa and 274 K.

8. INTERACTION PARAMETER ESTIMATION IN EQUATIONS OF STATE USING BINARY VLE DATA

We turn now our attention to the problem of estimation of interaction parameters for an equation of state using binary vapor liquid equilibrium (VLE) data. The problem was introduced in chapter 1, analyzed and stated in chapter 2. In this chapter a Least Squares (LS) and a Maximum Likelihood (ML) estimation procedures will be proposed and evaluated using the Trebble-Bishnoi equation of state. The procedures will be compared, from a computational viewpoint, with the simplified error in variables method. In addition, a constrained least squares estimation method will be proposed for the calculation of interaction parameters which prevent the equation of state to predict erroneous liquid phase splitting. Finally, based on these estimation methods, a systematic approach for the estimation of interaction parameters in equations of state will be presented.

8.1 Unconstrained Estimation

8.1.1 Proposed Implicit Least Squares Estimation Procedure

As it was mentioned in chapter 2 an equation of state may not be capable of predicting the phase behavior of certain mixtures without systematic deviations. These deviations can be significantly larger in

magnitude than the experimental error. In such cases, one should not attempt to estimate the best parameters in a statistical sense, but rather should view the parameter estimation problem as a *curve fitting exercise*. In other words, the objective should be to determine a set of interaction parameters (with as little computational effort as possible) which yields an *acceptable fit* within the limitations of the model.

Based on numerical experimentation we have chosen the following LS estimation procedure whereby the parameters are obtained by minimizing the following objective function:

$$S_{LS}(\mathbf{k}) = \sum_{i=1}^N \sum_{j=1}^2 q_{ij} \left[\ln f_{ij}^L - \ln f_{ij}^V \right]^2 \quad (57)$$

where q_{ij} are set equal to one. Paunovic et al. (1981) proposed a similar LS procedure by formulating the objective function as the non-weighted summation of squares of normalized fugacity differences. Peters et al. (1987) reported that use of the summation of squares of fugacity differences can easily lead to numerical instability. Skjold-Jorgensen (1983) has also suggested the use of Eq. 57 with $q_{ij}=1$.

8.1.2 Proposed Implicit Maximum Likelihood Estimation Procedure

For a binary, two phase system, at each experimental point i , and for each component j , the equilibrium constraints are given below

$$f_{ij}^L - f_{ij}^V = 0 \quad (58)$$

or equivalently

$$g_j(\hat{x}_i, \hat{y}_i, \hat{T}_i, \hat{P}_i; \mathbf{k}; \mathbf{u}) = 0; \quad i=1, \dots, N; j=1,2 \quad (59)$$

If we replace the true but unknown state variables with their measurements, then the above functions are not equal to zero due to the measurement errors even if the model were exact.

$$g_j(\hat{x}_i, \hat{y}_i, \hat{T}_i, \hat{P}_i; \mathbf{k}; \mathbf{u}) = e_{ij}; \quad i=1, \dots, N; j=1,2 \quad (60)$$

If the assumptions stated in section 2.5.2(c) hold, the parameter estimation problem reduces to the minimization of the following quadratic objective function

$$S_{ML}(\mathbf{k}) = \sum_{i=1}^N (\mathbf{e}_{i1}, \mathbf{e}_{i2}) \begin{bmatrix} \sigma_{i1}^2 & \sigma_{i12} \\ \sigma_{i12} & \sigma_{i2}^2 \end{bmatrix}^{-1} (\mathbf{e}_{i1}, \mathbf{e}_{i2})^T \equiv \sum_{i=1}^N \mathbf{e}_i^T \mathbf{Q}_i \mathbf{e}_i \quad (61)$$

where σ_{ij}^2 ($j=1,2$) is computed using the error propagation law. If the errors in the measurements of the state variables are not correlated, using a first order variance approximation for σ_{ij}^2 we obtain:

$$\sigma_{ij}^2 = \left[\frac{\partial g_j}{\partial x_1} \right]^2 \sigma_{x,i}^2 + \left[\frac{\partial g_j}{\partial T} \right]^2 \sigma_{T,i}^2 + \left[\frac{\partial g_j}{\partial y_1} \right]^2 \sigma_{y,i}^2 + \left[\frac{\partial g_j}{\partial P} \right]^2 \sigma_{P,i}^2 \quad (62)$$

and similarly for the σ_{i12} we obtain:

$$\sigma_{i12} = \left[\frac{\partial g_1}{\partial \bar{x}_1} \right] \left[\frac{\partial g_2}{\partial \bar{x}_1} \right] \sigma_{x,i}^2 + \left[\frac{\partial g_1}{\partial P} \right] \left[\frac{\partial g_2}{\partial P} \right] \sigma_{P,i}^2 +$$

$$\left[\frac{\partial g_1}{\partial y_1} \right] \left[\frac{\partial g_2}{\partial y_1} \right] \sigma_{y,i}^2 + \left[\frac{\partial g_1}{\partial T} \right] \left[\frac{\partial g_2}{\partial T} \right] \sigma_{T,i}^2 \quad (63)$$

where all the derivatives are evaluated at $\hat{x}_i, \hat{y}_i, \hat{T}_i, \hat{P}_i$.

The choice of the functional form of the residuals in the optimality criterion is of extreme importance and should be based on the following considerations:

- (a) On statistical grounds, the selection of the residual functions should be such that the errors, e_{ij} , are approximately normally distributed, since a quadratic objective function is to be used.
- (b) On computational grounds, the choice should be such that no iterative computations are needed for the calculation of the residuals. Otherwise there is no advantage in using an *implicit formulation* over the *error in variables method* which on statistical grounds has more realistic assumptions.
- (c) The choice of the residuals should be such that it avoids, if possible numerical instabilities (e.g. exponent overflow) and has favorable convergence characteristics.

Based on the above considerations and numerical experimentation with several binary systems instead of the residual function defined by

Eq. 44 we have chosen the following residual function:

$$g_j(x_i, y_i, T_i, P_i; \mathbf{k}; \mathbf{u}) = \ln f_{ij}^L - \ln f_{ij}^V \quad i=1, \dots, N; j=1, 2 \quad (64)$$

The calculation of the residuals is straightforward and does not require any iterative computations. As a result, the overall computational requirements are significantly less compared to the *error in variables method*.

8.1.3 Computation of the Parameter Estimates

The solution of the minimization problem was performed using the Gauss-Newton method. By linearizing the residual vector we obtain

$$\mathbf{e}_i(\mathbf{k}^{(j+1)}) = \mathbf{e}_i(\mathbf{k}^{(j)}) + \left[\frac{\partial \mathbf{e}^T}{\partial \mathbf{k}} \right]_i^T \Delta \mathbf{k}^{(j+1)} \quad (65)$$

Substituting Eq. 65 into S and taking $\partial S / \partial \mathbf{k}^{(j+1)} = \mathbf{0}$ we obtain the following linear system of equations

$$\mathbf{A} \Delta \mathbf{k}^{(j+1)} = \mathbf{b} \quad (66)$$

where

$$\mathbf{A} = \sum_{i=1}^N \left[\frac{\partial \mathbf{e}^T}{\partial \mathbf{k}} \right]_i \mathbf{Q}_i \left[\frac{\partial \mathbf{e}^T}{\partial \mathbf{k}} \right]_i^T \quad (67)$$

$$\mathbf{b} = \sum_{i=1}^N \left[\frac{\partial \mathbf{e}^T}{\partial \mathbf{k}} \right]_i \mathbf{Q}_i \mathbf{e}_i \quad (68)$$

In order to ensure convergence of the iterative procedure we used (a) Marquardt's suggestion for the solution of the system of the normal equations and (b) singular value decomposition of the normal equation matrix. Possible overstepping problems encountered during the minimization are treated using the step size policy suggested by Kalogerakis and Luus (1983).

8.1.4 Numerical Results and Discussion

Three binary systems were used in this study, namely methane-methanol (Hong et al. 1987), carbon dioxide-methanol (Hong and Kobayashi, 1988) and propane-methanol (Galivel-Solastiuk et al. 1986). The quadratic mixing rules with temperature independent interaction parameters, as proposed by Trebble and Bishnoi (1988), were used.

In Table 8.1 the parameter estimates with their standard error of estimate are shown for the methane-methanol system. Also shown is the type of the objective function that was used and the required CPU seconds per iteration. The values of the interaction parameters which are not shown in the tables are zero. As seen from the table the parameter estimates with all three estimation procedures do not differ significantly. The computational efficiency of the proposed implicit ML and LS estimation procedures are also evident from the table. For this system, use of only one parameter, k_d , is found to be *acceptable*. The

Table 8.1 Parameter Estimates for the Methane-Methanol System.

<i>Parameter</i>	<i>Standard Deviation (%)</i>	<i>Objective Function</i>	<i>CPU/iteration (CP seconds)</i>
$k_d = -0.1903$	$\pm 14.9^*$	$S_{LS}(\mathbf{k})$	0.004 NP ^{**}
$k_d = -0.2317$	± 0.03	$S_{ML}(\mathbf{k})$	0.014 NP
$k_d = -0.2515$	± 0.01	$S_{TP}(\mathbf{k})$	0.032 NP

* As computed under the null hypothesis that σ_{ij} is constant and $q_{ij}=1$.

** NP is the number of experimental points.

interaction parameter k_d was selected over k_a , k_b , k_c from the results obtained by the simple LS estimation procedure. Using the interaction parameter value of (-0.1903) for k_d which was obtained by LS estimation, the phase equilibrium calculations were performed. The calculated values of the liquid and vapor mole fractions at constant temperature and pressure were found to agree very well with the experimental data. Subsequently, ML estimation was performed and the value of (-0.2317) for k_d was obtained. Using the ML estimate for k_d isobaric-isothermal flash computations were performed and typical VLE predictions are shown in Figure 8.1.

Similar calculations were performed for the CO_2 - CH_3OH system. The parameter estimates are shown in Table 8.2. Two binary interaction parameters were used. For this system the minimization algorithms using S_{Tx} and S_{TP} converged with a Marquardt's parameter not equal to zero. For the isothermal-isobaric flash calculations the ML estimates were used. The results at 273 K are shown in Figure 8.2. By comparing the required computational times, it is seen that the LS estimation procedure has the smallest requirements whereas the estimation procedures which require phase equilibrium calculations during the minimization have significantly larger requirements. For example, S_{Tx} requires 20 times more CPU time per iteration compared to simple LS, whereas S_{TP} requires 80 times more CPU time for this particular problem.

For the majority of binary systems, use of one or two binary interaction parameters has been found to be adequate for the representation of the VLE data (Trebble, 1988). As seen from Figures 8.1

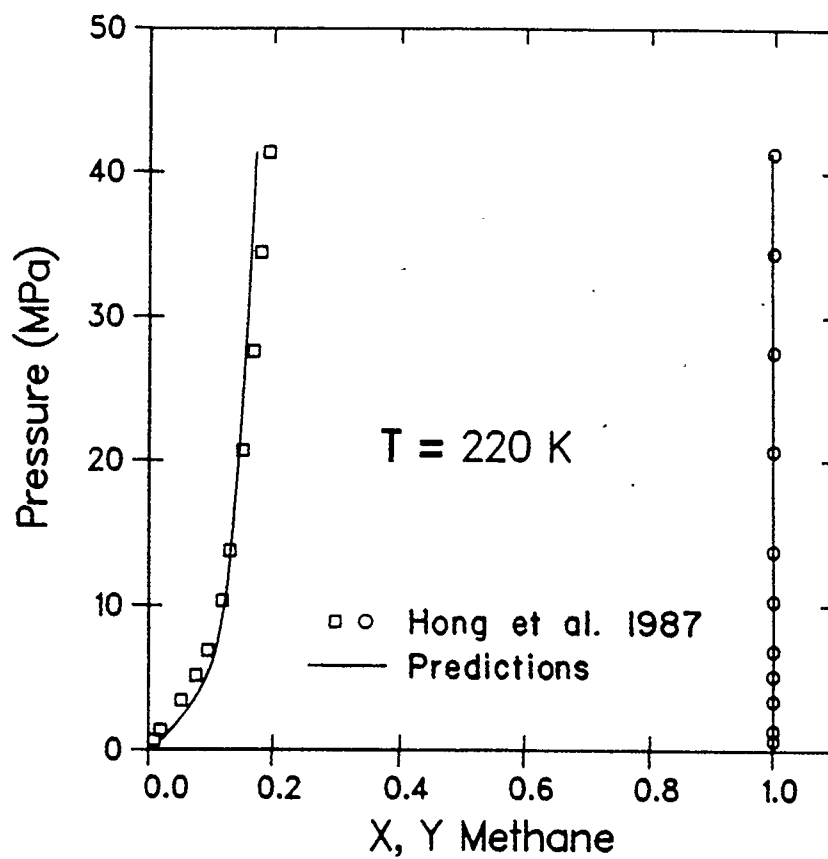


Figure 8.1 Vapor-Liquid Equilibrium for the Methane-Methanol System.

Table 8.2 Parameter Estimates for the CO₂-CH₃OH System.

<i>Parameter</i>	<i>Standard Deviation (%)</i>	<i>Objective Function</i>	<i>CPU/iteration (CP seconds)</i>
$k_a = 0.0605$	$\pm 9.54^*$	$S_{LS}(\mathbf{k})$	0.0054 NP ^{**}
$k_d = -0.1137$	± 15.86		
$k_a = 0.0504$	± 0.18	$S_{ML}(\mathbf{k})$	0.015 NP
$k_d = -0.0631$	± 0.60		
$k_a = 0.0511$	± 3.15	$S_{TX}(\mathbf{k})$	0.103 NP
$k_d = -0.0967$	± 7.63		
$k_a = 0.0566$	± 3.91	$S_{TP}(\mathbf{k})$	0.445 NP
$k_d = -0.2238$	± 1.14		

* As computed under the null hypothesis that σ_{ij} is constant and $q_{ij}=1$.

** NP is the number of experimental points.

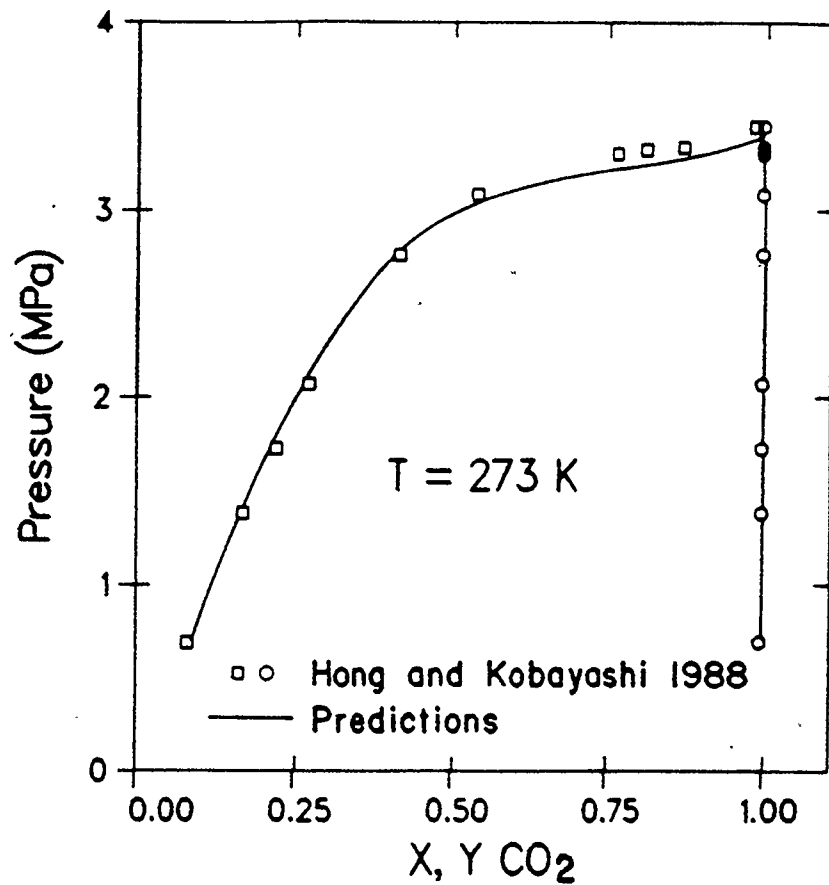


Figure 8.2 Vapor-liquid Equilibrium for the CO_2 - CH_3OH System.

and 8.2 the phase behavior of the binary systems of methane and carbon dioxide with methanol are represented by the EOS with a reasonable accuracy for engineering calculations. This was not the case for the *propane-methanol* system for which grossly biased predictions were obtained by using one, two or three parameters obtained by LS estimation. The improvement of the fit by increasing the number of parameters, especially from two to three was minimal. It is evident that the EOS with classical quadratic mixing rules is not capable of representing the behavior of this system with an accuracy that would make the ML estimation of the parameters meaningful. Nevertheless for comparison purposes, ML calculations were performed and the parameter estimates are shown in Table 8.3. Again, the computational requirements per iteration of S_{T_x} are 8 times more than the implicit ML and 33 times more compared to the simple LS procedure. The parameters obtained by LS estimation were used in this case to generate the phase equilibrium predictions by bubble point pressure calculations. The results at 343 K are shown in Figure 8.3. As seen the calculated bubble point pressures differ significantly from the experimental values. Moreover, erroneous liquid phase splitting is suggested. This is a typical case where one should reconsider the applicability of the mixing rules.

Finally, as seen from the above examples the computational requirements of the LS and the ML estimation procedures are very small when compared to the simplified *error in variables method* (S_{T_x} , S_{T_P}). In addition, the latter ones were found to converge very slowly as compared to the ML or the LS estimation procedures which implies that the overall

Table 8.3 Parameter Estimates for the Propane-Methanol System.

<i>Parameter</i>	<i>Standard Deviation (%)</i>	<i>Objective Function</i>	<i>CPU/iteration (CP seconds)</i>
$k_a = 0.1531$ $k_d = -0.2994$	$\pm 7.35^*$ ± 9.34	$S_{LS}(\mathbf{k})$	0.006 NP^{**}
$k_a = 0.1533$ $k_d = -0.3218$	± 0.27 ± 0.40	$S_{ML}(\mathbf{k})$	0.049 NP
$k_a = 0.2384$ $k_d = -0.3222$	± 0.58 ± 0.82	$S_{TX}(\mathbf{k})$	0.196 NP

* As computed under the null hypothesis that σ_{ij} is constant and $q_{ij}=1$.

** NP is the number of experimental points.

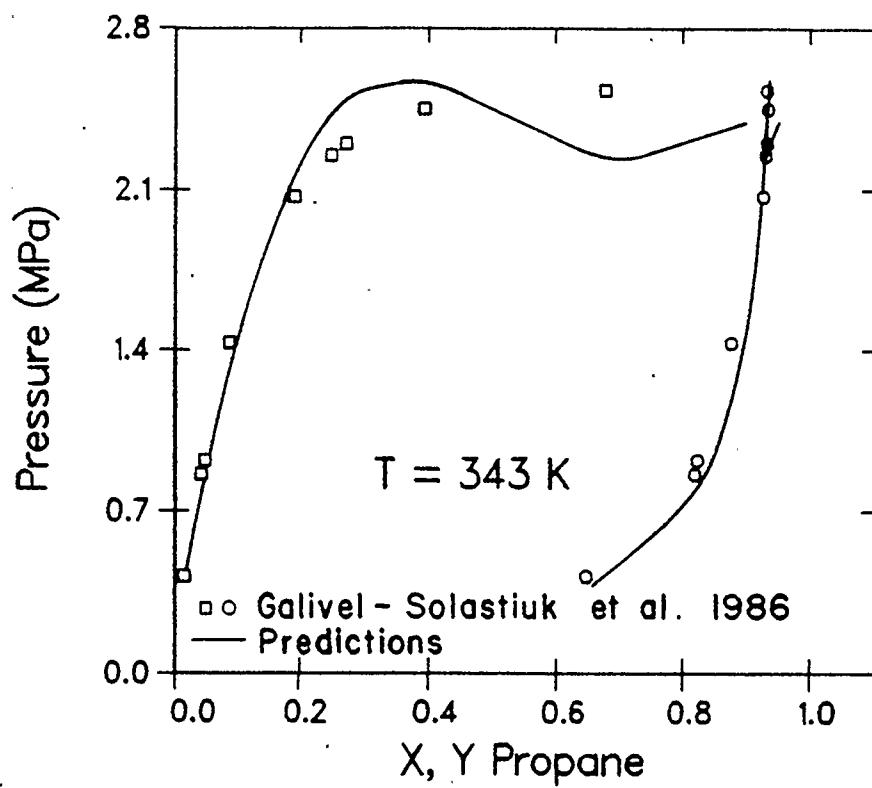


Figure 8.3 Vapor-liquid Equilibrium for the Propane-Methanol System.

computational requirements of the *error in variables method* are excessive by at least two orders of magnitude. However, it should be kept in mind that the measurements of all four state variables (T, P, x, y) are needed in order to apply the implicit formulation methods.

8.2 Constrained Least Squares Estimation

In this section, a constrained least squares interaction parameter estimation method is presented. It is used to estimate such interaction parameters which will enable the thermodynamic model to predict the correct phase behavior whenever it is found to predict erroneous liquid phase splitting. The propane-methanol system for which this problem was encountered will be examined. For this system the interaction parameters which are obtained by performing the constrained least squares estimation enable the equation of state to predict the correct phase behavior. However, since there are considerable deviations between the calculated and the experimental phase behavior the method will be illustrated first with two other examples.

8.2.1 Prediction of Erroneous Liquid Phase Separation

As it was seen in the previous section, when calculating the VLE for a binary system utilizing the interaction parameters from an unconstrained Least Squares (ULS) estimation procedure, there is a possibility that the EOS predicts erroneous liquid-liquid phase

separation. Similar observations were also made by other workers (Schwartzentruber et al. 1987; Trebble and Bishnoi, 1988; Trebble, 1988a). Such behavior is a consequence of the inadequacy of the thermodynamic model. In Figure 8.4 the experimental data along with the predictions using the Trebble-Bishnoi equation of state for the carbon dioxide-n-hexane system are shown. As seen, erroneous liquid phase splitting is suggested by the EOS.

Schwartzentruber et al. (1987) while correlating propane-methanol VLE data encountered this problem. They were the first to propose a procedure for the calculation of interaction parameters which would not yield prediction of erroneous liquid-liquid phase splitting. In their approach, the Aspen-Plus Data Regression System, commercially available by Aspen Technology Inc., was used for the estimation of all but one of the interaction parameters by fitting the VLE data. The remaining interaction parameter was obtained by solving the following equation

$$\min_{x_1} \frac{\partial \Delta G^{\text{mix}}}{\partial x_1^2} = 10^{-3} R T \quad (69)$$

where ΔG^{mix} is the Gibbs free energy change of mixing. Although, their procedure guarantees the stability of the liquid phase, the estimated interaction parameters are not optimal in the sense of corresponding to the constrained minimum of the optimality criterion.

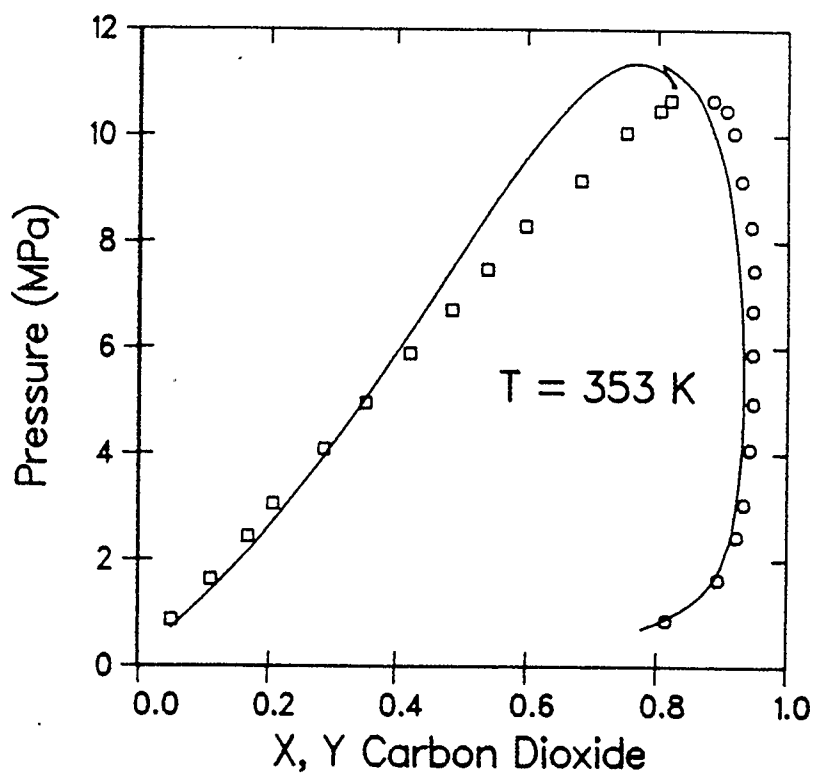


Figure 8.4 Prediction of Erroneous Liquid Phase Separation Using the Interaction Parameters from Unconstrained LS Estimation.

Liquid Phase Stability Criterion for a Binary System

For a binary liquid mixture the condition for a stable liquid phase is written as following

$$\left[\frac{\partial \ln f_1^L}{\partial x_1} \right]_{T,P} = \phi(z; \mathbf{k}) > 0. \quad (70)$$

where f_1^L is the fugacity of component 1 in the liquid phase, z is the vector of the two independent state variables and \mathbf{k} is the interaction parameter vector. The function ϕ is called stability function. For systems with azeotropic behavior z is selected to be $(T, x)^T$ whereas for systems where the pressure has a large derivative with respect to composition, it is $(T, P)^T$. In both cases the selection is such that the calculation of the dependent variables at each experimental equilibrium point is facilitated when solving the equilibrium equations given below

$$f_{ij}^L = f_{ij}^V \quad i=1,\dots,N; j=1,2 \quad (71)$$

In Figure 8.5 the stability function, as calculated at all the experimental points shown in Figure 8.4 for the CO_2 -n-Hexane system, is plotted against pressure. It is evident from the figure that the stability criterion is violated.

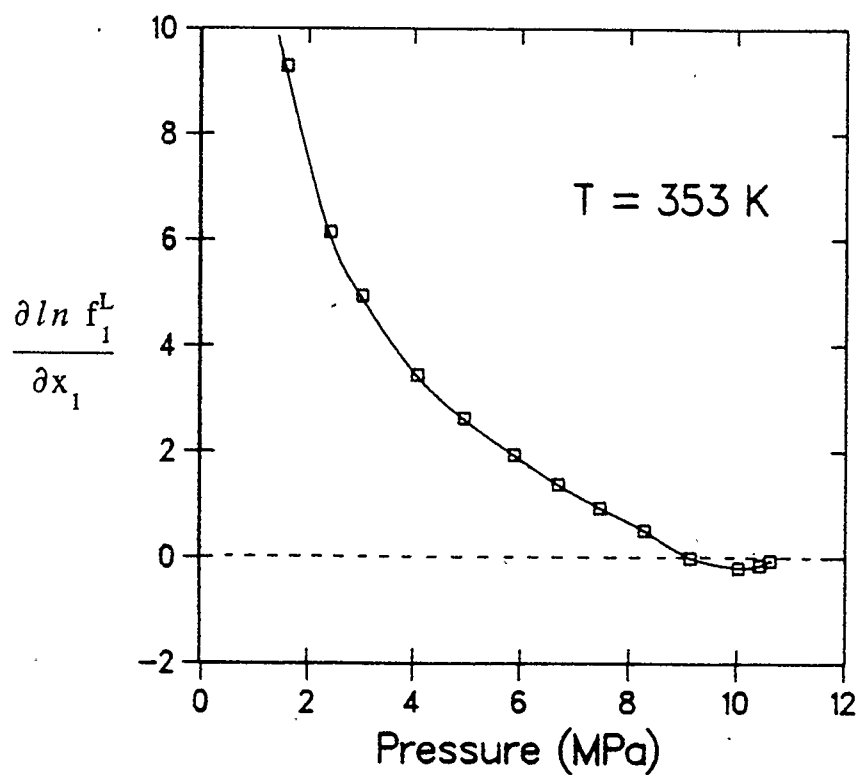


Figure 8.5 The Stability Function with Interaction Parameters from Unconstrained Least Squares Estimation for the CO_2 - n-Hexane System.

8.2.2 Formulation of the Constrained Estimation Problem

As it was seen in the previous section, for efficient estimation of \mathbf{k} , the following objective function should be minimized

$$S(\mathbf{k}) = \sum_{i=1}^N \mathbf{e}_i^T \mathbf{Q}_i \mathbf{e}_i \quad (72)$$

where \mathbf{e} is the residual vector defined by Eq. 64.

In order to estimate the interaction parameter vector \mathbf{k} which will ensure the stability of the liquid phase, the minimization should be performed subject to the condition that the stability of the liquid phase is ensured. Hence, the following constrained least squares (CLS) estimation problem should be solved

minimize

$$S(\mathbf{k}) = \sum_{i=1}^N \mathbf{e}_i^T \mathbf{Q}_i \mathbf{e}_i \quad (73a)$$

subject to

$$\left[\frac{\partial \ln f_1^L}{\partial x_1} \right]_{T,P} = \phi(z; \mathbf{k}) > 0. \quad (73b)$$

The solution of this minimization problem is complicated by the fact that ϕ is not only a function of the unknown parameters, \mathbf{k} but also of

the state variables. Although the LS performance index is calculated at a finite number of data points, the constraint should be satisfied over the entire feasible range of the state variables. Fortunately, if we consider that the region over which the constraint must be satisfied, is finite, then there exists a point, z_0 , where the functional is minimum. Hence the above constrained minimization problem reduces to:

minimize

$$S(\mathbf{k}) = \sum_{i=1}^N \mathbf{e}_i^T \mathbf{Q}_i \mathbf{e}_i \quad (74a)$$

subject to

$$\phi_0 \equiv \phi(z_0; \mathbf{k}) \geq \xi > 0. \quad (74b)$$

where ξ is a small positive constant.

If the point z_0 is known or can be computed, the above constrained minimization problem is reduced to a typical one in the sense that the Kuhn-Tucker conditions can be applied. Namely, by introducing the Lagrange multiplier λ , we augment the performance index to

$$S^*(\mathbf{k}, \lambda) = S(\mathbf{k}) + \lambda (\phi_0 - \xi) \quad (75)$$

and we search for the stationary points of $S^*(\mathbf{k}, \lambda)$.

8.2.3 Proposed Solution Method

Problem Reduction

Instead of searching for z_0 over the entire feasible region of the state variables we restrict the search only to the N given experimental data points. In this case, the point where ϕ is minimum can be readily determined. This simplification can only be employed if a sufficient number of well distributed experimental data points are available. Furthermore, ξ should be chosen in such a way that it takes into account the experimental error in the data.

A Quadratically Convergent Iterative Procedure

Let us consider the well known Gauss-Newton (GN) method. Given an estimate, $\mathbf{k}^{(j)}$, of the interaction parameter vector at the j th iteration, linearization of the residual vector and of the stability function yields the following equations

$$\mathbf{e}_i(\mathbf{k}^{(j+1)}) = \mathbf{e}_i(\mathbf{k}^{(j)}) + \left[\frac{\partial \mathbf{e}^T}{\partial \mathbf{k}} \right]_i^T \Delta \mathbf{k}^{(j+1)} \quad (76)$$

$$\phi_o(\mathbf{k}^{(j+1)}) = \phi_o(\mathbf{k}^{(j)}) + \left[\frac{\partial \phi_o}{\partial \mathbf{k}} \right]^T \Delta \mathbf{k}^{(j+1)} \quad (77)$$

Substituting equations 76 and 77 into S^* and taking $\partial S^*/\partial \mathbf{k}^{(j+1)} = \mathbf{0}$ and also $\partial S/\partial \lambda = 0$ we obtain the following linear system of equations

$$\mathbf{A} \Delta \mathbf{k}^{(j+1)} = \mathbf{b} - \frac{\lambda}{2} \frac{\partial \phi_o}{\partial \mathbf{k}} \quad (78)$$

$$\phi_o(\mathbf{k}^{(j)}) + \left[\frac{\partial \phi_o}{\partial \mathbf{k}} \right]^T \Delta \mathbf{k}^{(j+1)} = \xi \quad (79)$$

where

$$\mathbf{A} = \sum_{i=1}^N \left[\frac{\partial \mathbf{e}^T}{\partial \mathbf{k}} \right]_i \mathbf{Q}_i \left[\frac{\partial \mathbf{e}^T}{\partial \mathbf{k}} \right]_i^T \quad (80)$$

$$\mathbf{b} = - \sum_{i=1}^N \left[\frac{\partial \mathbf{e}^T}{\partial \mathbf{k}} \right]_i \mathbf{Q}_i \mathbf{e}_i \quad (81)$$

By solving Eq. 78 for $\Delta \mathbf{k}^{(j+1)}$ and substituting in Eq. 79 we obtain

$$\lambda = 2 \frac{\phi_o - \xi + \left[\frac{\partial \phi_o}{\partial \mathbf{k}} \right]^T \mathbf{A}^{-1} \mathbf{b}}{\left[\frac{\partial \phi_o}{\partial \mathbf{k}} \right]^T \mathbf{A}^{-1} \left[\frac{\partial \phi_o}{\partial \mathbf{k}} \right]} \quad (82)$$

Selection of ξ

Since we search for the minimum of ϕ over the experimental data points only, and instead of the true values of the state variables, x , T and P , we use their measurements which have a certain experimental error, we should select ξ to ensure that ϕ is always positive. The suggested value of x is $1.96 \sigma_\phi$ corresponding to the 95 per cent confidence interval respectively. This is illustrated qualitatively in Figure 8.6. The value of ξ is obtained at the conditions where the minimum of ϕ lies, by a first order variance approximation for σ_ϕ^2 with respect to the state variables x , T and P , and is given by the following equation

$$\sigma_\phi^2 = \left[\frac{\partial \phi}{\partial x} \right]^2 \sigma_x^2 + \left[\frac{\partial \phi}{\partial T} \right]^2 \sigma_T^2 + \left[\frac{\partial \phi}{\partial P} \right]^2 \sigma_P^2 \quad (83)$$

8.2.4 Computational Algorithm

Once an estimate of the parameter vector, $\mathbf{k}^{(j)}$, at the j^{th} iteration is available, one can obtain the estimate for the next iteration by following steps (i) to (vi):

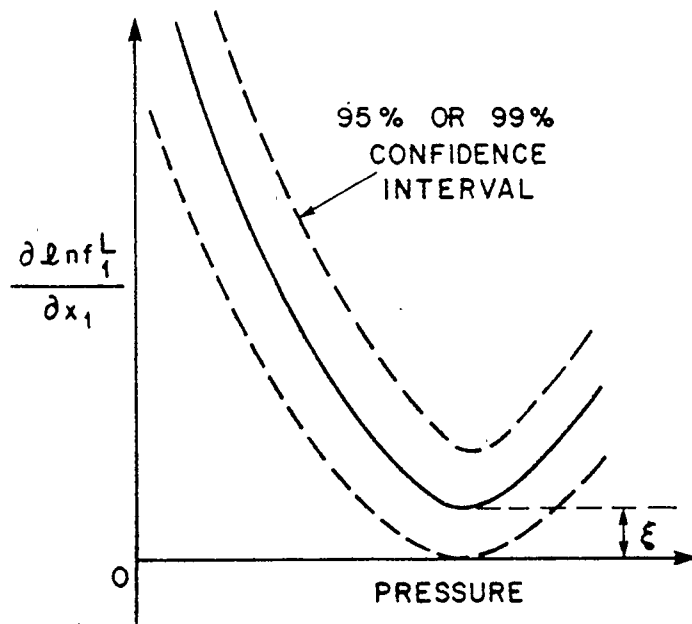


Figure 8.6 Selection of Lower Bound for ϕ

- (i) compute $\left[\frac{\partial \mathbf{e}^T}{\partial \mathbf{k}} \right]_i$, \mathbf{e}_i and ϕ at each data point,
- (ii) keep the experimental point where ϕ becomes minimum,
- (iii) set up matrix A, vector b and compute λ ,
- (iv) decompose matrix A and compute $\frac{\partial \phi_o}{\partial \mathbf{k}}$,
- (v) compute $\Delta \mathbf{k}^{(j+1)}$ from Eq. 78. and update \mathbf{k} .

The solution of the system of the normal equations was obtained exactly the same way as it was in the case of unconstrained estimation.

8.2.5 Numerical Results and Discussion

The methodology is illustrated with two examples. Experimental VLE data for the carbon dioxide - n-Hexane system are available at 313, 353 and 393 K. by Li et al. (1981). The phase diagram for this binary mixture is characterized by the absence of liquid-liquid immiscibility and the existence of a continuous critical locus connecting the critical points of the pure components. The second binary system is the n-Hexane-Ethanol (Gmehling et al., 1982) for which 78 experimental VLE data at six different temperatures are available.

(a) *Carbon Dioxide-n-Hexane*

First, unconstrained minimization was performed using the data for the carbon dioxide-n-Hexane system. The parameter estimates are shown in Table 8.4. These parameter values when used in the Trebble-Bishnoi equation of state resulted in the prediction of erroneous phase behavior, as it was shown in Figure 8.4. Subsequently, constrained minimization was performed and the parameter values are also shown in Table 8.4. Using these parameter estimates the VLE phase behavior is again calculated and the results are shown in Figure 8.7. As seen, these predictions do not indicate any liquid phase separation, however, this is only accomplished with some sacrifice in the overall fit of the VLE data.

The prediction of the correct phase behavior is verified by the calculation of the stability function at all the experimental points. The calculated values of the stability function ϕ , with the parameters from CLS estimation are shown in Figure 8.8. As it is seen they are all positive and hence the liquid phase stability criterion is satisfied. In Figure 8.9 the minimum value of the stability function, ϕ , at each one of the three experimental temperatures is plotted. As seen, by using the proposed constrained least squares estimation method the condition for liquid phase stability is not violated at any of the experimental data points. For this system the phase behavior is represented reasonably well and the parameters calculated by the constrained least squares estimation should suffice.

Table 8.4 Binary Interaction Parameter Estimates for the
CO₂-*n*-Hexane System.

<i>Parameter Value</i>	<i>Standard Deviation</i> (Per Cent)	<i>Minimization Type</i>
k _b = 0.1977	16.9*	Unconstrained
k _c = -1.0699	15.4	
k _b = 0.1345	27.7	Constrained
k _c = -0.7686	23.4	

* As computed under the null hypothesis that σ_{ij} is constant and $q_{ij}=1$.

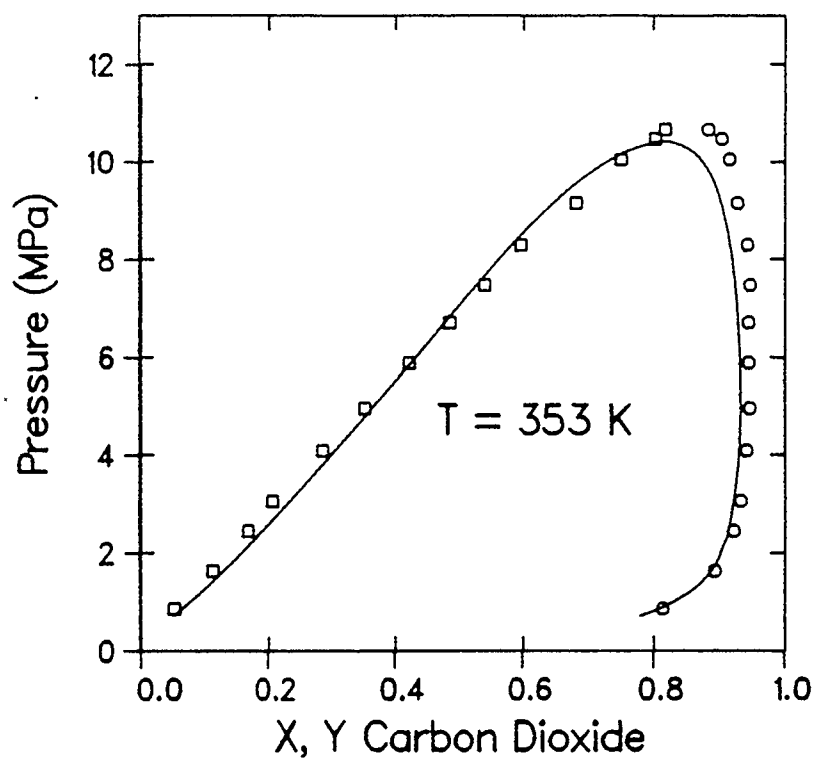


Figure 8.7 VLE Predictions for CO₂-n-Hexane with Interaction Parameters from Constrained Least Squares Estimation

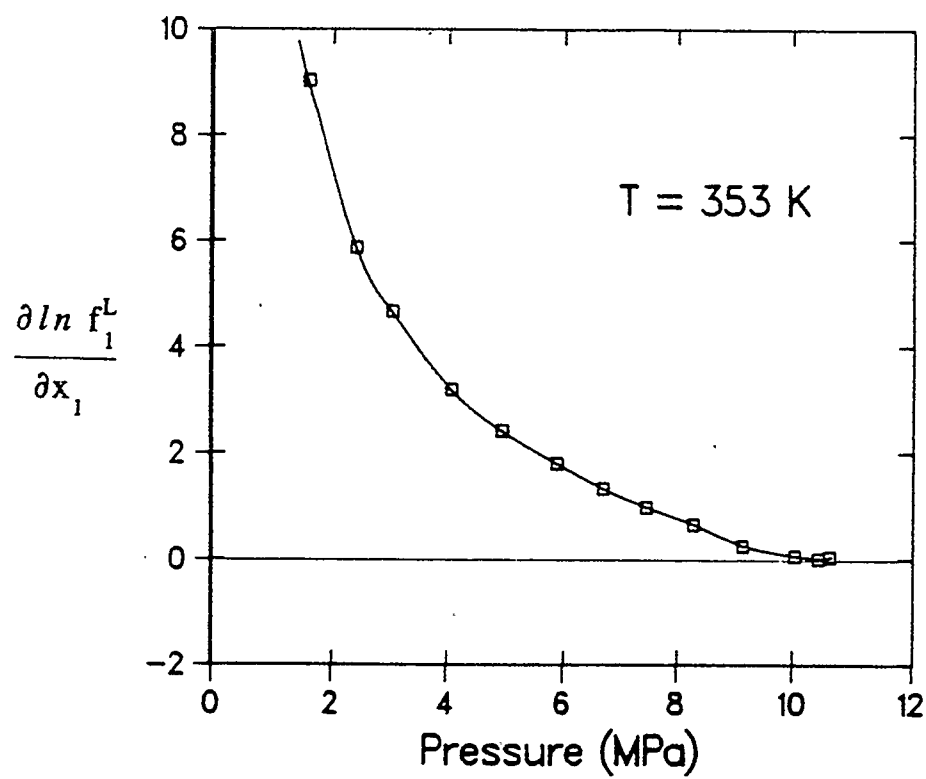


Figure 8.8 The Stability Function with Interaction Parameters from Constrained Least Squares Estimation for the CO₂- n-Hexane System.

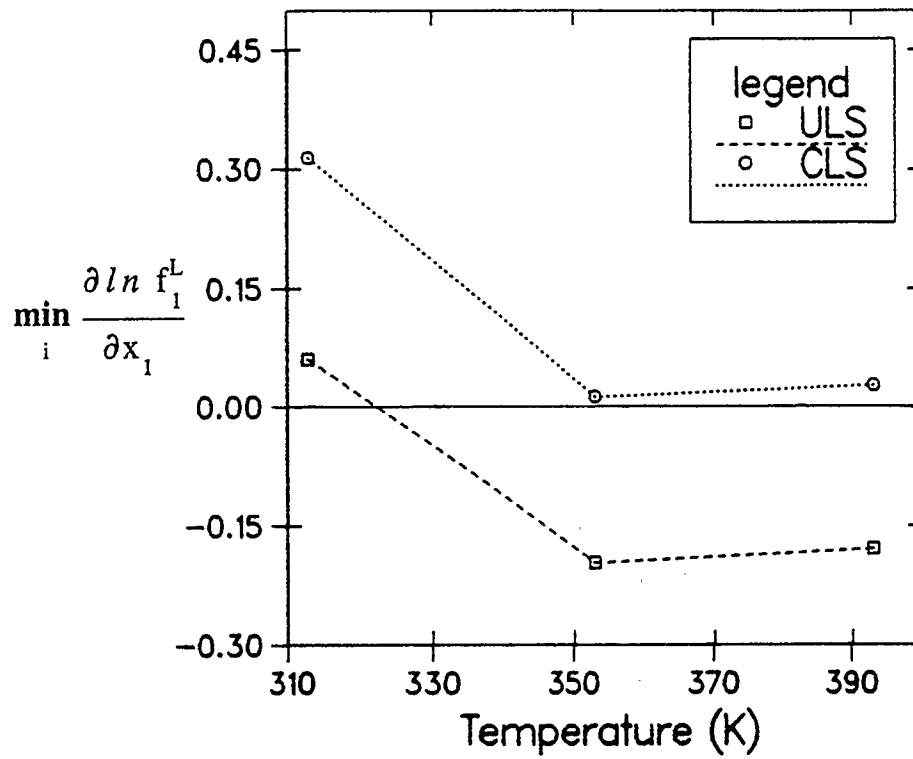


Figure 8.9 The Minimum Value of the Stability Function at each Temperature with Interaction Parameters from ULS and CLS Estimation

(b) *n-Hexane-Ethanol*

Similar calculations were performed for the *n*-Hexane-ethanol system. The parameter estimates are shown in Table 8.5. In Figure 8.10 the VLE predictions together with the experimental data at 323 K are shown. As seen, using the parameters from unconstrained minimization, erroneous liquid phase separation is predicted. The correct phase behavior is obtained when the parameters are estimated with the proposed constrained LS estimation method. This is illustrated in Figure 8.11 where the VLE predictions using these parameters are shown. The phase equilibrium and stability function calculations were performed at all the experimental temperatures. In Figure 8.12 the minima of the stability function, calculated by using both the interaction parameter sets, are shown. The stability criterion which was violated using the interaction parameters from the unconstrained estimation is positive at all the experimental data points when the interaction parameters from the constrained estimation are used.

It is interesting to plot the Gibbs free energy change of mixing for the binary liquid mixture at a temperature and pressure where liquid phase separation is suggested by the EOS with the interaction parameters from unconstrained optimization. This is depicted by the solid line in Figure 8.13. It is the familiar curve which indicates liquid splitting. However, when the Gibbs free energy change of mixing is calculated by utilizing the parameters from constrained optimization, the dashed curve is obtained. This curve indicates a stable liquid phase.

Table 8.5 Binary Interaction Parameter Estimates for the
n-Hexane - Ethanol System.

<i>Parameter Value</i>	<i>Standard Deviation</i> (Per Cent)	<i>Minimization Type</i>
$k_a = 0.4743$	2.00*	Unconstrained
$k_d = 0.3722$	1.90	
$k_a = 0.3211$	9.30	Constrained
$k_d = 0.2555$	10.1	

* As computed under the null hypothesis that σ_{ij} is constant and $q_{ij}=1$.

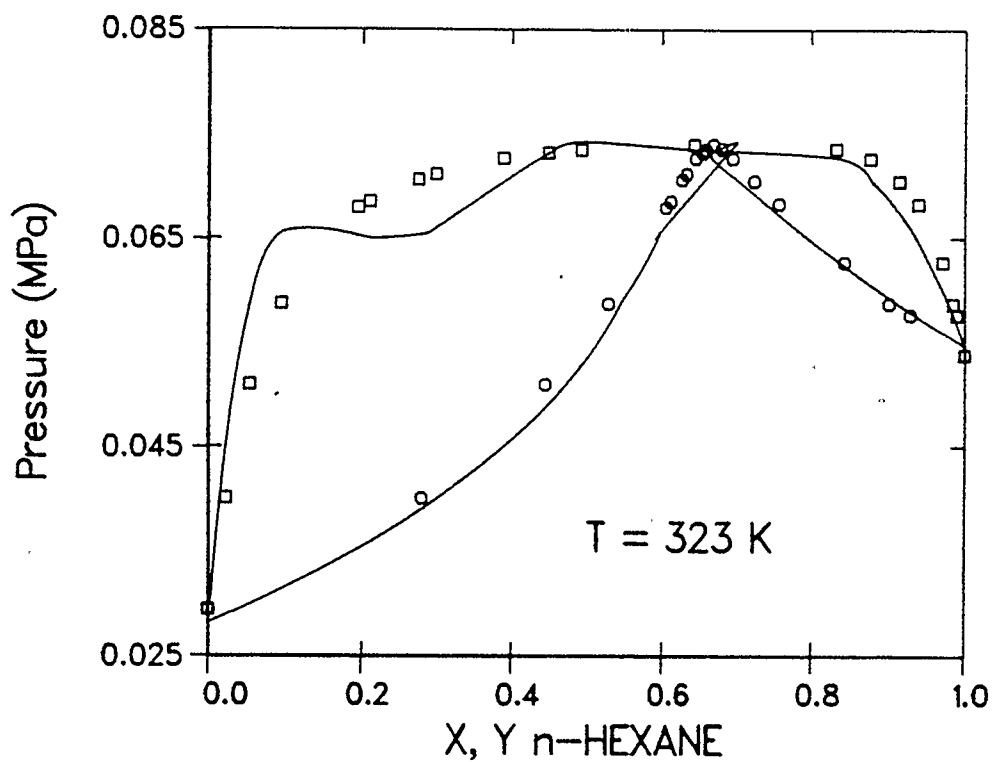


Figure 8.10 VLE Predictions for the n-Hexane-Ethanol System with Interaction Parameters from Unconstrained LS Estimation.

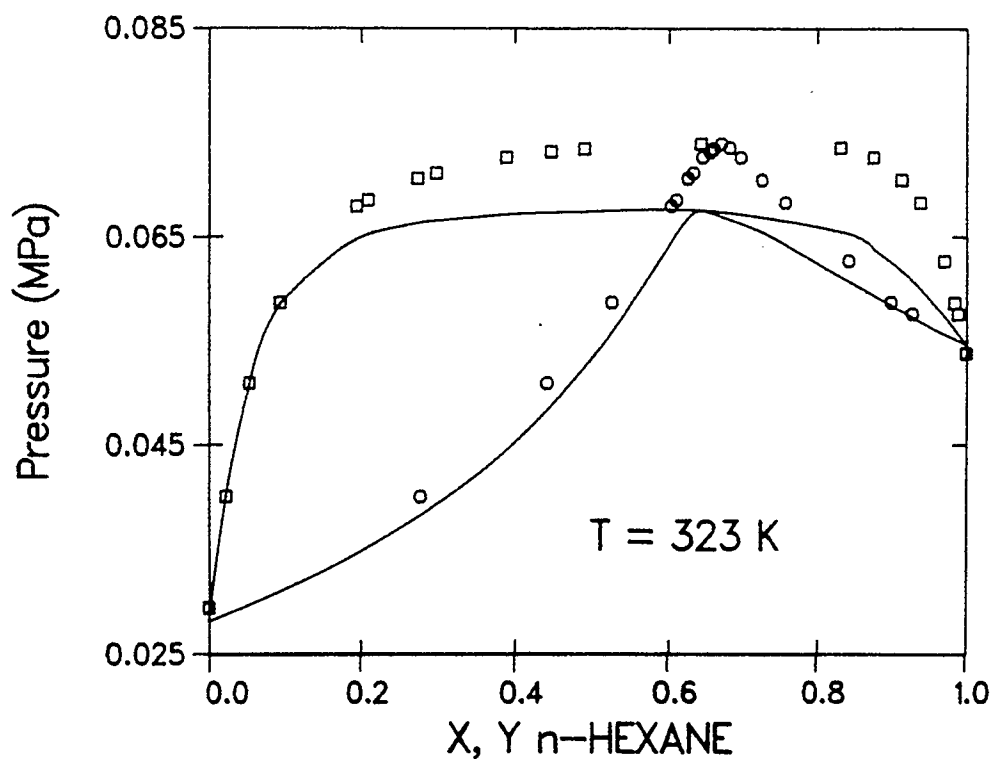


Figure 8.11 VLE Predictions for the n-Hexane-Ethanol System with Interaction Parameters from Constrained LS Estimation.

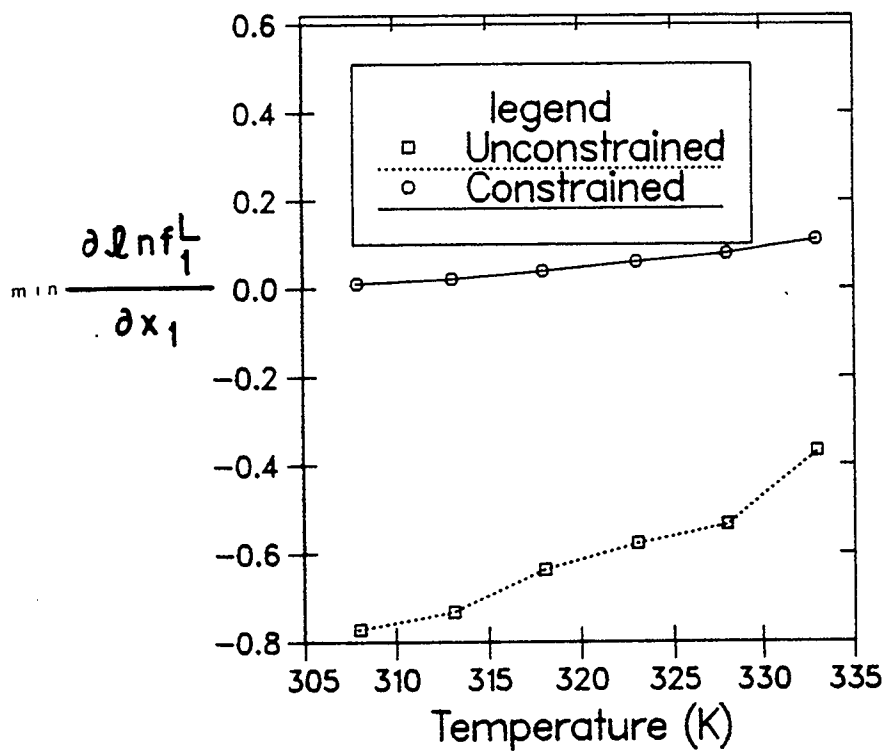


Figure 8.12 The Minimum Value of the Stability Function at each Temperature with Parameters from ULS and CLS Estimation.

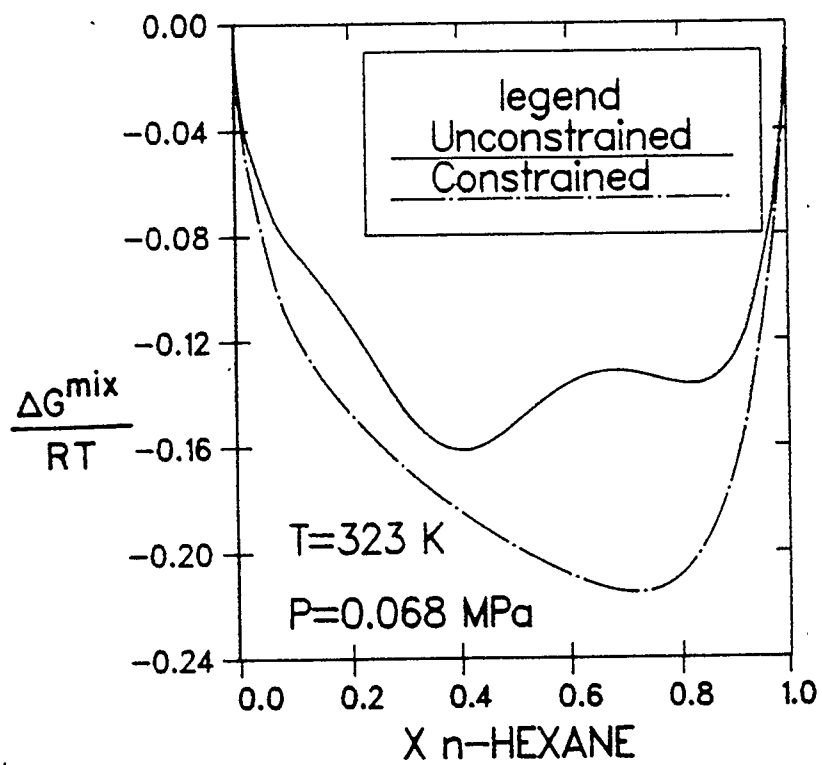


Figure 8.13 Gibbs Free Energy Change of Mixing for the n-Hexane - Ethanol System

8.2.6 A Systematic Approach to the Interaction Parameter Estimation Problem in Equations of State

The above mentioned estimation methods can be used to synthesize a systematic approach to the parameter estimation problem when using binary VLE data and having no prior knowledge regarding the adequacy of the thermodynamic model (EOS). In this case, the following approach for parameter estimation, also depicted in Figure 8.14, is advocated.

- (a) Use the proposed simple LS estimation procedure and determine the binary interaction parameters.
- (b) Plot the data and the model predictions and *judge* whether the fit is *acceptable*. If the fit is *acceptable*, proceed to the next step. Otherwise one may wish to change the EOS or the mixing rules or keep the thermodynamic model as it is and examine the predicted phase behavior. If the phase behavior is correct the LS estimates should suffice. If it is not correct then the proposed Constrained LS estimation should be performed.
- (c) Using the determined parameters as initial guesses, obtain the optimum parameter values by using the proposed implicit ML estimation procedure.

At this point it is up to the user whether to proceed with further

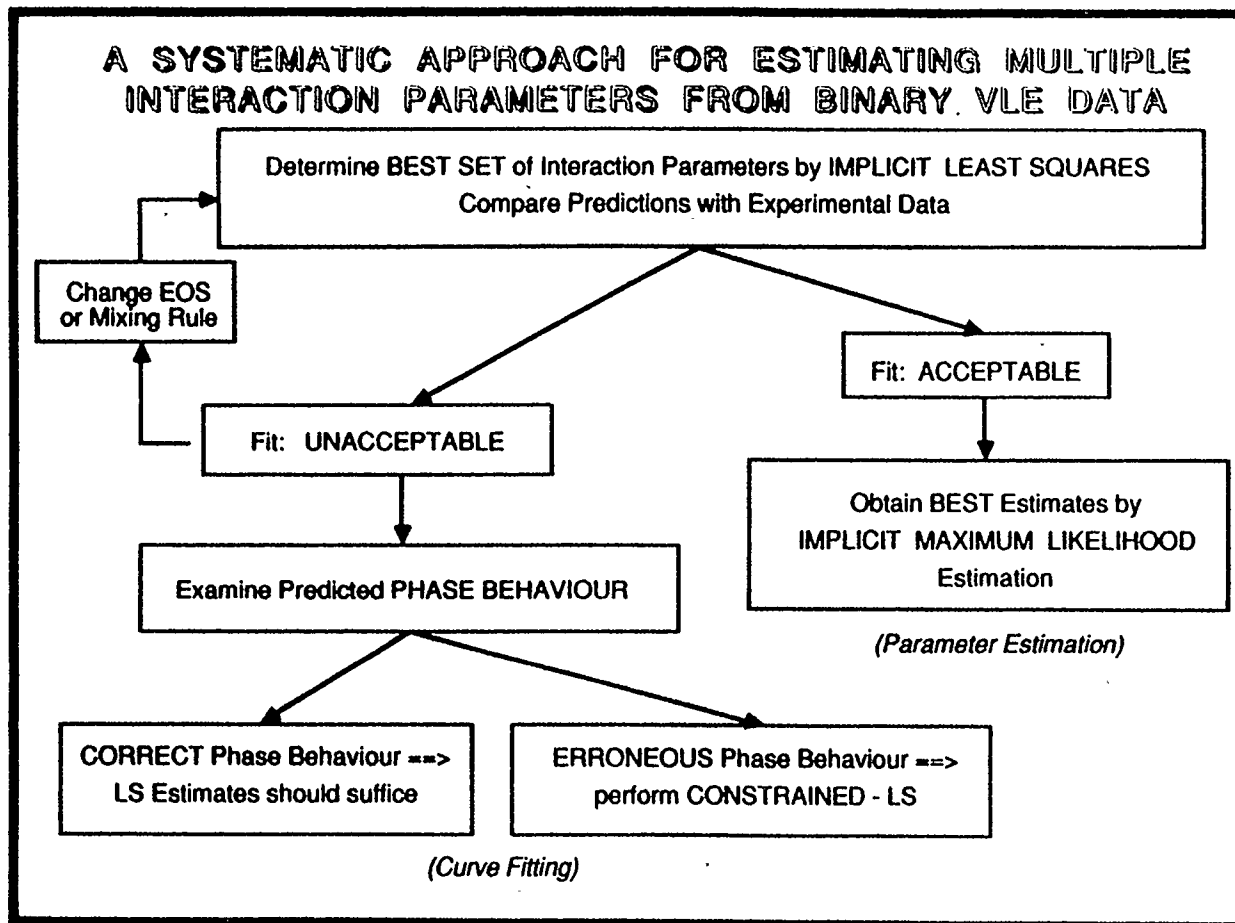


Figure 8.14 A Systematic Approach for the Interaction Parameter Estimation Problem in Equations of State

investigations such as computation of the standard error of parameter estimates, computation of the standard error of estimate of the model prediction, detection of erroneous measurements (outliers), performance of model adequacy tests, etc.

Step (a) is very important when using EOS which utilize more than one binary interaction parameters. In such cases we have to select the best combination of interaction parameters to be used, besides determining their optimal values. For example, the Trebble-Bishnoi EOS can utilize up to four interaction parameters and hence, the number of possible combinations that should be investigated is $\sum_{i=1}^4 \binom{4}{i} = 15$.

In general, it is desirable to utilize as few interaction parameters as possible. Therefore, the investigation begins by considering all possible cases with one parameter. Among them, the best is used for the generation of the VLE predictions. Upon examination, we decide whether the fit is *acceptable*. If it is, we proceed to determine the statistically optimal parameter value by using the implicit ML procedure. If the fit is not *acceptable* one should proceed to utilize two binary interaction parameters. Again, all possible two parameter combinations should be examined and the VLE predictions be generated with the optimal set of parameters. If necessary, we proceed with three or more parameters. It is noted that the decision whether the fit is *acceptable* is subjective and based on experience rather than a rigorous statistical test.

The methane-methanol system which was discussed in chapter 8 provides an example where ML estimation of the binary interaction

parameters for the EOS is justified. The EOS can very well represent the experimental phase behavior. In Figure 8.15 the VLE predictions for the n-Pentane-Acetone system are shown. Experimental data for this system at three temperatures are available (Cambell et al. 1986). The calculations in Figure 9.12 are with the LS estimate of the parameter, k_a , which is equal to $0.0977 \pm 2.08 \%$. The values of the other interaction parameters are zero. It is noted that use of more than one parameters does not result in any improvement of the fit. For this system, the predicted phase behavior is consistent with the experimentally observed.

The propane-methanol system which was discussed in the first section of this chapter provides an example which we believe illustrates the need for improved mixing rules. For that system constrained LS estimation was also performed. The calculated interaction parameters are $k_a = 0.1193 \pm 25.6 \%$ and $k_d = -0.3196 \pm 22.9 \%$. In Figure 8.16 the minimum values of the stability function calculated at each experimental temperature are shown. The calculations were done with the Trebble-Bishnoi equation of state and using the interaction parameters obtained by the Unconstrained Least Squares (ULS) and those by the Constrained Least Squares (CLS) Estimation. As seen, the stability criterion is not violated when the above reported interaction parameters are used. The calculated phase behavior is consistent with the experimental data. However, the deviations between the experimental data and the predictions are large. This is shown in Figure 8.17. For this system the interaction parameters obtained by CLS are not sufficient and one should consider different mixing rules in order to be able to

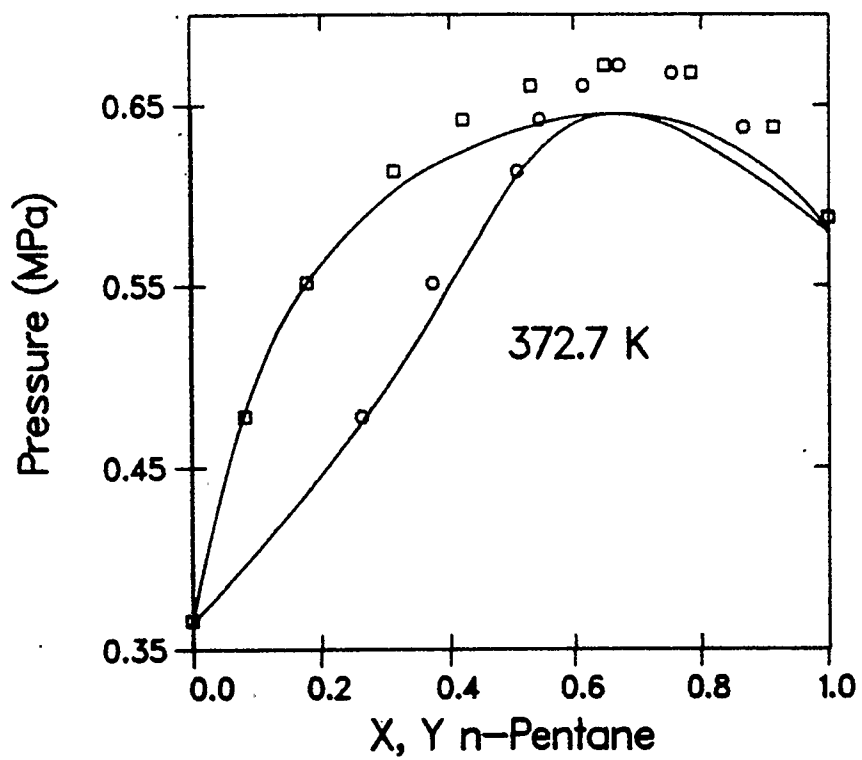


Figure 8.15 VLE Predictions for the n-Pentane-Acetone System.

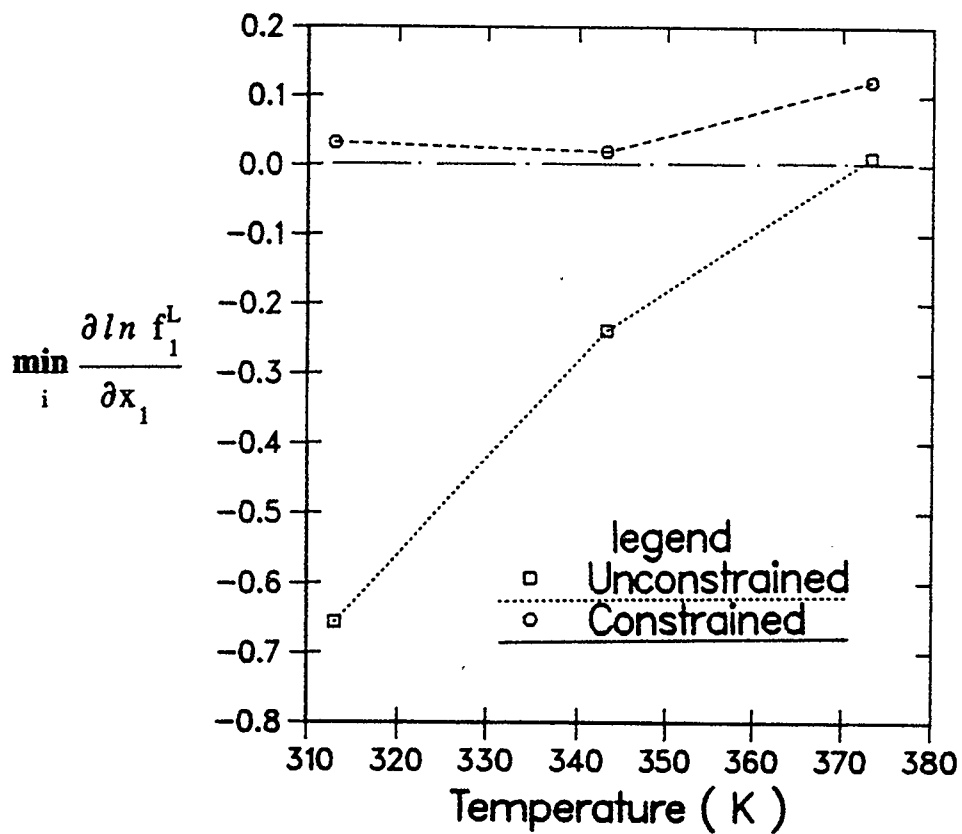


Figure 8.16 The Minimum Values of the Stability Function at each Temperature with Interaction Parameters from ULS and CLS Estimation.

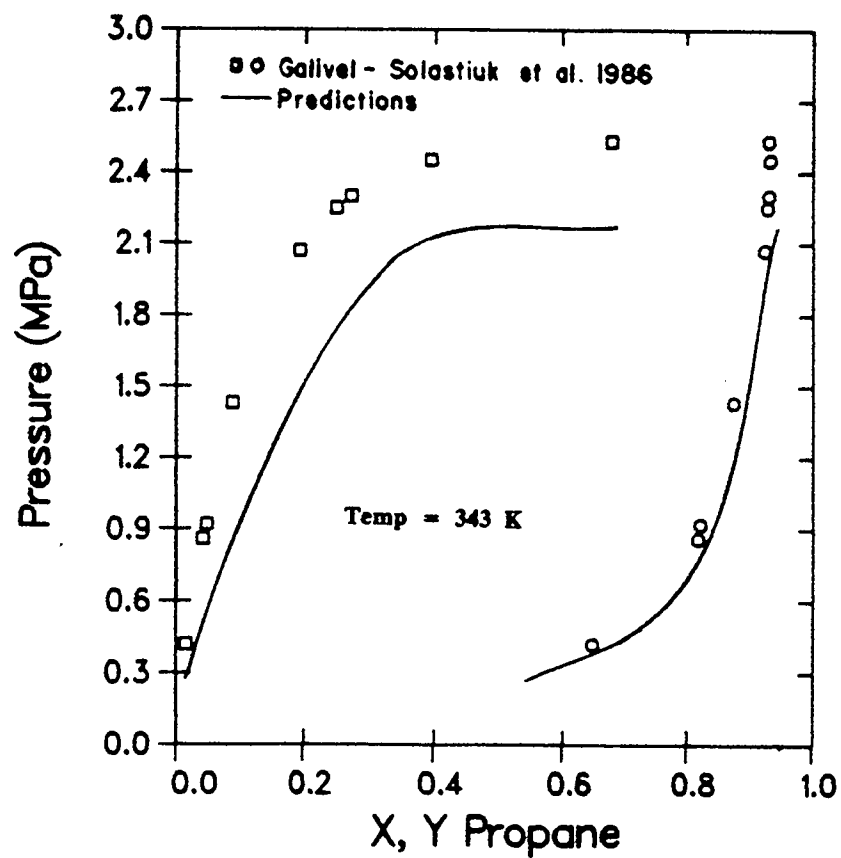


Figure 8.17 VLE Predictions for the Propane-Methanol System with Interaction Parameters from Constrained LS Estimation

represent the correct phase behavior. On the other hand CLS estimation is very useful for systems like the CO_2 - n-Hexane and n-Hexane-Ethanol.

9 SIMULTANEOUS REGRESSION OF BINARY VLE AND VLLE DATA

9.1 Introduction and Problem Statement

According to Rowlinson and Swinton (1982) the phase diagrams for binary mixtures can be classified into six principal types. In five of these categories the mixtures exhibit liquid-liquid phase separation. It is therefore essential for process design purposes to have both vapor-liquid equilibrium (VLE) and vapor-liquid-liquid equilibrium (VLLE) experimental data. These data are either needed directly for process design or more importantly for the development of empirical thermodynamic models with predictive capabilities.

For systems where both VLE and VLLE data are available, all the data should be used in the estimation of the interaction parameters. In this chapter, an implicit LS estimation procedure for the simultaneous regression of binary VLE and VLLE data is proposed. In addition, an implicit ML estimation procedure is proposed to obtain the statistically best interaction parameters whenever the thermodynamic model represents the data without any systematic deviations. As the efforts for the improvement of the mixing rules for EOS intensify and better models are developed, the suggested ML estimation procedure should be particularly helpful due to its computational efficiency.

Let us assume that for a binary system M VLLE experiments have been performed. Usually, such information is available in the form of a set of data indicating the temperature, T , the pressure, P , and the mole

fraction of one of the components in all the phases at equilibrium (vapor, liquid-I and liquid-II). If \hat{z} is the vector of the measurements, it is related to the vector of the *true* but unknown state variables, $z_i = (T_i, P_i, y_i, x_i^I, x_i^{II})^T$, by the following equation

$$\hat{z}_i = z_i + \varepsilon_i \quad i=1,\dots,M \quad (84)$$

where the vector ε_i represents the errors in the measurements at the i th experiment. These errors are assumed to be normally distributed with zero means and known variances. The EOS is considered a functional relationship among the state variables, z , the unknown interaction parameters, k , and the precisely known parameters, u . The latter are the pure component EOS parameters, the critical constants etc.

Given the above information and by taking into account the phase equilibrium relationships we can determine the parameter vector, k , by minimizing a suitable optimality criterion. This criterion is a measure of the ability of the EOS to correlate the experimental data.

9.2 Proposed Implicit ML and LS Estimation Procedures

The implicit LS and ML estimation procedures for the regression of the VLE data, which were presented in chapter 8, can be easily extended to the case where VLLE data are also available. The objective function for VLLE data regression alone is

$$S^{VLL}(\mathbf{k}) = \sum_{i=1}^M \mathbf{r}_i^T \mathbf{W}_i \mathbf{r}_i \quad (85)$$

where \mathbf{r}_i represent the residuals from the i th experiment and are defined as following

$$\mathbf{r}_i = \begin{bmatrix} r_1 \\ r_2 \\ r_3 \\ r_4 \end{bmatrix}_i = \begin{bmatrix} \ln f_1^I - \ln f_1^V \\ \ln f_2^I - \ln f_2^V \\ \ln f_1^{II} - \ln f_1^V \\ \ln f_2^{II} - \ln f_2^V \end{bmatrix}_i \quad (86)$$

The chosen form of the residuals is similar to the one used for VLE data regression and is based on the isofugacity conditions at each three phase equilibrium point

$$f_{ij}^V = f_{ij}^I = f_{ij}^{II} \quad i=1,\dots,M; j=1,2 \quad (87)$$

The residuals are calculated using the measured values, \hat{z}_i , of the state variables. The weighting matrix \mathbf{W} is the identity matrix if LS estimation is performed or the inverse of the covariance matrix \mathbf{V} of the residuals when ML estimation is used. The elements of this matrix can be related to the known variance of the errors in the measurements of the state variables ($T, P, y, \mathbf{x}^I, \mathbf{x}^{II}$) by the error propagation law. The covariance matrix has the following form

$$V_i = \begin{bmatrix} \sigma_1^2 & \sigma_{12} & \sigma_{13} & \sigma_{14} \\ \sigma_{12} & \sigma_2^2 & \sigma_{23} & \sigma_{24} \\ \sigma_{13} & \sigma_{23} & \sigma_3^2 & \sigma_{34} \\ \sigma_{14} & \sigma_{24} & \sigma_{34} & \sigma_4^2 \end{bmatrix}_i \quad (88)$$

The diagonal elements, σ_j^2 ($j=1,4$), of the covariance matrix are given by

$$\sigma_{j,i}^2 = \left[\frac{\partial r_j}{\partial x_1} \right]^2 \sigma_{x,i}^2 + \left[\frac{\partial r_j}{\partial T} \right]^2 \sigma_{T,i}^2 + \left[\frac{\partial r_j}{\partial y_1} \right]^2 \sigma_{y,i}^2 + \left[\frac{\partial r_j}{\partial P} \right]^2 \sigma_{P,i}^2 \quad (89)$$

where the mole fraction x_1 is equal to x_1^I for σ_1^2 and σ_2^2 , and equal to x_1^{II} for σ_3^2 and σ_4^2 . Similarly, we obtain the elements σ_{12} and σ_{34} . In particular

$$\begin{aligned} \sigma_{12,i} = & \left[\frac{\partial r_1}{\partial x_1} \right] \left[\frac{\partial r_2}{\partial x_1} \right] \sigma_{x,i}^2 + \left[\frac{\partial r_1}{\partial P} \right] \left[\frac{\partial r_2}{\partial P} \right] \sigma_{P,i}^2 + \\ & \left[\frac{\partial r_1}{\partial y_1} \right] \left[\frac{\partial r_2}{\partial y_1} \right] \sigma_{y,i}^2 + \left[\frac{\partial r_1}{\partial T} \right] \left[\frac{\partial r_2}{\partial T} \right] \sigma_{T,i}^2 \end{aligned} \quad (90)$$

where $x_1 = x_1^I$. The covariance $\sigma_{34,i}$ is calculated from Eq. 9 by using $x_1 = x_1^{II}$ and the residuals r_3 and r_4 instead of r_1 and r_2 respectively. Since the residuals r_1 and r_2 are correlated with r_3 and r_4 , the

covariances σ_{13} , σ_{14} , σ_{23} and σ_{24} do exist. These elements, σ_{jk} ($j=1,2$; $k=3,4$) for the i^{th} experiment can be obtained from

$$\sigma_{jk, i} = \left[\frac{\partial r_j}{\partial P} \right] \left[\frac{\partial r_k}{\partial P} \right] \sigma_P^2 + \left[\frac{\partial r_j}{\partial y_1} \right] \left[\frac{\partial r_k}{\partial y_1} \right] \sigma_{y,i}^2 + \left[\frac{\partial r_j}{\partial T} \right] \left[\frac{\partial r_k}{\partial T} \right] \sigma_{T,i}^2 \quad (91)$$

In the above equations all the derivatives are evaluated at \hat{z}_i , and it is assumed that the variances of the measurement errors are known.

9.3 Simultaneous Regression of Binary VLE and VLLE Data

It is evident from the above analysis that when both the VLE and the VLLE data are to be used for the estimation of the interaction parameters, the objective function that should be minimized is

$$S(\mathbf{k}) = \sum_{i=1}^N \mathbf{e}_i^T \mathbf{Q}_i \mathbf{e}_i + \lambda \sum_{i=1}^M \mathbf{r}_i^T \mathbf{W}_i \mathbf{r}_i \quad (92)$$

where λ is a user supplied weighting factor which in the case of ML estimation should be set equal to one. When LS estimation is performed, λ can be chosen to assign a higher or lower weight to the three phase data. The weighting matrices \mathbf{Q} and \mathbf{W} are equal to the identity matrix when LS estimation is performed. For ML estimation, \mathbf{Q} and \mathbf{W} should be the inverse of the covariance matrices of the residuals.

The advantage of using implicit estimation methods is their computational efficiency due to the absence of any iterative phase

equilibrium calculations during the minimization of the objective function. This is particularly important when VLLE data are used, since the iterative solution of the four equilibrium equations is avoided. The minimization is performed by using the Gauss-Newton method exactly the same way as it was described in chapter 8.

9.4 Numerical Results and Discussion

As an example, we consider the experimental data for the system *Hydrogen Sulfide - Water* (Selleck et al., 1952). In particular, 53 VLE data points at five temperatures together with five VLLE data points were available for the regression of the binary interaction parameters. The above binary system is a typical type III mixture in the classification of Rowlinson and Swinton (Rowlinson and Swinton, 1982). Its characteristic is that the three phase VLLE locus is at slightly lower pressures than the vapor pressures of *hydrogen sulfide*. The upper critical end point (UCEP) for the *hydrogen sulfide-water* system is very close to the critical point of *hydrogen sulfide* (373.2 K, 8.94 MPa). Selleck et al. (1952) reported the values of 373.45 K and 9.00 MPa for the UCEP.

In Table 9.1 the estimated parameters with LS or ML estimation together with their standard deviation and covariance are given. As seen, the parameters obtained by least squares regression of the VLE data are just slightly different from those obtained by the regression of the VLLE data. As expected, by performing simultaneous regression of

Table 9.1 Interaction Parameters for the H₂S - H₂O System
Using the VLE and VLLE Data by Selleck et al. (1952)

<i>Parameter</i>	<i>Standard Deviation</i>	<i>Covariance</i>	<i>Data</i>	<i>Method</i>
k _a = 0.1957 k _d = -0.5297	0.0070* 0.0185*	0.13x10 ⁻³ *	VLE	LS
k _a = 0.2011 k _d = -0.5410	0.0152* 0.0385*	0.55x10 ⁻³ *	VLLE	LS
k _a = 0.1972 k _d = -0.5332	0.0065* 0.0170*	0.11x10 ⁻³ *	VLE+VLLE	LS
k _a = 0.1978 k _d = -0.5869	0.0013 0.0031	0.38x10 ⁻⁵	VLE	ML
k _a = 0.1421 k _d = -0.4309	0.84x10 ⁻⁴ 0.26x10 ⁻²	0.85x10 ⁻⁷	VLLE	ML
k _a = 0.1432 k _d = -0.4512	0.82x10 ⁻⁴ 0.70x10 ⁻³	0.22x10 ⁻⁷	VLE+VLLE	ML

* Computed under the null hypothesis that the model is exact and the residuals are normally distributed with zero mean and constant variance.

the two and three phase data the estimated parameters are again almost identical. In Figure 9.1 the phase equilibrium predictions obtained by using the interaction parameters from the simultaneous regression are shown as dotted curves together with the experimental data. In the same figure, the solid curves represent the predictions which are based on zero interaction parameters. As seen, the introduction of the binary interaction parameters improves dramatically the ability of the equation of state to represent the data.

The ability of the EOS to represent the data without systematic deviations justifies the use of maximum likelihood estimation. The results of the ML calculations are also shown in Table 9.1. As seen, when only the VLE data are used the ML estimate of k_a is different from its LS estimate. By performing ML estimation using the VLLE data alone, different values for the parameters are obtained. The parameters obtained by the simultaneous ML estimation using the VLE and the VLLE data are very close to those obtained by the ML estimation based on the VLLE data alone and have the smallest standard deviation and covariance.

In Figure 9.2 the equilibrium predictions based on the ML estimates are shown. As seen, the incorporation of the three phase data results in parameters which yield slightly improved liquid phase compositions, however, the vapor phase compositions have become slightly worse. The calculations at the other temperatures indicated the same behavior for the liquid composition. The vapor composition was found to be either slightly worse or the same.

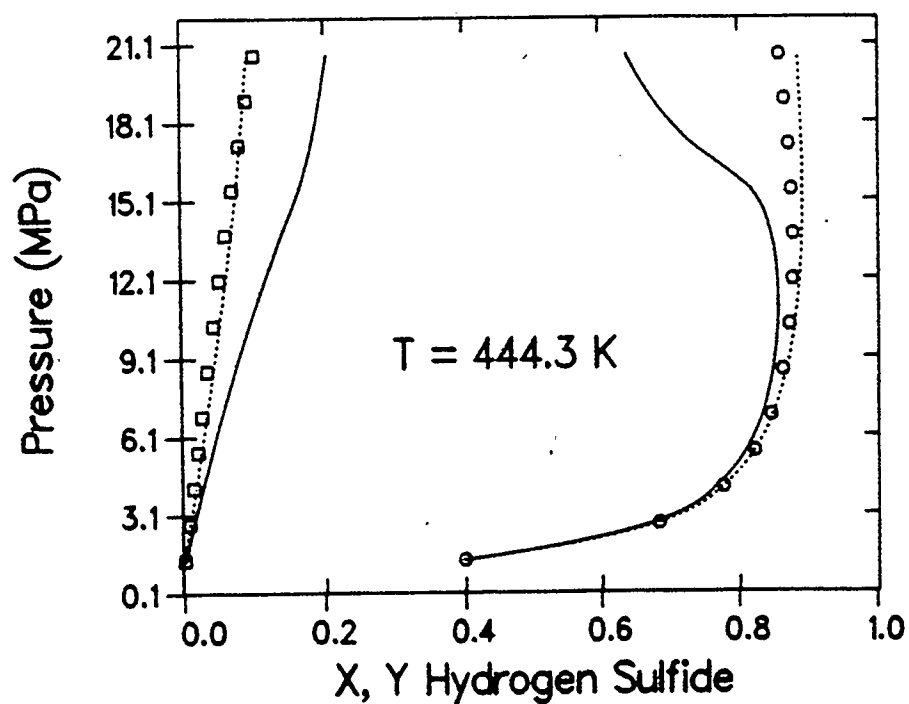


Figure 9.1 VLE for the Hydrogen Sulfide - Water System. (—) Zero Interaction Parameters. (...) Parameters Obtained by Simultaneous LS Regression of Selleck's VLE and VLLE Data.

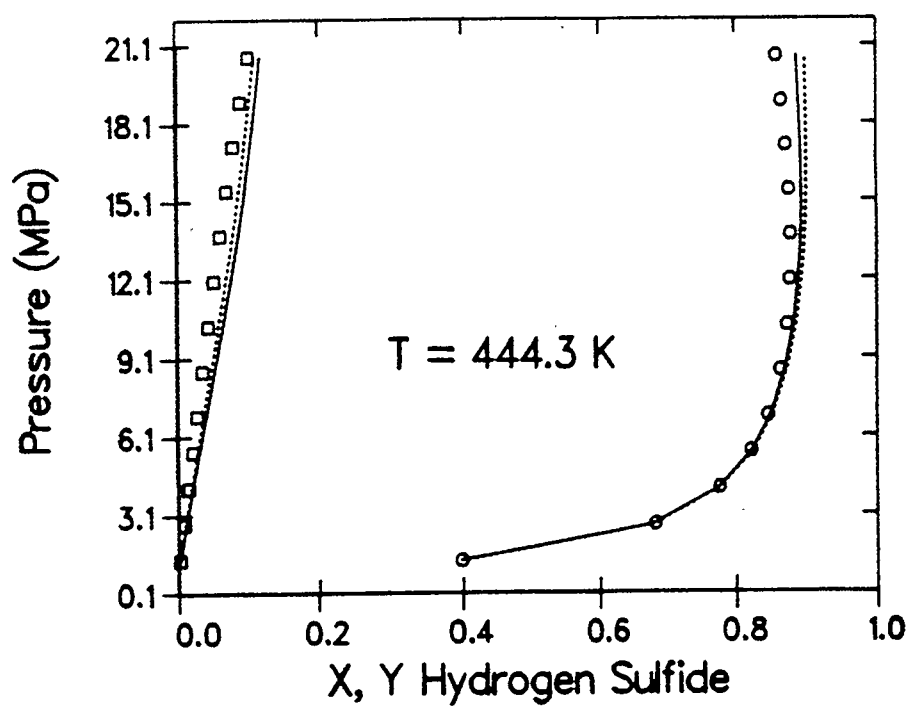


Figure 9.2 VLE for the $\text{H}_2\text{S}-\text{H}_2\text{O}$. (—) Parameters Obtained by ML Regression of Selleck's VLE Data. (...) Parameters Obtained by Simultaneous ML Regression of Selleck's VLE and VLLE Data.

In Figure 9.3 the experimental three phase data by Selleck et al. (1952) together with the calculated three phase VLLE locus are shown. The dashed curve is calculated with the interaction parameters obtained by ML estimation using the VLE data, the solid line by using the parameters from the simultaneous ML estimation and the dotted curve by using zero values. It is clear from the figure how important is the contribution of the interaction parameters to the predictive capabilities of the EOS. It also appears from the figure that by using the interaction parameters from the simultaneous ML estimation the calculated temperatures are slightly worse than those obtained by using the parameter estimates from the VLE data regression. Indeed the root mean square deviation (rmsd) is 0.89×10^{-3} when the calculations are performed using the parameters from the ML regression of the VLE data alone whereas it is 0.44×10^{-2} when the parameters from the simultaneous regression are used. However, this is not a contradictory result because the phase equilibrium calculations for the vapor and liquid mole fractions were found to be better in the latter case.

The above results indicate that different parameters may be obtained by the inclusion of the three phase data. However, the phase predictions do not change significantly. From a statistical point of view, if VLLE data are available then all the experimental information, namely both VLE and VLLE data should be used for the estimation of the binary interaction parameters. The definite advantage of performing the simultaneous regression, when it is possible, is the fact that the parameters are more well defined in terms of smaller standard error of

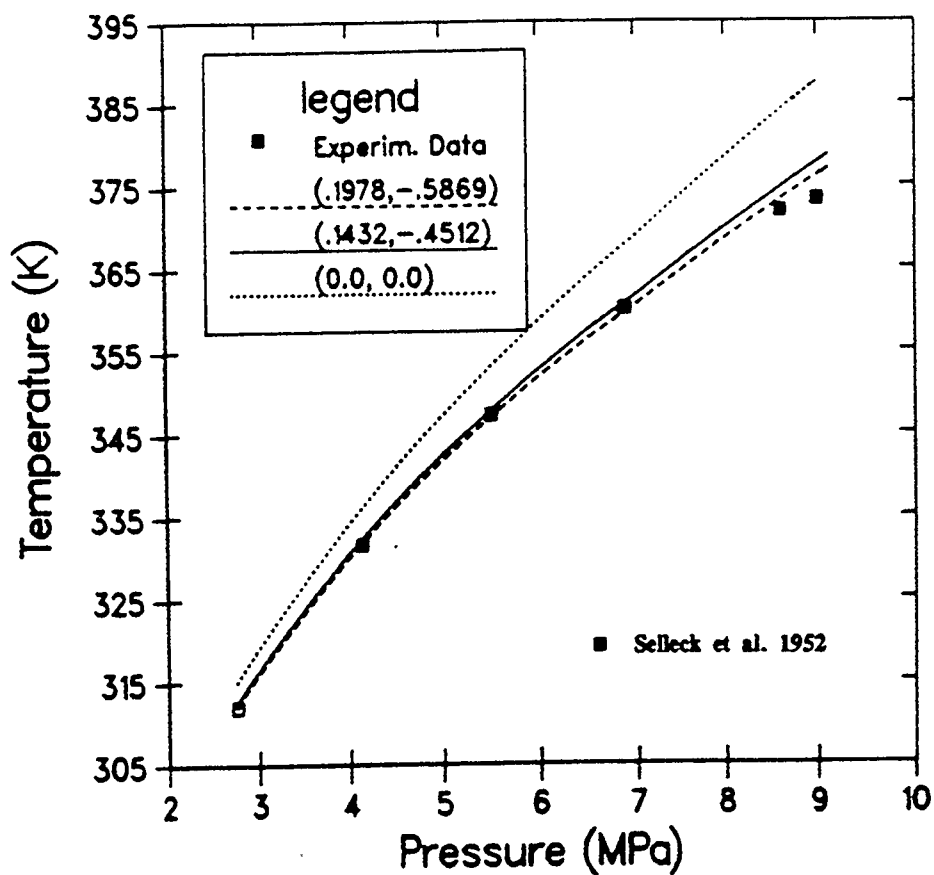


Figure 9.3 Three Phase Temperature-Pressure Locus for H₂S - H₂O.
 (—) Parameters from Simultaneous ML Estimation,
 (- - -) Parameters from ML Estimation Using VLE Data,
 (...) Zero Interaction Parameters

estimate and a reduced correlation among the parameter values. Hence, the recommended interaction parameter values are those from the simultaneous ML estimation ($k_a=0.1432$ and $k_d=-0.4512$).

It is noted that the inclusion of the three phase data does not increase the computational requirements compared with the time required for the estimation using the VLE data alone. The ML estimation, generally requires about five times more computational time compared with least squares for the regression of either VLE or VLLE data.

9.4.1 Effect of Inconsistent Data

Recently, new experimental VLLE data for the hydrogen sulfide-water system became available (Carroll and Mather, 1989a). They found that the three phase locus extends up to 9.39 MPa and 379.35 K. This UCEP is about 6 °C higher than that reported by Selleck et al. (1952). The same researchers also presented a new interpretation (Carroll and Mather, 1989b) for the smoothed data of Selleck et al. In particular, they concluded that the extrapolations for the aqueous phase concentrations are incorrect. Also, since the UCEP was 6 degrees lower than that found by Carroll and Mather, Selleck et al. misinterpreted the results at 377.55 K by ignoring the existence of the three phase point.

In view of this recent experimental work, the interaction parameters were estimated again using the correct VLE data by Selleck et al. and the VLLE data by Carroll and Mather. The correct VLE data are those reported by Selleck et al. excluding their extrapolated results

and the point at 377.55 K where three phases were observed by Carroll and Mather. The results from the parameter estimation are shown in Table 9.2.

As seen from the table, the LS parameter estimates are almost identical. However, the parameters calculated by ML estimation are different. The two and three phase equilibrium calculations were performed using the parameters from Table 9.2. As it was the case with the parameters from Table 9.1 the phase behavior results are similar. The recommended parameter values are $k_a=0.2102$ and $k_d=-0.5462$. It is interesting to see how the phase behavior predictions are compared with those obtained by using the interaction parameters from the regression of all the data by Selleck et al. ($k_a=0.1432$ and $k_d=-0.4512$).

In Figure 9.4 the dotted lines represent the calculated phase behavior by using the interaction parameters (0.2102, -0.5462) from the simultaneous ML regression of Selleck's correct VLE data with Mather's VLLE data. Also shown are the experimental data and the calculations based on the interaction parameters obtained from the simultaneous regression of Selleck's VLE and VLLE data (0.1432, -0.4512). It is evident that when the consistent data set is used the interaction parameters enable the equation of state to represent the liquid phase compositions more accurately. The vapor phase compositions, although they are slightly worse, they are still very close to the experimental data.

Table 9.2 Interaction Parameters for the H₂S - H₂O System
Using the VLLE Data by Carroll and Mather and
the Correct VLE Data by Selleck et al.

<i>Parameter</i>	<i>Standard Deviation</i>	<i>Covariance</i>	<i>Data</i>	<i>Method</i>
$k_a = 0.2209$ $k_d = -0.5862$	0.0120* 0.0300*	0.31x10 ⁻³ *	VLE	LS
$k_a = 0.2324$ $k_d = -0.6054$	0.0232* 0.0581*	0.13x10 ⁻² *	VLLE	LS
$k_a = 0.2281$ $k_d = -0.6030$	0.0122* 0.0310*	0.37x10 ⁻³ *	VLE+VLLE	LS
$k_a = 0.1796$ $k_d = -0.4688$	0.0044 0.0120	0.52x10 ⁻⁴	VLE	ML
$k_a = 0.2349$ $k_d = -0.5667$	0.21x10 ⁻⁴ 0.14x10 ⁻³	0.11x10 ⁻⁸	VLL	ML**
$k_a = 0.2102$ $k_d = -0.5462$	0.72x10 ⁻⁴ 0.38x10 ⁻³	0.13x10 ⁻⁷	VLE+VLLE	ML

* Computed under the null hypothesis that the model is exact and the residuals are normally distributed with zero mean and constant variance.

** Convergence was achieved with a value of 0.4 for the Marquardt's directional parameter

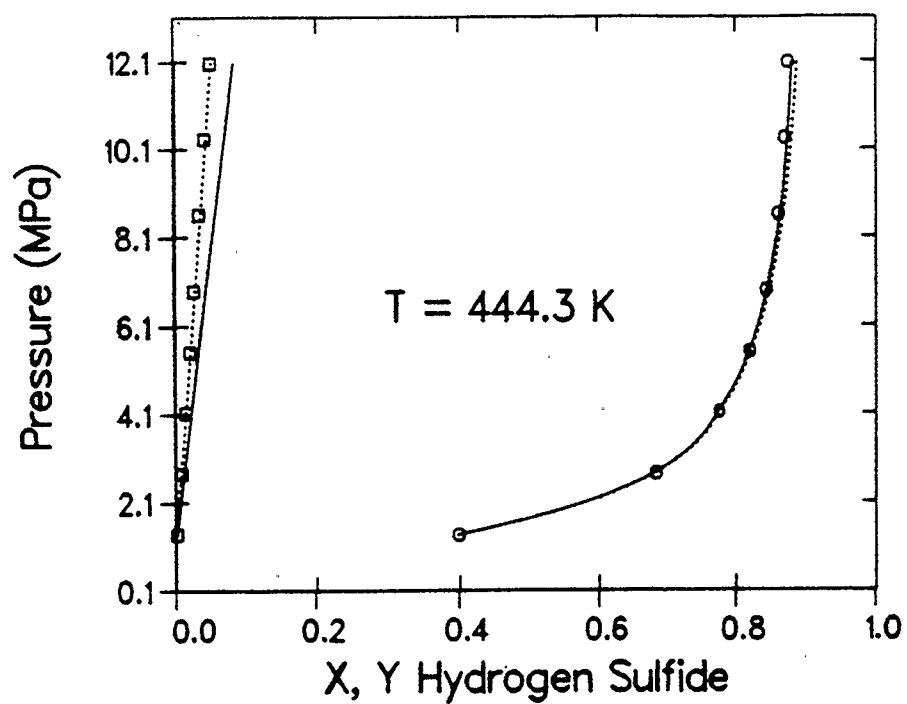


Figure 9.4 VLE for the Hydrogen Sulfide - Water System. (—) Parameters Obtained by the ML Regression of Selleck's VLE and VLLE Data. (...) Parameters Obtained by the ML Regression of Selleck's Correct VLE Data and Mather's VLLE Data.

In Figure 9.5 the calculated three phase temperature-pressure locus together with the experimental data are shown. As seen, the reported data are consistent only up to 7.0 MPa. Using the two sets of parameters the root mean square deviations were calculated for the temperature and the mole fractions in the aqueous liquid, hydrogen sulfide liquid and vapor phases. These results are shown in Table 9.3. The interaction parameters obtained from the regression of the consistent data set result in a significant improvement of the predictions for the aqueous liquid phase compositions. Also, the temperature predictions are better as it is also seen in Figure 9.5. The hydrogen sulfide liquid and the vapor phase compositions are slightly worse but considering the magnitude of the deviations the differences are not significant.

To conclude this chapter, it is mentioned that the inclusion of the three phase equilibrium data, whenever they are available, in the interaction parameter estimation database does not increase the computational requirements substantially. In addition the inclusion of the three phase data results in the estimation of interaction parameters with better statistical properties and hence it is recommended.

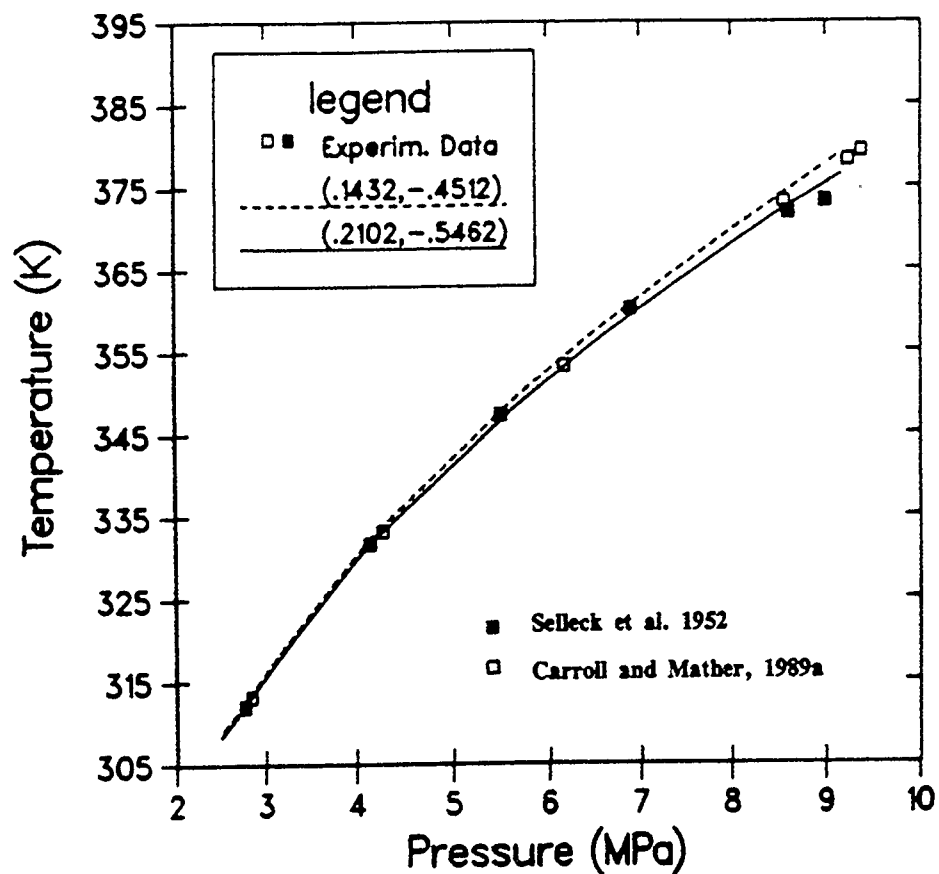


Figure 9.5 Three Phase Temperature-Pressure Locus for H₂S - H₂O.
 (—) Parameters obtained by the ML Regression of Selleck's VLE and VLLE Data. (- - -) Parameters Obtained by the ML Regression of Selleck's Correct VLE Data and Mather's VLLE Data.

Table 9.3 Root Mean Square Deviations in Three Phase Calculations

<i>Parameter</i>	<i>Root Mean Square Deviations in</i>			
	<i>Temperature</i>	\bar{x}^I	\bar{x}^{II}	<i>y</i>
$k_a = 0.1432$ $k_d = -0.4512$	0.27×10^{-2}	0.6305	0.0130	0.71×10^{-2}
$k_a = 0.2102$ $k_d = -0.5462$	0.11×10^{-2}	0.1433	0.0224	0.88×10^{-2}

10. CONCLUSIONS AND RECOMMENDATIONS

10.1 Conclusions

An experimental apparatus for the determination of the equilibrium conditions in hydrate forming systems was built and its ability to provide reliable data was validated. The apparatus was used to obtain equilibrium formation data for ethane hydrate in aqueous solutions of NaCl, KCl, CaCl₂ and KBr. Particularly, fifty experiments were performed at temperatures and pressures between 265.36-282.98 K and 0.488-2.188 MPa respectively. First, six experiments for hydrate formation in pure water were performed in order to compare the results with those obtained in other laboratories and establish the validity of the new apparatus and the procedure. Subsequently, experiments with aqueous solutions of NaCl, KCl and CaCl₂ were performed followed by experiments in aqueous solutions of binary mixtures of these salts. A ternary solution and finally a four-component solution with these three salts and KBr were also studied. The measured pressures and temperatures are believed to be known within ± 10 kPa and ± 0.06 K respectively.

The experimental data obtained in this work as well as all the available data in the literature were predicted using a method which was developed in this work. The method predicts the incipient hydrate formation conditions in light hydrocarbon-water systems in the presence of single or mixed electrolytes. The maximum and minimum percent deviations between the experimental data and the predictions were found

to be 7.50 and 0.76 respectively. The validity of the calculation method makes it a useful tool for the investigation of hydrate formation conditions in sea or ground water. The method can also facilitate studies for water desalination and gas storage via gas hydrate formation.

A simple predictive method to calculate the inhibiting effect of methanol on hydrate formation from mixtures of natural gas components was also presented. Its simplicity arises from the fact that it uses only an equation of state to represent vapor and liquid phases in addition to the van der Waals and Platteeuw thermodynamic model for the solid hydrate. The calculated hydrate formation conditions generally compare very well with the experimental data. Equilibrium phase compositions in the hydrating region were also calculated and found to agree very well with the experimental measurements available in the literature. The usefulness of the method as a design tool was demonstrated by considering the design of a methanol dehydration unit.

The problem of estimating efficiently the interaction parameters in an equation of state was also examined. A computationally efficient method for the regression of binary vapor-liquid equilibrium data was proposed and evaluated. The method consists of an implicit least squares estimation procedure and an implicit maximum likelihood estimation procedure. First, the best combination of interaction parameters is determined by least squares and second, the statistically best parameter values are obtained by maximum likelihood. Conditions under which the least squares estimates suffice are discussed. The required CPU time by

the implicit least squares method was found to be three to eight times less than that required by the implicit maximum likelihood and ten to ninety times less than the simplified error in variables method. The computational efficiency is due to the absence of any phase equilibrium calculations during the minimization of the objective function. The method was extended for the simultaneous regression of binary vapor-liquid and vapor-liquid-liquid equilibrium data. The incremental computational requirements by the inclusion of the three phase data are not significant.

In addition, a constrained least squares method was developed for the estimation of the binary interaction parameters subject to the condition that no liquid phase separation is predicted by the equation of state. The estimation problem is solved by a quadratically convergent algorithm based on the Gauss-Newton method which takes into account the criterion for the stability of the liquid phase. The method was shown to be able to suppress the prediction of erroneous liquid phase separation whenever this happens.

Finally, it was found that although the equation of state calculates a limit for the dissolution of methane in water it is not clear that this limit is related to the limits of supersaturation which were observed in the laboratory. Also, the tangent plane analysis is another way of representing the phase behavior for binary hydrate forming systems.

10.2 Recommendations

In order to improve the the accuracy of the predictions of the equilibrium hydrate formation conditions, the ability of the thermodynamic model which describes the hydrate phase (van der Waals and Platteeuw model) should be improved. Some of the assumptions made by van der Waals and Platteeuw should be replaced by more realistic ones when calculating the Langmuir constants.

It was recognized while doing this study that there is not any thermodynamic model that could describe an aqueous liquid phase where other molecules in addition to electrolytes are also present in non-negligible amounts. Systems like water-methanol-electrolytes and water-carbon dioxide-electrolytes are not only important in hydrates research but also in biochemical systems and in systems encountered when fighting water pollution. Hence, there is a need for such thermodynamic models and efforts should be directed towards this objective.

The experimental program, initiated in the present work should be continued. It is suggested to investigate the carbon dioxide hydrate formation conditions in the presence of electrolytes. These data will be used to extend the predictive method of chapter three or propose a new one for the cases where the solubility of the hydrate forming substance in water in the presence of salts can not be ignored.

The calculation methods presented in this work should be extended to the case where a hydrocarbon liquid phase is also present. In such systems the need for improved thermodynamic models will be more

pronounced.

Numerous researchers deal with the problem of the improvement of an equation of state or the development of a new one. The estimation methods presented here should be used to determine parameters in such efforts and to compare alternative thermodynamic models. It is also recommended that the constrained least squares estimation method presented here be improved, particularly by examining the stability constraint not only at the experimental data but at other conditions as well.

REFERENCES

- Anderson T.F, D.S. Adams and E.A. Greens II, 1978. Evaluation of Parameters for Nonlinear Thermodynamic Models, *AIChE Journal* 24 (1) : 20-29.
- Anderson, F.E., and Prausnitz, J.M., 1986. Inhibition of Gas Hydrates by Methanol, *A.I.Ch.E.J.*, 32, No 8, 1321-1333.
- Baker, L.E., A.C. Pierce, and K.D. Luks, 1982. Gibbs Free Energy Analysis of Phase Equilibria, *Soc. Pet. Eng. J.*, 731-742.
- Barker J.W., and R.K. Gomez, 1989. Formation of Hydrates During Deepwater Drilling Operations, *Journal of Petroleum Technology*, 297-301.
- Barduhn, A.J., H.E. Toelson, and Y.C. Hu, 1962, The Properties of Some New Gas Hydrates and their Use in Demineralizing Sea Water, *AIChE J.*, 8 (2), 176-183.
- Berez, E., and Balla-Achs, M., 1983. *Studies in Inorganic Chemistry 4: Gas Hydrates*, Elsevier, Amsterdam.
- Bishnoi, P.R., A.A. Jeje, N.E. Kalogerakis, and R. Saeger, 1985. The Kinetics of Formation and Decomposition from Mixtures of Natural Gas Components-Experimental Data and Development of Generalized Predictive

Rate Expressions, annual report, *Energy Mines and Resources*, Ottawa, Canada.

Bishnoi, P.R., N.E. Kalogerakis, A.A. Jeje, P.D. Dholabhai, and P. Englezos, 1986. The Kinetics of Formation and Decomposition of Hydrates from Mixtures of Natural Gas Components, final report, *Energy Mines and Resources*, Ottawa, Canada.

Bishnoi, P.R., Gupta, A.K., Englezos P. and Kalogerakis, N., 1989a. Multiphase Equilibrium Flash Calculations for Systems Containing Gas Hydrates, *Fluid Phase Equilibria*, **53**, 97-104.

Bishnoi, P.R., N.E. Kalogerakis, and P. Englezos, 1989b. Kinetics of Gas Hydrate Formation: Intrinsic and Global Rates. Invited paper at the Norwegian Petroleum Society Annual Conference on *Multiphase Flow-Technology & Consequences for Field Development '89*, Stavenger, Norway, May 8-9.

Bond D.C. and N.R. Russell, 1949. Effect of Antifreeze Agents on the Formation of Hydrogen Sulfide hydrate, *Petr. Tr. AIME*, **179**, 192-198.

Box M.J., 1970. Improved Parameter Estimation, *Technometrics* **12** (2) :219-229.

Britt H.I., and R.H. Luecke, 1973. The Estimation of Parameters in

Nonlinear, Implicit Models, *Technometrics* **15** (2) : 233-247.

Byk S.S., and V.I. Fomina, 1968. Gas Hydrates, *Russ. Chem. Rev.*, **37** (6), 469-491.

Campbell, J.M., 1981. *Gas Conditioning and Processing*, Vol. 2. Campbell Petroleum Series, Inc., Norman, OK 5th edition.

Cambell, S.W., R.A. Wilsak, and G. Thodos, 1986. Isothermal Vapor-Liquid Equilibrium Measurements for the n-Pentane-Acetone System at 372.7, 397.7, and 422.6 K, *J. Chem. Eng. Data*, **31**, 424-430.

Carnahan, B., Luther, H.A., and Wilkes, J.O., 1969. *Applied Numerical Methods*, Wiley & Sons, Inc.,

Carroll, J.J., and A.E. Mather, 1989a. Phase Equilibrium in the System Water-Hydrogen Sulfide: Experimental Determination of the LLV Locus. *Can. J. Chem. Eng.*, **67**, 468-470.

Carroll, J.J., and A.E. Mather, 1989b. Phase Equilibrium in the System Water-Hydrogen Sulfide: Modelling the Phase Behavior with an Equation of State *Can. J. Chem. Eng.*, **67**, 999-1003

Davidson, D.W., 1973. *Water: A comprehensive Treatise*. Vol. 2. Frank, F: editor. Plenum Press, New York, Chap. 3.

Davidson, D.W., Garg, S.K., Gough, S.R., Hawkins, R.E., and Ripmeester, J.A., 1977. Characterization of Natural Gas Hydrates by Nuclear Magnetic Resonance and Dielectric Relaxation, *Can. J. Chem.*, 55, 3641-3650.

Deaton, W.M. and E.M.Jr Frost, 1937. Gas Hydrates in Natural Gas Pipe Lines, *Oil and Gas Journal*, 36, (1), 75.

Deaton, W.M. and E.M.Jr Frost, 1946. Clathrate Hydrates and Their Relation to the Operations of Natural Gas Pipe Lines, *USD of the Interior*.

Dharmawardhana, P.B., Parrish, W.R., and Sloan, E.D., 1980. Experimental Thermodynamic Parameters for the Prediction of Natural Gas Hydrate Dissociation Conditions, *Ind. Eng. Chem. Fundam.*, 19, 410-414.

Dholabhai, P.D., P. Englezos, N.E. Kalogerakis and P.R. Bishnoi, 1990. Equilibrium Conditions for Methane Hydrate Formation in Aqueous Mixed Electrolyte Solutions, *Can. Journal of Chemical Engineering* (Submitted).

Dholabhai, P.D., 1989. Incipient Equilibrium Conditions for Methane Hydrate Formation in Aqueous Mixed Electrolyte Solutions, *M.Sc. Thesis*, University of Calgary.

Englezos, P., 1986. A Model for the Formation Kinetics of Gas Hydrates

from Methane, Ethane, and their Mixtures, M.Sc. Thesis, University of Calgary.

Englezos, P., N. Kalogerakis, P.D. Dholabhai and P.R. Bishnoi, 1987a. Kinetics of Formation of Methane and Ethane Gas Hydrates, *Chem. Eng. Sc.*, **42**, No 11, 2647-2658.

Englezos, P., N. Kalogerakis, P.D. Dholabhai and P.R. Bishnoi, 1987b. Kinetics of Gas Hydrate Formation from Mixtures of Methane and Ethane, *Chem. Eng. Sc.*, **42**, No 11, 2659-2666.

Englezos, P. and Bishnoi, P.R., 1988a. Prediction of Gas Hydrate Formation Conditions in Aqueous Electrolyte Solutions, *A.I.Ch.E.J.*, **34** (10), 1718-1721.

Englezos, P. and Bishnoi, P.R., 1988b. Gibbs Free Energy Analysis for the Supersaturation Limits of Methane in Liquid water and the Hydrate-Gas-Liquid water Phase Behavior, *Fluid Phase Equilibria*, **42**, 129-140.

Englezos P., N. Kalogerakis and P.R. Bishnoi, 1989a. Estimation of Binary Interaction Parameters for Equations of State Subject to Liquid Phase Stability Requirements, *Fluid Phase Equilibria*, **53**, 81-88.

Englezos P., N. Kalogerakis and P.R. Bishnoi, 1989b. Simultaneous

Regression of VLE and VLLE Data, 5th International IUPAC Workshop, Gradisca, Italy, September 6-8, 1989, *Fluid Phase Equilibria* in press.

Englezos, P., N. Kalogerakis and P.R. Bishnoi, 1990a. Formation and Decomposition of Gas Hydrates of Natural Gas Components, *Journal of Inclusion Phenomena and Molecular Recognition in Chemistry*, **8**, 89-101.

Englezos P., Z. Huang and P.R. Bishnoi, 1990b. Prediction of Natural Gas Hydrate Formation Conditions in the Presence of Methanol Using the Trebble-Bishnoi Equation of State, *Journal of Canadian Petroleum Technology* in press.

Englezos, P., N. Kalogerakis, M.A. Trebble and P.R. Bishnoi, 1990c. Estimation of Multiple Binary Interaction Parameters in Equations of State Using VLE Data. Application to the Trebble-Bishnoi EOS, 4th International IUPAC Workshop, Thessaloniki, Greece, October 24-26, 1988, *Fluid Phase Equilibria* in press.

Fabries J-F., and H. Renon, 1975. Method of Evaluation and Reduction of Vapor-Liquid Equilibrium Data of Binary Mixtures, *AIChE Journal* **21**(4):735-743.

Fisher, R.A., 1922. The Mathematical Foundations of Theoretical Statistics, *Philosophical Transactions of the Royal Society*, A. **222**, 306-368.

Galivel-Solastiuk F., S. Laugier and D. Richon, 1986. Vapor-Liquid Equilibrium Data for the Propane-Methanol and Propane-Methanol-Carbon Dioxide System, *Fluid Phase Equilibria* 28: 73-85.

Gmehling, J., U. Onken, and W. Arlt, 1982. Vapor-Liquid Equilibrium Data Collection (Supplement 1). DECHEMA Chemistry Data Series, Vol I, Part 2c.

Gupta, A.K., 1989. Ph.D. Dossier, University of Calgary.

Hammerschmidt, E.G., 1934. Formation of Gas Hydrates in Natural Gas Transmission Lines, *Ind. Eng. Chem.*, 26, No. 8, 851-855.

Hammerschmidt, E.G., 1939. Preventing and Removing Hydrates in Natural Gas Pipe Lines, *Gas* 15 (5), 30-34.

Handa, Y.P., and Tse, J.S., 1986. Thermodynamic Properties of Empty Hydrate Lattices of Structure I and Structure II Clathrate Hydrates, *J. Phys. Chem.*, 90, No. 22, 5917-5921.

Hayduck W., 1982. IUPAC Solubility Data Series, Volume 9.

Hayduck W., 1986. IUPAC Solubility Data Series, Volume 24.

Heidemann, R.A., 1974. Three Phase Equilibrium Using Equations of State, *AIChE J.*, **20**, 847-855.

Holder G.D., and V.T. John, 1983. Thermodynamics of Multicomponent Hydrate Forming Mixtures, *Fluid Phase Equilibria*, **14**, 353-361.

Holder G.D., S.P. Zetts, and N. Pradhan, 1988. Phase Behavior in Systems Containing Clathrate Hydrates, *Reviews in Chemical Engineering* 1-69.

Holder, G.D., Gorbin, G., and Papadopoulos, K.D., 1980. Thermodynamic and Molecular Properties of Gas Hydrates from Mixtures Containing Methane, Argon, and Krypton, *Ind. Eng. Chem. Fundam.*, **19**, 282-286.

Holder, G.D., Malekar, S.T., and Sloan, E.D., 1984. Determination of Hydrate Thermodynamic Reference Properties from Experimental Hydrate Composition Data, *Ind. Eng. Chem. Fundam.*, **23**, No. 1, 123-126.

Hong J.H., and R. Kobayashi 1988. Vapor-Liquid Equilibrium Studies for the Carbon Dioxide-Methanol System, *Fluid Phase Equilibria* **41**: 269-276.

Hong J.H., P.V. Malone, M.D. Jett and R. Kobayashi, 1987. The Measurement and Interpretation of the Fluid Phase Equilibria of a Normal Fluid in a Hydrogen Bonding Solvent: The Methane-Methanol System, *Fluid Phase Equilibria* **38**: 83-86.

Houghton G.A., M. McLean and P.D. Ritchie, 1957. Compressibility, Fugacity and Water-Solubility of Carbon Dioxide in the Region 0-36 Atm and 0-100 °C, *Chem. Eng. Sci.*, **6**, 132-137.

Istomin V.A., 1987. A Model of Gas Hydrates Taking into Account the Guest-Guest Interactions, *J. Phys. Chem.*, **61**, 1404-1407.

John V.T., and G.D. Holder, 1982. Hydrates of Methane+n-Butane Below the Ice Point, *J. Chem. Eng. Data* 1982, **27**, 18-21.

John V.T., and G.D. Holder, 1981. Choice of Cell Size in the Cell Theory of Hydrate Phase Gas-Water Interactions, *J. Phys. Chem.*, **85**, 1811-1814.

John V.T., and Holder, G.D., 1982. Contribution of Second and Subsequent Water Shells to the Potential Energy of Guest-Host Interactions in Clathrate Hydrates, *J. Chem. Phys.*, **86**, 455-459.

John V.T., and G.D. Holder, 1985. Langmuir Constants for Spherical and Linear Molecules in Clathrate Hydrates. Validity of the Cell Theory, *J. Phys. Chem.*, **89**, 3279-3285.

John, V.T., Papadopoulos K.D., and Holder, G.D., 1985. A Generalized Model for Predicting Equilibrium Conditions for Gas Hydrates, *A.I.Ch.E.J.*, **31**, No. 2, 252-259.

Kalogerakis N., and R. Luus 1983. Improvement of Gauss-Newton Method for Parameter Estimation through the Use of Information Index, *Ind. Eng. Chem. Fundam* 22: 436-445.

Katz, D.L., *Trans AIME* 160, 140 (1945).

Kemeny S., and J. Manczinger 1978. Treatment of Binary Vapor-Liquid Equilibrium Data, *Chem. Eng. Sc.* 33: 71-76.

Kemeny S., and J. Manczinger, S. Skjold-Jorgensen and K. Toth, 1982. Reduction of Thermodynamic Data by Means of the Multiresponse Maximum Likelihood Principle, *AIChE Journal* 28(1): 20-30

Kim H.C., P.R. Bishnoi, R.A. Heidemann and S.S. Rizvi, 1987. Kinetics of Methane Hydrate Decomposition, *Chem. Eng. Sc.*, 42, 1645-1653.

Knox, W.G., Hess, M., Jones, G.E., and Smith, H.B., 1961. The Hydrate Process, *Chem. Eng. Prog.*, 57, (2), 66-76.

Kobayashi R. and D.L Katz 1949. Methane Hydrate at High Pressure, *Petroleum Transactions, AIME*, 66-70.

Kubota, H., Shimizu, K., Tanaka, Y., and Makita, T., 1984. Thermodynamic Properties of R13 (CClF_3), R23 (CHF_3), R152a ($\text{C}_2\text{H}_4\text{F}_2$), and Propane

Hydrates for Desalination of Seawater, *J. Chem. Eng. Japan* 17 (4), 423-429.

Lewis, G.N., and M. Randall, 1961. Thermodynamics, 2nd edition, revised by K.S. Pitzer and L. Brewer, McGraw Hill, N.Y.

Li Y-H., K.H. Dillard and R.L. Robinson 1981. Vapor-Liquid Phase Equilibrium for Carbon-Dioxide-n-Hexane at 40, 80, 120 °C. *J. Chem. Eng. Data* 26, 53-58.

Ma Y.M., and J.P. Kohn, 1964. Multiphase and Volumetric Equilibria of the Ethane-Methanol System at Temperatures Between -40 °C and 100 °C, *J. Chem. Eng. Data*, 9, 3-8.

Makogon Y.F., 1981. *Hydrates of Natural Gas*. W.J. Cieslewicz. Translation Penn Well Publishing Co., Tulsa, Oklahoma.

Makogon Y.F., 1987. Les Hydrates de Gaz: de l' energie congelee, *LA RECHERCHE*, 192, 1192-1200.

Marshall D.R., S. Saito and R. Kobayashi 1964. Hydrates at High Pressures: Part I. Methane-Water, Argon-Water, and Nitrogen-Water Systems, *AIChE J.* 10 (2), 202-205.

McKoy, V., and Sinanoglu, O., 1963. Theory of Dissociation Pressures of

Some Gas Hydrates, *J. Chem. Phys.*, **38**, No. 3, 2946-2956.

Meissner, H.P., and C.L. Kusik, 1972. Activity Coefficients of Strong Electrolytes in Multicomponent Aqueous Solutions, *AIChE J.*, **18** (2), 294-298.

Menten, P.D., Parrish, W.R., and Sloan, E.D., 1981. Effect of Inhibitors KCl , $CaCl_2$, and CH_3OH on Cyclopropane Hydrate Formation Conditions, *Ind. Eng. Chem. Process Design Develop.*, **20**, No. 2, 399-401.

Michelsen, M.L., 1982. The Isothermal Flash Problem. Part I. Stability, *Fluid Phase Equilibria*, **9**, 1-19.

Neau E., and A. Peneloux, 1981. Estimation of Model Parameters. Comparison of Methods Based on the Maximum Likelihood Principle, *Fluid Phase Equilibria* **6**: 1-19.

Ng, H.-J., and Robinson, D.B., 1976. The Measurement and Prediction of Hydrate Formation in Liquid Hydrocarbon-Water Systems, *Ind. Eng. Chem. Fundam.*, **15**, No. 4, 293-298.

Ng H.-J., and D.B. Robinson 1977. The Prediction of Hydrate Formation in Condensed Systems, *AIChE J.* **23** (4), 477-482.

Ng, H.-J., and Robinson, D.B., 1983. Equilibrium Phase Compositions and

Hydrating Conditions in Systems Containing Methanol, Light Hydrocarbons, Carbon Dioxide and Hydrogen Sulfide, *Gas Processors Association*, Tulsa, Oklahoma, Research Report RR-66.

Ng, H.-J., and Robinson D.B., 1984. The Influence of Methanol on Hydrate Formation at Low Temperatures, *Gas Processors Association*, Tulsa, Oklahoma, Research Report RR-74.

Ng, H.-J., and Robinson, D.B., 1985. Hydrate Formation in Systems Containing Methane, Ethane, Propane, Carbon Dioxide or Hydrogen Sulfide in the Presence of Methanol, *Fluid Phase Equilibria*, **21**, 145-155.

Ng, H.-J., Chen, C.-J., and Robinson, D.B., 1985. Hydrate Formation and Equilibrium Phase Compositions in the presence of Methanol: Selected Systems Containing Hydrogen Sulfide, Carbon Dioxide, Ethane, or Methane, *Gas Processors Association*, Tulsa, Oklahoma, Research Report RR-87.

Ng, H.-J., Chen, C.-J., and Robinson, D.B., 1987. The Influence of High Concentrations of Methanol on Hydrate Formation and the Distribution of Glycol in Liquid-Liquid Mixtures, *Gas Processors Association* Tulsa, Oklahoma, Research Report RR-106.

Ohgaki K., F. Sano and T. Katayama, 1976. Isothermal Vapor-Liquid Equilibrium Data for Binary Systems Containing Ethane at High Pressures,

J. Chem. Eng. Data, **21**, 55-58.

Paranjpe S.G., S.L. Patil, V.A. Kamath and S.P. Godpole, 1987. Hydrate Equilibria for Binary and Ternary Mixtures of Methane, Propane, Isobutane, and n-Butane: Effect of Salinity, *SPE*, 379-389.

Parrish, W.R., and Prausnitz, J.M., 1972. Dissociation Pressures of Gas Hydrates Formed by Gas Mixtures, *Ind. Eng. Chem. Process Design Develop.*, **11**, 26-34.

Patino-Leal H., and R.M. Reilly, 1982. Statistical Estimation of Parameters in Vapor-Liquid Equilibrium, *AIChE Journal* **28**(4): 580-587.

Paunovic R., S. Jovanovic and A. Mihajlov 1981. Rapid Computation of Binary Interaction Coefficients of an Equation of State for Vapor-Liquid Equilibrium Calculations. Application to the Redlich-Kwong-Soave Equation of State *Fluid Phase Equilibria* **6**: 141-148.

Peneloux A., R. Deyvieux, E. Canals and E. Neau 1976. The Maximum Likelihood Test and the Estimation of Experimental Inaccuracies. Application to Data Reduction for Vapor-Liquid Equilibrium, *Journal de Chim. Phys.* **73**: 706-716.

Peng, D.Y., and D.B. Robinson, 1976. A New Two-Constant Equation of State, *Ind. Eng. Chem. Fundam.*, **15**, 59-64.

Peters, C.J., De Roo and R.N. Lichtenthaler, 1987. Measurements and Calculations of Phase Equilibria of Binary Mixtures of Ethane+Eicosane. Part I: Vapor+liquid Equilibria, *Fluid Phase Equilibria* **34**, 287-308.

Pitzer, K.S., 1973. Thermodynamics of Electrolytes I. Theoretical Basis and General Equations, *J. Phys. Chem.*, **77** (2), 268-277.

Pitzer, K. S., and G. Mayorga, 1973. Thermodynamics of Electrolytes II. Activity and Osmotic Coefficients for Strong Electrolytes with One or Both Ions Univalent, *J. Phys. Chem.*, **77** (19), 2300-2308.

Redlich, O., and Kwong, J.N.S., 1949. On the Thermodynamics of Solutions. V: An Equation of State. Fugacities of Gaseous Solutions, *Chem. Rev.*, **44**, 233-244.

Robinson, D.B., and Ng, H.-J., 1986. Hydrate Formation and Inhibition in Gas or Gas Condensate Streams, *J. Can. Pet. Technology*, 26-30.

Robinson, D.B., and Mehta, B.R., 1971. Hydrates in the Propane-Carbon Dioxide-Water System, *J. Can. Pet. Technology*, 33-35.

Roo, J.L., Peters, G.J., Lichtenthaler, R.H., and Diepen, G.A.M., 1983. Occurrence of Methane Hydrate in Saturated and Unsaturated solution of

Sodium Chloride and Water in Dependence of Temperature and Pressure, *A.I.Ch.E.J.*, **29**, (4), 651-657.

Rowlinson, J.S., and F.L. Swinton, 1982. *Liquids and Liquid Mixtures*, Butterworths & Co (Publishers) Ltd.

Salazar-Sotelo D., A. Boireaut and H. Renon 1986. Computer Calculations of the Optimal Parameters of a Model for the Simultaneous Representation of Experimental, Binary and Ternary Data, *Fluid Phase Equilibria* **27**: 383-403.

Schwartzentruber J., F. Galivel-Solastiuk and H. Renon 1987. Representation of the Vapor-Liquid Equilibrium of the Ternary System Carbon Dioxide - Propane - Methanol and its Binaries with a Cubic Equation of State. A new Mixing Rule, *Fluid Phase Equilibria* **38**: 217-226.

Schwetlick H., and V. Tiller 1985. Numerical Methods for Estimating Parameters in Nonlinear Models with Errors in the Variables, *Technometrics* **27** (1): 17-24.

Schroeter, J.P., and R. Kobayashi and M.A. Hildebrand 1983. Hydrate Decomposition Conditions in the System Hydrogen Sulfide-Methane-Propane. *Ind. Eng. Chem. Fundamentals*, **22**, 361-364.

Selleck, F.T., L.T. Carmichael, and B.H. Sage 1952. Phase Behavior in the Hydrogen Sulfide-Water System, *Ind. Eng. Chem.*, **44** (9):2219-2226.

van der Waals, J.H., and Platteeuw, J.C., Clathrate Solutions, *Adv. Chem. Phys.*, **2**, 1-57, 1959.

Skjold-Jorgensen S., 1983. On Statistical Principles in Reduction of Thermodynamic Data, *Fluid Phase Equilibria* **14**: 273-288.

Sloan E.D. Jr., 1989. Clathrate Hydrates of Natural Gases, *Marcell Dekker, Inc.*, New York, NY.

Smirnov L.F., 1987. Kinetics of Gas Hydrate Formation, *Theor. Foundations in Chem. Eng.*, 465-474.

Song K.Y., and R. Kobayashi, 1982. Measurement and Interpretation of the Water Content of a Methane-Propane Mixture in the Gaseous State in Equilibrium with Hydrate, *Ind. Eng. Chem. Fundam.*, **21**, 391-395.

Song K.Y., and R. Kobayashi, 1987. Water Content of Carbon Dioxide in Equilibrium with Liquid Water and/or Hydrates, *SPE Formation Evaluation*, 500-508.

Stewart P.B. and Munjal, 1970. Solubility of Carbon Dioxide in Pure Water at -5 °C to 25 °C, and 10 to 45 Atm Pressure, *J. Chem. Eng. Data* **15** (1), 67-71.

Sutton T.L., and J.F. MacGregor, 1977. The Analysis and Design of Binary Vapor-Liquid Equilibrium Experiments. Part I: Parameter Estimation and Consistency Tests, *Can. J. Chem. Eng.* **55**: 602-608.

Tester J.W., R.L. Bivins, and C.C. Herrick, 1972. Use of Monte Carlo in Calculating the Thermodynamic Properties of Water Clathrates. *AIChE J.*, **18** (6): 1220-1230.

Treble M.A., and P.R. Bishnoi 1987. Development of a New Four-Parameter Equation of State, *Fluid Phase Equilibria* **35**: 1-18.

Treble M.A., and P.R. Bishnoi 1988. Extension of the Treble-Bishnoi Equation of State to Fluid Mixtures, *Fluid Phase Equilibria* **40**: 1-21.

Treble M.A., 1988a. Correlation of VLE Data for Binary Mixtures of 1-Alkanols and Normal Hexane with the Treble-Bishnoi Equation of State, *Fluid Phase Equilibria*, **42**: 117-128.

Treble M.A., 1988b. Personal Communication.

Unruh C.H., and D.L. Katz, 1949. Gas Hydrates of Carbon Dioxide-Methane Mixtures. *Petroleum Transactions, AIME* 83-86.

Valko P., and S. Vajda, 1987. An Extended Marquardt-Type Procedure for

Fitting Error-in-Variables Models, *Comput. Chem. Eng.* **11** (1): 37-43.

van der Waals J.H. and J.C. Platteeuw, 1959. Clathrate Solutions, *Adv. Chem. Phys.*, **2**, 1-57.

van Ness H-C., F. Petersen and P. Rasmussen, 1978. Vapor-Liquid Equilibrium: Part V. Data Reduction by Maximum Likelihood, *AIChE Journal* **24** (6): 1055-1063.

Vysniauskas A. and P.R. Bishnoi, 1983. A Kinetic Study of Methane Hydrate Formation, *Chem. Eng. Sc.*, **38** (7), 1061-1072.

Vysniauskas A. and P.R. Bishnoi, 1985. Kinetics of Ethane Hydrate Formation, *Chem. Eng. Sc.*, **40** (2), 299-303.

Weber W., S. Zeck and H. Knapp, 1984. Gas Solubilities in Liquid Solvents at High Pressures: Apparatus and Results for Binary and Ternary Systems of N₂, CO₂ and CH₃OH, *Fluid Phase Equilibria*, **18**, 253-278.

Wilcox W.I., D.B. Carson and D.L. Katz, 1941. Natural Gas Hydrates, *Ind. Eng. Chemistry*, **33** No 5, 662-665.

Wu B.-J., D.B. Robinson and H.-J. Ng, 1976. Three and Four-Phase Hydrate Forming Conditions in Methane+Isobutane+Water, *J. Chem. Thermodynamics*, **8**, 461-469.

Zemaitis, J.F., D.M. Clark, M. Rafal and N.C. Scriven, 1986. Handbook of Aqueous Electrolyte Thermodynamics, *DIPPR/AIChE*, New York, NY.